Republic of Iraq
Shiite Endowment Diwan

Quarterly Refereed Journal for Natural and Engineering Sciences

Issued by
Al-`Abbas Holy Shrine
International Al-`Ameed Centre for Research and Studies

Licensed by
Ministry of Higher Education
and Scientific Research

Fourth Year, Seventh Volume, Issue 13 and 14
Ramadhan, 1439, June 2018

Secretariat General
of Al-'Abbas
Holy Shrine

Al-Ameed Interna-
tional center
for Research and Studies

Print ISSN: 5721 – 2312
Online ISSN: 0083 – 2313
Consignment Number in the Housebook and Iraqi
Documents: 1996, 2014
Postal Code: 56001
Mailbox: 232

Al-Abbas Holy Shrine. International Al-`Ameed Centre for Research and Studies.

ALBAHIR : Quarterly Refereed Journal for Natural and Engineering Sciences \ Issued by Al-Abbas Holy Shrine International Al-`Ameed Centre for Research and Studies. - Karbala, Iraq : Abbas Holy Shrine International Al-`Ameed Centre for Research and Studies.- Karbala, Iraq : AL- Abbas Holy Shrine International Al-`Ameed Centre for Research and Studies, 1433 hijri = 2012 -

Volume : Illustrations; 24 cm

Quarterly.- Fourth Year, Seventh Volume, Issue 13 and 14 (June 2018)-

ISSN : 5721-2312

Includes bibliographical references.

Text in English ; summaries in Arabic.

1. Science--Periodicals. A. title.

Q1 .A8365 2018 VOL. 7 NO. 13-14

Cataloging center and information systems

Tel: +964 032310059
Mobile: +9647602355555
http://albahir.alkafeel.net
Email: albahir@alkafeel.net

Publication Conditions

In as much as Al-`Bahir- effulgent- Abualfadhal Al-`Abbas cradles his adherents from all humankind, verily Al-Bahir journal does all the original scientific research under the conditions below:

1. Publishing the original scientific research in the various scientific sciences keeping pace with the scientific research procedures and the global common standards; they should be written either in Arabic or English .
2. The research should not be published before under any means .
3. The research should adhere the academic commonalties; the first page maintains the title, researcher name /names, address, mobile number under condition that the name, or a hint , should never be mentioned in the context and keywords should be written in Arabic and English as there is an abstract in Arabic and English.
4. The Research studies should be delivered to us either via Journal website http://albahir.alkafeel.net , after filling the two standard format the first with the name of the researcher and the second without in Word .
5. The page layout should be (2)cm .
6. The font should be of (16 bold),Time New Roman, subtitles of (14 bold) and also the context.
7. The space should be single, indentation should not be, as 0 before, 0 after and no spacing, as 0 before, 0 after.
8. There should be no decoration and the English numeral should proceed to the last text.
9. Any number should be between two brackets and then measurement unit, for instance: (12) cm .
10. All sources and references should be mentioned at the end of the article and categorized in conformity with Modern Language Association (MLA) , for instance :

Name of Author/ Authors, Journal Name Volume Number (Year) pages from - to.

Similarly done in the Arabic article withy a proviso that superscript should be employed.

11. There should be a caption under a diagram in 10 dark , Arabic and English; for instance:

Title or explanation; number of the Fig.

Similarly done with tables.

12. Diagrams , photos and statics should be in colour with high resolution without scanning.

13. The marginal notes, when necessary, should be mentioned at the end of the article before the references.

14. Wherever there is the word " figure" should be abbreviated as Fig. and table should be Table.

15. The pages never exceed 25 pages.

16. The Formulae should be written in Math Type.

17. All the ideas and thoughts reveal the mindset of the researcher not the journal and the article stratification takes technical standards.

18. All the articles are subject to :

a- The researcher is notified that his paper is received within 14 days in maximum.

b- The article is to be sent to the researcher as soon as it does not meet the requirement of the publication conditions.

c- The researcher is notified that his article is accepted.

d- The articles need certain modification , as the reviewers state, are sent to the researchers to respond in a span of a month from the date of dispatch.

e- The researcher is to be notified in case the article is rejected.

f- The researcher is to be granted an edition containing his article.

19. Priorities are given in concordance to :

a. The articles participated in the conferences held by the publication institute.

b. The date of receiving.

c. The date of acceptance.

d. The importance and originality of the article.

e. The diversity of the fields the articles maintain in the meant edition.

20. The researchers should appeal to the modifications the language and scientific reviewers find in the articles.

21. The researcher should fill the promise paper having the publication rights of the Scientific Al-Bahir Journal and adhering to integrity conditions in writing a research study.

In the Name of Allah
Most Compassionate, Mort Merciful

Edition Word

In the Name of Allah, Most Merciful, Most Gracious, thanks be upon the Creator of the universe, peace be upon the most eloquent in Arabs , the most evident , the most efficacious, the most righteous and upon his immaculate benevolent progeny

Al-Bahr journal , scientific and peer-reviewed, comes to the fore as a ground to the researchers and academics since its first publication . Today as the eleventh and twelfth edition heaves into effect to be an essential source of information in publishing the specialized research studies and cuddling the contemporary data to keep pace with the crestive development in the research fields.

None could feel the ambience of Al-Bahr journal but those who experience its loci and fathom the intent of its incharges , thus it is of delectation for us to lay the hand of readership on such a research bouquet to augment knowledge.

The current edition ramifies into the natural and engineering sciences to have a niche among the other journals , as such we , with the bless of Allah, grow momentum and a cynosure to all researchers, academics and readership as here comes the journal with a vesture , we do hope all the success and sapience to you all.

Consultation and Editaril

Proposed New Technique for Smart Earthing System

*Ali Abdulabbas Abdullah, **Inaam Ibrahim Ali, **Alameer Abbas Thamir
*Al-Najaf Eng. Tech. College, AATU, Najaf, Iraq
**Electrical Dept., University of Technology, UOT, Baghdad, Iraq

Received Date: 1 / 6 / 2017
Accepted Date: 5 / 10 / 2017

الخلاصة

اخطاء الخط الواحد المتلامس مع الارض واخطاء الخطين المتلامسين مع الارض تحدث في نظام توزيع القدرة والتي تؤدي الى رجوع تيار خطأ عالي الى هذاالنظام من خلال موصل التأريض . هذا البحث يقترح طريقة تأريض ذكية لتقليل هذا التيار. متحكم المنطق المضبب استخدم في هذه التقنية لغرض زيادة او تقليل قيمة مقاومة التأريض التي تصل نقطة التعادل للمحولة الى نقطة الارض بالاعتماد على تيار الخطأ المقاس. استخدمت ميزة المحاكاة في برنامج الماتلاب لاختبار اداء هذه التقنية. هذه التقنية طبقت في نموذج لنظام توزيع القدرة ذو المستوى (11) كيلو فولت والذي صمم وفق بيانات حقيقية اخذت من محطة توزيع ثانوية في مدينة كربلاء. تقنية التأريض الذكية هذه تتعامل مع أي خطأ ارضي غير متماثل والذي يحدث عند أي موقع في شبكة التوزيع مع أي مقاومة خطأ.

الكلمات المفتاحية

الخطأ الأرضي ذو الخط الواحد، الخطأ الأرضي ذو الخطين، نظام التأريض الذكي، متحكم المنطق المضبب.

Abstract

Single line to ground and double line to ground faults occurred in distribution power system which leads to high fault current that is returned to this system through earthing conductor. This paper proposed smart earthing technique to reduce this current. The fuzzy logic controller is used in this technique to increase or decrease the earthing resistance which connects the neutral of the substation transformer to the earth point depending on the measured faulted current. MATLAB/ Simulink is used to test the performance of this technique. This technique applied to (11) KV distribution power system model with real data from distribution substation in Karbala city. This smart earthing technique deals with any unsymmetrical earthing fault that occurs at any location in the distribution network with any fault resistance.

Keywords

SLG: single line to ground fault; DLG: double line to ground fault; smart earthing system; FLC: fuzzy logic controller.

1. Introduction

Under normal or safe operating condition, the electrical equipment of power system network operates at rated voltage and current. Occasionally, asymmetrical earthing faults occur in power system causing this system to operate in an abnormal condition. So, the voltage and current magnitudes deviate from their normal ranges. In some cases, very high current will return to supply equipment such as generator or transformer, while in others, earthing faults are not necessary to be solid short circuit faults and this will lead to reduction in the magnitude of the current that returns to the system [1]. Whenever there is increase in this magnitude, there will be more damage to power system equipment and vice versa. The faulted current passes through an earthing conductor which connects the neutral point of the system to the earth. So, the magnitude of this faulted current depends on how the neutral point is connected to the earth (earthing techniques) which signifies the importance of earthing in power system network. For these reasons there is a need to search for earthing system and to suggest a new earthing technique to reduce the damage.

Physically, the neutral earthing is the connection of transformer neutral point, generator neutral point or star point of loads or circuits to the earth [2]. The conductor which satisfies this connection is called earthing conductor. The distribution system has several neutral points and the points of the same system are not necessarily connected to the earth by the same technique.

There are two main objectives of system earthing, the first is the detection of earthing faults and the second is to determine the returned fault current in order to prevent the hazard voltage between the structure of the faulted equipment and the earth caused by its high magnitude [3].Earthing of power system has many advantages. The main advantage is that the power system can be divided into several subsystems without interconnected zero sequences. Another advantage is that earthing system can be considered as the most important parameter which affectsearthing faults. Thisresults that it significantly affects the behavior of distribution power system when subjected to earthing faults.

In this paper, a new technique of smart earthing system by using control circuit composed of FLC and controller block will be proposed. This technique is considered a new technique because that it composed of different earthing resistances values that activated depending on operation condition to compensateany change that occurs in fault resistance value or location keeping the returning current magnitude in low level. The control circuit is used to control the operation of the bank of earthed resistances for the purpose of reducing earthing fault current that passes through earthing conductor. This smart earthingtechniqueis applied to distribution

system model of (11) KV which implemented in MATLAB simulation by using real data of substation located in Karbala city. This work deals with unsymmetrical earthing faults (SLG and DLG).

2. Literature Review

Researchers where interested to study this subject because of its importance and great effect on the protection of distribution power systems and their employees. For examples: a research is presented about sizing high resistance grounding in power system with consideration of system earthing capacitance. This research discussed the problems that concerned with earthing capacitance in high voltage and gave the procedure of determining earthing capacitance of the system, the greatest value permitted for high earthing resistance and the pickup setting of an over current relay [4]. The main neutral grounding methods that including un-grounding neutral method, neutral grounding by using a Peterson coil method and neutral grounding by using low resistance value method are discussing in [5]. The methods which used to ground the neutral point of Shanghai Fengxian (35) kV and (10) kV power grid are discussed in [6]. Discuss the phasor diagram and flow directions of the faulted current in case of single phase to ground bolted fault when the HRG method is used in power system be done in [7]. The researches mentioned above discussed the traditional earthing techniques used in different applications. These techniques deal with any earthing fault without the need to know the fault characteristics. So, many problems can occur such as breakdown of the insulation when there is failure in fault detection or damage to the system equipment.

3. Earthing techniques

Earthing technique has small influence under normal operation of the distribution system, but becomes very important and effective when an earthing fault occurs [8]. The neutral point can be isolated from the earth (unearthed) or connected to the earth by using different techniques. These techniques aresolidly earthing, resistance earthing, reactance earthing andpeterson coil earthing. Solidly and LRG are called effective eathing techniques but the HRG, unearthing and resonance techniques are called ineffective earthing technique [9].

4. Smart Earthing system

In this type of earthing, operation condition of the power system determine an earthing connection to the neutral point of the substation transformer. This is done by connecting the neutral point of the distribution system to the earth by using bank of resistances. There are so many cases of the earthing fault which may occur in distribution system due to different magnitudes of the fault resistance and the location of this fault. So, in each case certain magnitude of the faulted current that returns through an earthing conductor is produced. In some cases, the faulted current is very high

reaching values up to thousands of amperes and consequently can cause shutdown if there is a compatible protection system or can entirely damage the equipment which may lead to arc explosion resulting in burning or electrical shock to the personnel that could be working adjacent to the equipment faulted. In other cases, the faults may occur at a remote location or across high fault resistance which causes failure in detection of this fault [10, 11, 12]. So, the fault current magnitude is considered as a critical factor in the power system and it is directly related to earthing method being applied [13]. To detect the fault current passing through an earthing conductor and to reduce it to low level for each case of earthing fault, the connection between the neutral point of substation transformer to earth changes in very short period depending on magnitude of this current. i.e. the smart earthing system overcomes these problems by increasing the equivalent earthing resistance according to the magnitude of returning current to allow low value of this current to passes through earthing conductor. So, nearly neglecting the effect of fault resistance and fault location is the result. The progress of smart earthing technique is represented by the flow chart as shown in Fig (1). This figure represents the flowchart of controlling an earthing fault current by using bank of resistances which controlled by FLC and controller block. The smartearthing system consists of measurement device, FLC, Processor block and bank of resistances.This smart earthing system is applied in distribution system model of (11) KV which implemented in MATLAB simulation.

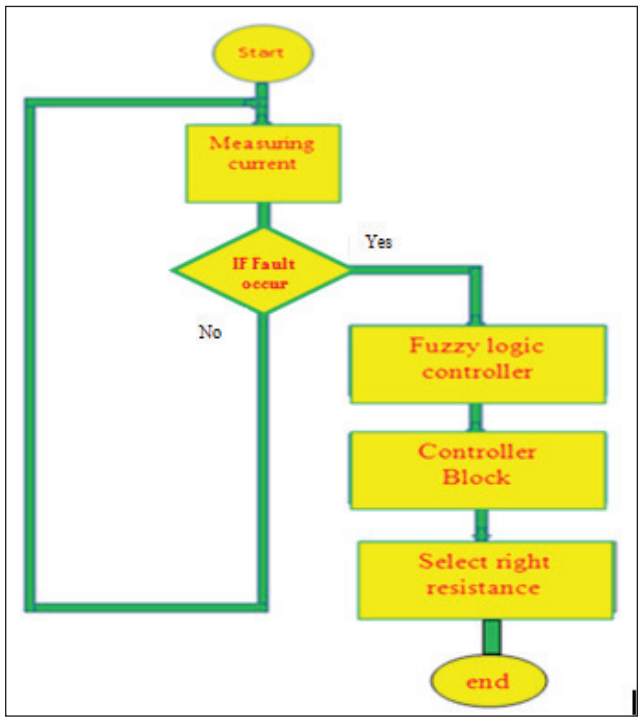

Fig (1): Flow chart of smart earthing technique.

4.1. Fuzzy logic controller

When utilizing fuzzy logic, the solution to the issue can be cast in terms that human operators can understand, so that their experience can be used in the design of the controller. This makes it easier to mechanize tasks that are already effectively performed by humans. It represents a technique that eases the control of a complicated system without having knowledge of mathematical description for this system. Fuzzy logic in reality represents an accurate problem-solving methodology.The most important advantages of the fuzzy logic system are:

• Capability to deal with the uncertainty and nonlinearity.

- Simplicity of implementation.
- Using of linguistic variables.
- Simplicity of adding new data or rules to the old fuzzy system as required.

The four main stages in fuzzy knowledge-based control are:

- Fuzzification
- Rule base
- Inference engine
- Defuzzification

There are need to control the operation of the bank of earthing resistances by changing the output signal of FLC according to measured current by ammeter located in the return path of faulted current.

Fuzzification converts a set of crisp inputs to the corresponding fuzzy sets. The defuzzification process decides the crisp output" by resolving the applicable rules into a single output value. Fuzzification process used (13) triangle membership functions to represent the input from ammeter. Also, Defuzzification process consists of (13) trapezoidal membership functions to represent the output of FLC. Inference step described by creating of rules and computing degree of membership. 13 rules are used in this fuzzy logic controller and the rule viewer of fuzzy controller as shown in Fig (2).

The input status words are Class 0, Class 1, Class 2, Class 3, Class 4, Class 5, Class 6, Class 7, Class 8, Class 9, Class 10, Class 11 and Class 12. This class refers to the magnitude of the fault current in the earthing system and the increasing of a number of the classesrefers to increasing this current. The output status words are No action, Part 1, Part 2, Part 3, Part 4, Part 5, Part 6, Part 7, Part 8, Part 9, Part 10, Part 11 and Part 12.The rule base are:

If the measured fault current belongs toclass 0, then take no action.

If the measured fault current belongs to class 1, then connect part 1 of the bank.

If the measured fault current belongs to class 2, then connect part 2 of the bank.

If the measured fault current belongs to class 3, then connect part 3 of the bank.

If the measured fault current belongs to class 4, then connect part 4 of the bank.

If the measured fault current belongs to class 5, then connect part 5 of the bank.

If the measured fault current belongs to class 6, then connect part 6 of the bank.

If the measured fault current belongs to class 7, then connect part 7 of the bank.

If the measured fault current belongs to class 8, then connect part 8 of the bank.

If the measured fault current belongs to class 9, then connect part 9 of the bank.

If the measured fault current belongs to class 10, then connect part 10 of the bank.

If the measured fault current belongs to class 11, then connect part 11 of the bank.

If the measured fault current belongs to class 12, then connect part 12 of the bank.

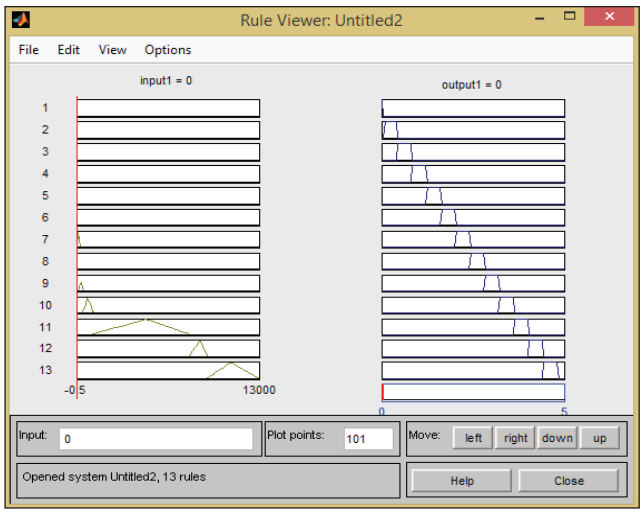

Fig (2): the rule viewer of fuzzy logic controller.

4.2. Controller block and Embedded MATLAB Function

This is a block of sub designed model implemented to receive the controlled signal output from FLC. According to this signal it will send 13 signals output to the earthing resistances block to activate some part of these resistances and separate the other parts. This activated resistance is responsible for reducing the faulted current passing through an earthing conductor. So, the constructions of controller block are:

- One input port which received the output controlled signal from FLC.
- 13 output ports used to control the resistances.
- Many Embedded MATLAB Function blocks.

4.2.1. Embedded MATLAB Function block

An Embedded MATLAB Function block allows using a MATLAB function within Simulink model. The Embedded MATLAB Function block is obtained from the User Defined Functions Library and it is inserted into a model in the same method as any other Simulink block. Embedded MATLAB Function blocks support a subset of the functions obtainable in MATLAB. These functions involve functions in common categories such as Arithmetic functions like plus, minus, and power, Matrix operations and Trigonometric functions like sin, cos, sinh, and cosh. The Embedded MATLAB Function block deals with inputs of any type that Simulink supports.The construction of the controller block shown in Fig (3).

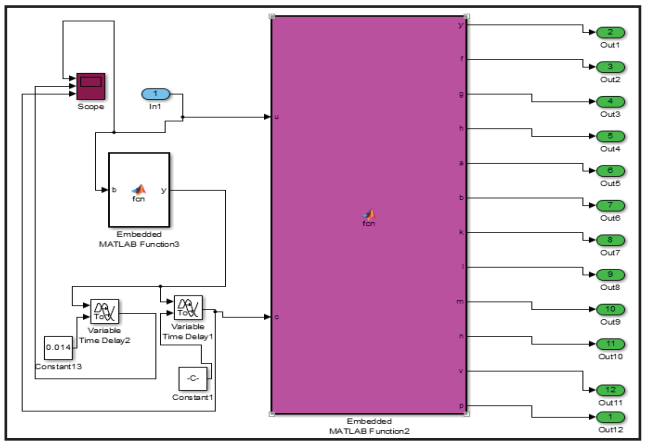

Fig (3): the internal design of controller block.

4.3. Earthing resistance

Neutral earthing resistance (NER) is used in electrical power distribution facilities to limit earthing fault current and to avoid many problems related to use of solidly earthing and unearthing techniques.NER can be categorized into low resistance grounding

(LRG) and high resistance grounding (HRG) and both of these types are applied to reduce the earth fault current and they differ from each other by the level of earth fault current allowed to flow. The two main techniques of connecting medium voltage system neutrals to earth point are carried out by using neutral grounding resistance (HRG method and LRG method). The most important issue regarding the use of resistance in earthing process is to select a proper value for this resistance. There are different opinions about what is better to use, high resistance or low resistance for distribution power system. In fact, there is no standard for defining earthing resistance [4]. Some considerations such as charging current value and pickup current should be taken in to account for selecting the value of earthing resistance. The value of this resistance must be less than earthing capacitance value. If this condition is not satisfied, a great part of current will return through this capacitance to the system if there is an earthing fault in distribution power system. This will result in increase in the electrical system's charging current leading to high transient over voltage. So, the system charging current should be known to apply an earthing resistance. The charging current for an electrical distribution system can be measured or estimated. Typical charging currents are less than (15) A for (11) KV power system [14]. This means that the neutral grounding resistance setting is normally selected so that it let-through a current greater than the total capacitive charging current, 3ICo, of the system when an earthing fault occurs. This determines the rate of fault damage which is considered acceptable under earth fault condition.

The other condition is that the resistance mustn't allow reducing the faulted current to a value less than the pickup current of the protection device (over current device). So, the pickup current should be set at value greater than that of the current passing through neutral earthing conductor by safety factor. So, using of the bank of earthing resistances provide the solution to this problem by change the equivalent earthing resistance value i.e. change the connection between neutral of the system and the earth by using resistances of different value. Note also the value of these resistances selected by applying the consideration above. It provides a dynamically earthing resistance that changed its value in very short time (in mille seconds) so as to treats the wide variations which exist in earthing faults. This leads to keep the faulted current through earthing conductor in small range of amperes which doesn't causes problems to the power system. Earthing resistance might be connected to the neutral point of a power transformer or across the broken delta secondary of the three phase to earth connected distribution transformers.

At normal operation, the earthing conductor doesn't carry current and the measurement device (ammeter) measures zero current approximately. This makes the magnitude

of signal input to FLC zero. So, the earthing connection in this case is implemented by using the lowest resistance value and there is no need to change it.

When earthing fault occurs in power system, the fault current will return to the system through earthing conductor and the magnitude of this current depends on the fault resistance and location in distribution power system. So, the ammeter measures this faulted current and sends its magnitude to FLC. The fuzzy controller immediately processes the magnitude of this fault and decides the magnitude of its output signal according to its rules. This magnitude varies from zero to (5) V and it will be sent to controller block. Accordingly, the controller block will send 13 controlling signals output to disconnect a resistance which operates at the normal condition and activates other part of resistances from bank of earthing resistances to reduce the faulted current that passes through an earthing conductor as required (the higher the NER value, the lower the faulted current magnitude) [15].

5. Advantages of changing the value of earthing resistance

1-Reduce faulted current that returns to the system.

2-More safety when there is failure in protection or detection device.

3-Easy to detect the earthing fault in case of the current magnitude is very small.

4-Overcomes on the problems that exist when using fixed value of resistance (high resistance or low resistance value).

5-Reduce the overvoltage problem.

6. TYPES OF FAULTS

In general, there are two types of faults may be occurred in three-phase power distribution systems. These faults are symmetrical and unsymmetrical fault which may be short circuit or open circuit. Short-circuit faults can occur between lines, or between lines and earth. Short circuits may be one-line to earth, line to line, two-lines to earth, three-lines without connected to earth and three-lines to earth. Unsymmetrical fault short circuit divides to three subtypes which are SLG fault, line to line fault and DLG fault. Earth fault typically means an unintentional connection of power line with metallic parts being connected with the earth. An asymmetrical earth fault current is a current that passes to earth and has a magnitude that depends on the techniques of system earthing. In this work, many faults of SLG and DLG type are used due to two reason; the first are these faults depends on how the neutral point connected to earth. And the second are the single-line to earth fault is proven to be a type of fault that most possibly occurs in the distribution network with the neutral un-effectively grounded system [16]. These faultsare tested in (11) KV distribution

system model. The magnitude of the fault current depends on location of fault in the system and fault resistance. So SLG and DLG faults will be tested across different fault resistance values and locations.

7. MATLAB SIMULATION

The power model implemented using MATLAB/SIMULINK to test the smart earthing system under SLG, and DLG faults occurred in the (11) KV distribution system. The MATLAB / Simulink simulation model is illustrated in Fig (4). This model represents real power network which powered from distribution substation on Karbala city. It composed from three phase programming voltage source of (33) KV connected (Yn). Three phase two winding transformer of capacity (31.5) MVA to transform (33) KV to (11) KV which connected as follow:

Winding 1 is delta

Winding 2 is Yn

This transformer is representing distribution substation and the neutral of this transformer connected to earth by using smart earthing technique. This substation consists from 6 feeders of (5) MVA. The feeder 1 supplies the load by using three phase distribution line of length (5) km, the feeder 2 supplies the load by using three phase distribution line of length (7.5) km, the feeder 3 supplies the load by using three phase distribution line of length (10) km, the feeder 4 supplies the load by using three phase distribution line of length (2.5) km, the feeder 5 supplies the load by using three phase distribution line of length (12.5) km and the feeder 6 supplies the load by using three phase distribution line of length (15) km. Three-phase ammeter and three-phase voltmeter were used to measure the current and voltage respectively. All feeders' supplies 12 transformers of capacity (400) KVA to transform (11) KV to (0.4) KV with connection as follow:

Winding 1 is delta

Winding 2 is Yn

This transformer supplied four lines to the consumers which are three phase line and neutral. This neutral of solidly connection to earth and each one of these transformers supplies loads of (340) kW connected as Yn. Three phase fault block are used to act as SLG or DLG fault.

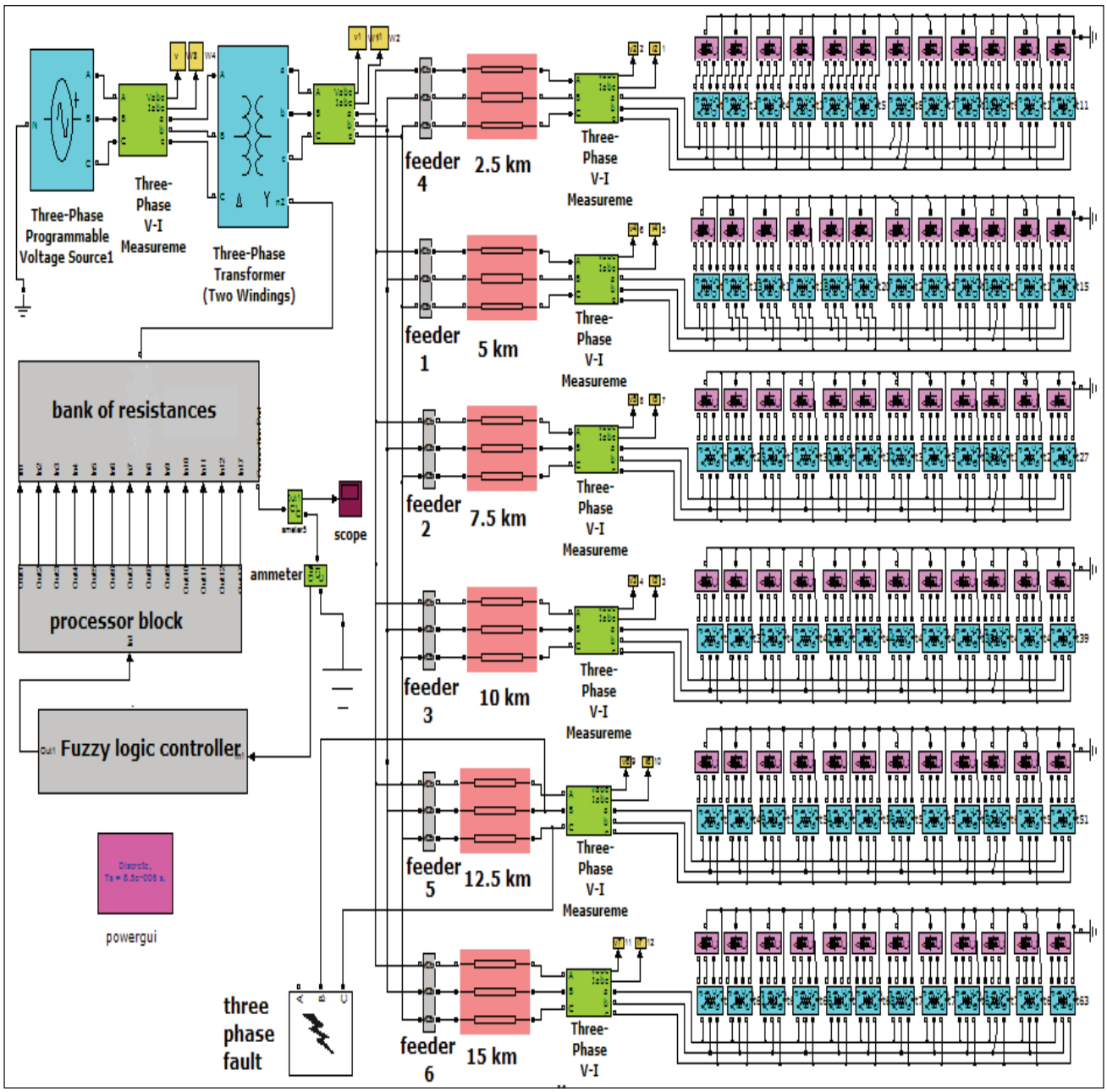

Fig (4): Simulink model of distribution system earthed by smart earthing system.

8. SIMULATION RESULTS

The faulted current which returned to the (11) kV distribution power system through earthing conductor causes big problem to this system. So, the smart earthing is suggested to reducing this faulted current. In this section, many cases of single line to earth faults and double line to earth faults are occurred in this power system and the simulation results of the faulted current due to these fault cases will show in Figs (5)-(10). This simulation results are measured by the ammeter that located in earthing conductor. The showing of this figures will ordered according to the type of unsymmetrical earthing fault and location of this fault by refers to the number of feeder and the distance.

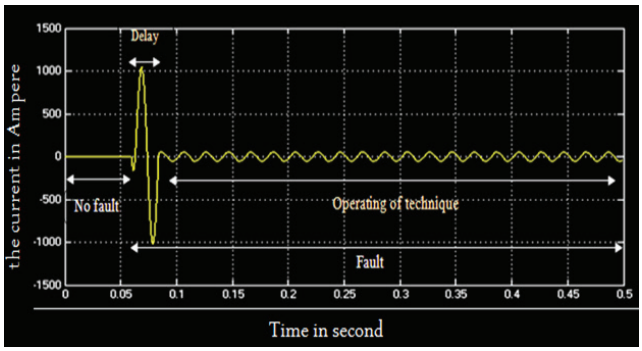

Fig (5): SLG fault at (0.06) sec located in feeder 2 after (7.5) km with Rf=(5.4) ohm.

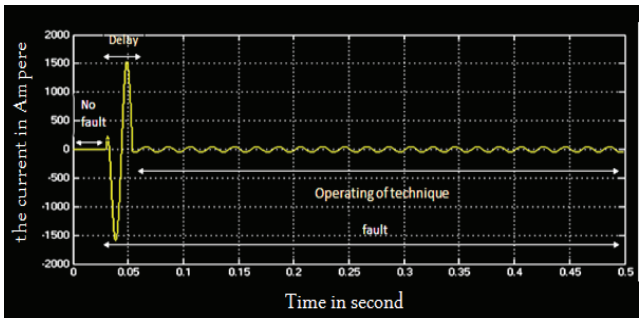

Fig (6): SLG fault at (0.03) sec located in feeder 1 after (5) km with Rf=(3.2) ohm.

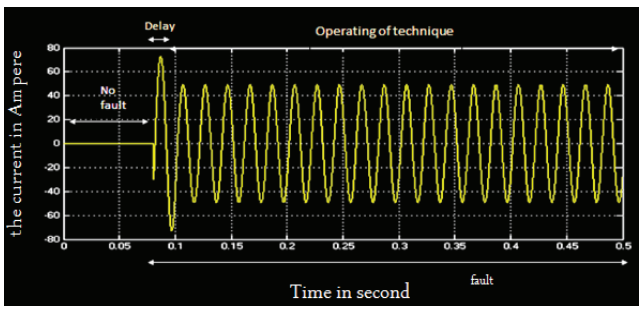

Fig (7): SLG fault at (0.08) sec located in feeder 6 after (15) km with Rf=(120) ohm.

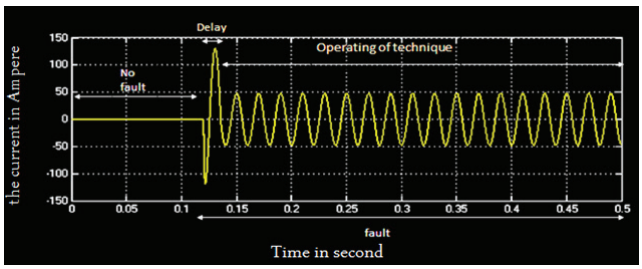

Fig (8): DLG fault at (0.12) sec located in feeder 5 after (12.5) km with Rf=(63) ohm.

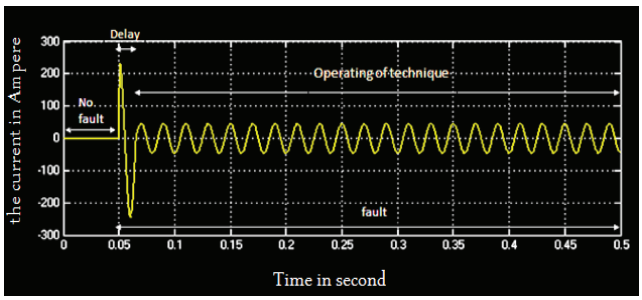

Fig (9): DLG fault at (0.05) sec located in feeder 4 after (2.5) km with Rf=(35) ohm.

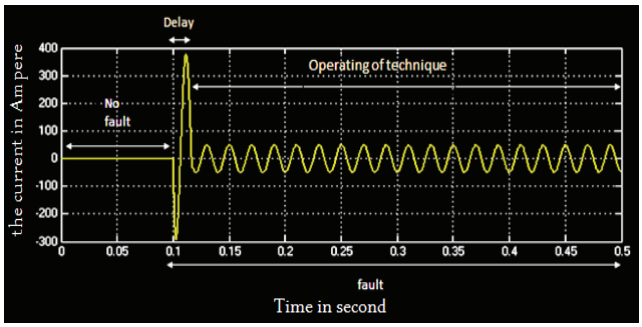

Fig (10): DLG fault at (0.1) sec located in feeder 3 after (10) km with Rf=(17.8) ohm.

8.1. Results discussion

The total period of simulation of these techniques is adjusted to (0.5) sec and divided into three periods which are the period of normal operation before the fault occurrence, delay period and period of technique operation.

At normal operation, the connection between the transformer neutral and the earth is done by using the lowest resistance value and the current through this resistance equals to zero. The time delay period equals to (20) m sec leading to passing one unlimited cycle of the fault current. In this period, the control process is done.

When the fault occurs, its current magnitude depends on fault resistance value and location but these Simulink results show

that the neutral earthing current is equal to the same magnitude (around (50) A) in each faulted case which reduces the system equipment damage. To compare these results, some researches results and discussions will addressed below:

Lawrence J. Kingrey, Ralph D. Painter and Anthony S. Locker, IEEE, 2011 [17] made a comparison between HRG and LRG method for grounding the medium voltage system. In the second point of this comparison, they wrote that a LGR let through current (400) A and HGR let through current less than (6) A. In the last point, the system application voltages for LGR is in ((2.4) and (4.16) kV) and for LGR (from (2.4) to (69) kV).So, HRG cannot be used in (11) KV due to high charging current in this voltage level((11) KV) compared to it requirement (6.5) A. The LGR limits the neutral earthing current to (400)A causes equipment damage leadingto that the fault clearing time should be in cycles due to high current magnitude as mentioned in the third point and the problem occurs when the fault isn't detected.

Eng. Hasan Z. Al-Amari and Dr. Abdallah I. Fadel, IEEE, 2013 [18], In this research, the significance and influence of neutral grounding resistance method in (30) KV Western Libyan power system network and its effect in limiting and determining the bolted single line to ground fault current for a network fed by a single or multi sources were addressed. The (10)ohm-neutral grounding resistance installed in (30) KVnetwork decreases the single line to ground fault current toless than (2) kA, (4) kA and (5) kA in the (30) KV network for single,double and triple feeding source respectively.When there is failure in protection device, these magnitudes of fault current cause more damage to the system equipment.

This smart technique allows to 50 A in any earthing fault which reduce the damage less than of LGR technique (400) A or (300) Ain (21.4) ohm as applied in (33/11) KV substation transformer in Karbala city. HRG and non-earthing technique limit the fault current to very low level which allows increasing the fault clearing time reaching to hours but there is high overvoltage in the two healthy phases during this time. This requires increasing the insulation level of the power system equipment. In the smart earthing technique, the fault should be cleared in short time (seconds) leading to there is no need for increase the insulation level.

9. Conclusion

1- The current let through earthing conductor in (11) KV system should be greater than (15) A for any fault condition. This magnitude was estimated for system charging current.

2- Damage problem is very important factor in selecting earthing technique for distribution system and it determined by the current allowed passing through neutral earthing conductor.

3- Bank of resistances is used to connect the neutral point to the earth and its controller is solved by using fuzzy logic controller and controller block. In this bank, there are 13 earthing resistances of different values applied to reduce the faulted current through an earthing conductor. These resistances are connected in parallel connection by using relays. The activation of these resistances depends on the magnitude of the faulted current that returns to (11) KV distribution system. Different values of these earthing resistances are selected to compensate any change that occurs in fault resistance value or location keeping the returning current magnitude in a low level. This will reduce the damage to the system equipmentand allows increasing the fault clearing time for some seconds making the allocation of the earth fault easier. The insulation level doesn't required to increase because the fault clearing time in seconds compared to that in high resistance and non-earthingtechnique which may reach to hours.The obtained results for this earthing technique are remarkable and comparable with respect to the conventional applicable techniques.

References

[1] Tao Cui, Xinzhou Dong, Zhiqian Bo and Andrzej Juszczyk, "HilbertTransform-Based Transient/ Intermittent Earth Fault Detection inNon-effectively Grounded Distribution Systems", IEEE, IEEE Transactions on Power Delivery, Vol. 26, Issue 1, pp. 143-151, January, (2011).

[2] HNIN NU WAI and KYAW SAN LWIN, "Design and Performance ofPrimary Substation Earthing System (230/33 kV)", International journal ofscientific engineering and technology research, Vol.03, Issue 07,pp.1245-250, May, (2014).

[3] Bystrík DOLNÍK and Juraj KURIMSKÝ, "Contribution to earth faultcurrent compensation in middle voltage distribution networks",Przegląd Elektrotechniczny, pp. 220-224, (2011).

[4] Joseph Sottile, Thomas Novak and AnupTripathi, "Best Practices forImplementing High-Resistance Grounding in Mine Power Systems",IEEE, IEEE Transactions on Industry Applications, Vol. 51, Issue 6, pp.5254 – 5260, (2015).

[5] Yundong Song, Shun Yuan, Chunfang Zhao and YanfengJia, "Analysisand Selection of Neutral Grounding Modes in Cable DistributionNetwork", IEEE,International Conference on Power Engineering, Energyand Electrical Drives, pp.518-521, April, (2007).

[6] Siming Hua, Hua Zhang, Feng Qian, Chunjie Chen and Meixia Zhang,"The Research on Neutral Grounding Scheme of Fengxian 35 kV and 10kV Power Grid", Journal of Energy and Power Engineering, pp. 897-901,July, (2013).

[7] Dev Paul PE, "Phasor Diagram of a Single-Phase-Ground Fault Currentin a High-Resistance Grounded Power System", IEEE, 2017 IEEE/

IAS53rd Industrialand Commercial Power Systems Technical Conference(I&CPS), pp. 1-6, (2017).

[8] Abdallah R. Al-Zyoud1, A. Alwadie, A. Elmitwally, and AbdallahBasheer, "Effect of Neutral Grounding Methods on the Earth FaultCharacteristics", PIERSProceedings, Prague, Czech Republic, pp. 1144-1151, July 6-9, (2015).

[9] Xiangjun Zeng, Yao Xu and Yuanyuan Wang, "Some Novel Techniquesfor Insulation Parameters Measurement and Petersen-Coil Control inDistributionSystems", IEEE, IEEE Transactions on IndustrialElectronics, Vol. 57, Issue 4, pp.1445-1451, April, (2010).

[10] M. Michalik, W. Rebizant, M. Lukowicz, Seung-Jae Lee and Sang-HeeKang, "High-impedance fault detection in distribution networks with useof wavelet-based algorithm", IEEE, Vol. 21, Issue 4, pp. 1793-1802, October, (2006).

[11] N. I. Elkalashy, M. Lehtonen, H. A. Darwish, M. A. Izzularab and A. I.Taalab, "Modeling and Experimental Verification of a High Impedance Arcing Fault in MVNetworks", IEEE, 2006 IEEE PES Power SystemsConference and Exposition, pp.1950 -1956, (2006).

[12] Nagy I. Elkalashy, MattiLehtonen, Hatem A. Darwish, Mohamed A.Izzularab and Abdel-Maksoud I. Taalab, "DWT-Based Investigation ofphase currents for Detecting High Impedance Faults Due to Leaning Treesin Unearthed MV Networks", IEEE, 2007 IEEE Power EngineeringSociety General Meeting, pp. 1-7, (2007).

[13] Yan Gao, Xiangning Lin, Pei Liu and Zhiqian Bo, "A GeneralizedMorphological Transform Based Faulty Feeder Selector Suitable for theNon-Effectively Grounded Power Systems", IEEE, 2007 IEEE PowerEngineering Society General Meeting, pp. 1-6, (2007).

[14] J. C. Das, "Ground Fault Protection for Bus-Connected Generators in anInterconnected 13.8-kV System" IEEE, IEEE Transactions OnIndustry Applications, Vol. 43, Issue 2, pp. 453-461,March/April, (2007).

[15] Mahdi MozaffariLegha and Saeed Shokoohian, "A New Algorithms forFaulted Phase Earthing Protection Relays on 20kV Networks", Specialtyjournal of Engineering and Applied Science, Vol. 1 (2), pp. 1-6, (2016).

[16] Ning Tong, Xiangning Lin, Rui Zhang and Shan He, "Fault Identification Method Based on the Neutral Point Medium Resistance Switching-on for the Distribution Network", IEEE, 2014 IEEE PES Asia-Pacific Power and Energy Engineering Conference (APPEEC), pp. 1-5, (2014).

[17] Lawrence J. Kingrey, Ralph D. Painter and Anthony S. Locker, "ApplyingHigh-Resistance Neutral Grounding in Medium-Voltage Systems", IEEE, Vol. 47, Issue 3, pp. 1220-1231, May/June, (2011).

[18] Hasan Z. Al-Amari and Abdallah I. Fadel, "10 ohm Neutral GroundingResistance in 30kV Western Libyan Network and Effects", IEEE, Power Engineering Conference (UPEC), pp. 1-6, (2013).

The role of Some Tumour Associated Genes (CA9, WT1, PRAME) in diagnosis and prognosis of Breast Cancer.

*Maisaa G. Jumaa and **Jawdat N. Gaaib
*Department of microbiology, College of medicine, University of Maisan, Maisan, Iraq.
** Department of Clinical Laboratories, College of Applied Medical Science, University of Karbala, Karbala, Iraq.

Received Date: 5 / 3 / 2017
Accepted Date: 30 / 3 / 2017

الخلاصة

هناك مجموعة من المستضدات المرتبطة بالورم (TAAS) والتي قد يتردد التعبير عنها في أنواع مختلفة من السرطان. قد يلعب التعبير عن هذه الجينات دورا حاسما في التشخيص و التنبوء المبكر بمرض السرطان، كما انها تعد من اهم الاهداف التي قد يستهدفها العلاج المناعي. تهدف الدراسة الحالية الى تحديد مستويات التعبير لثلاثة من هذه الجينات المرتبطة بالورم (CA9, WT1 and PRAME) في الدم المحيطي المأخوذ من مرضى سرطان الثدي بالمقارنة مع عينات دم لمرضى اورام الثدي الحميدة ولأشخاص اصحاء كمجاميع سيطرة. تم تقدير القيمة التشخيصية لهذه الجينات من خلال مقارنة مستويات التعبير مع كل من حجم الورم, و حالة العقد الليمفاوية. جمعت عينات الدم المحيطي (PB) من 55 مريضة مصابة بسرطان الثدي و20 عينة من المتبرعين الأصحاء، و 10 نساء كان حديثا قد تم تشخيص اصابتهم باورام الثدي الحديثة, استخدمت المجموعتين الاخيرتين كمجاميع سيطرة وتم تحليل العينات جزيئيا باستخدام تقنية عكس تفاعل سلسة البلمرة (RT-PCR). أشارت نتائج الدراسة إلى أن من بين 55 عينةلسرطان الثدي، كانت 50 (91٪) عينة ايجابية لجين(14.54٪) 8 ،CA9 من العينات موجبة لجين WT1 و 5 (9.09٪) من العينات موجبة لجين PRAME. كان تعبير جينCA9في عينات السرطان أعلى بكثير بالمقارنة مع عينات الأورام الحميدة والاصحاء، في حين أن كل من الجينين الأخرينلم يظهرا تعبير في عينات الاورام الحميدة وعينات الاصحاء. عند مقارنة التعبير الجينيللجينات الثلاثة بالنسبة إلى وضع العقدة الليمفاوية, أظهرت نتائج الجينات الثلاثة أن أعلى نسبة العينات الإيجابية 25 (50٪) و 5 (60٪) و 4 (80٪) للجينات CA9، WT1 وPRAME على التوالي، كانت في حالة العقدة الليمفاوية المتعددة. وفقا لحجم الورم أظهرت النتائج أن هنالك علاقة ذات دلالة إحصائية بين زيادة التعبير للجينات CA9 و WT1 مع الاورام ذو الحجم 2،0-2،9، في حين أن جينPRAME كانت أعلى نسبة العينات الإيجابية مع حجم الورم 1،0-1،9. كأستناتج أثبتت الدراسة الحالية أن جينCA9 يمكن أن يكونذو قيمة تفريقية للتميز بين أورام الثدي الخبيثة من تلك غير الخبيثة، كذلك تشير النتائج الى القيمة التشخيصية والتنبؤية لهذا الجين. من ناحية أخرى قد يحتاج الجينانWT1 وPRAME الى المزيد من الدراسات الجزيئية للكشف عن دورهم في امراضية سرطان الثدي.

الكلمات المفتاحية

الجينات المرتبطة بالورم، CA9, WT1, PRAME، سرطان الثدي

Abstract

The aim of the present study is to assess the possible diagnostic and prognostic significance of certain tumour associated genes (CA9, WT1, and PRAME) in relation to tumour size and lymph node status. In order, the expression of these factors were measuredin the peripheral blood of breast cancer patients (N=55), patients with benign breast lesions (N=10) and apparently healthy controls (N=20). Quantitative real time polymerase chain reaction (qRT-PCR) was used to assess the expression of the target biomarkers. In the breast cancer samples 50(91%) samples were CA9-positive,8(14.54%) wereWT1-positive and 5(9.09%) were PRAME-positive samples. The expression of CA9-positive was significantly higher in breast cancer sample compared to benign tumour samples and healthy controls. For lymph node status, the results of all three genes showed that the highest percentage of positive samples 25(50%), 5(60%) and 4(80%) for CA9, WT1 and PRAME genes respectively, were multiple for lymph node status. The tumour size was significantly associated with the increasedCA9 and WT1 genes expression with tumour size 2.0-2.9 cm, while for PRAME gene the highest percentage of positive samples were with tumour size 1.0-1.9 cm. This study showed that CA9 gene can be a useful tool for discrimination between malignant and non-malignant breast tumours, the results may also indicatethe diagnostic and prognostic values for this gene. However, further analysis of a bigger cohort are required to consolidate these initial findings.

Keywords

Breast cancer, WT1, CA9, PRAME

.1 Introduction

Breast cancer is the one of the most common malignancy that diagnosed in women around the world, with high frequency in the western countries, and it represents the most important cancer related death among women [1]. One of the current challenges in the breast cancer management is the imperative need to find out a biomarkers that are sensitive and specific enough to detect early neoplastic changes which will facilitate the detection of breast cancer at an early stage, and monitoring the progression of breast cancer and the patient response therapy programs.

Tumour associated antigens (TAAs) could serve as a distinctive molecular markers and specific targets for immunotherapies, since these antigens are molecules not expressed normal tissues, but they are preferentially expressed by tumour cells [2]. There are several types of TAAs such as cancer germline antigens which considered a good target to future immunotherapies since these antigens can be expressed on tumour cells and normal germ cells but not in other normal somatic tissues. Other types of TAAs are expressed in normal tissues but overexpressed in tumour cells. These TAAs can show changes recognized by the immune response either through their loss or de novo aberrant expression. Many TAAs that shown to be specifically recognized by T cells have been identified [3,4].

For breast cancer immunotherapy, many tumour antigens used that are expressed on normal tissues but are overexpressed or mutated on tumour cells, examples TAAs that associated with over expression in tumour cells are WT1, PRAME, and CA9. The Wilms' tumour gene (WT1) was initially identified in hereditary and sporadic cases of Wilms' tumour in which the gene was either mutated or overexpressed [5]. WT1 is one of the genes that involved in growth regulation and/or differentiation of cells. Previous studies showed that the WT1expression is limited to particular cell types, including ovarian granulosa, testicular sertoli cell, mammary duct and lobule cells, splenic parenchyma, and glomerular podocytes[6,7].

Although its expression is restricted to adult tissues, WT1 is also widely expressed in many cancer types, in which the gene act as an oncogene as interference with WT1 function induces apoptosis and inhibits proliferation, making WT1 a target for cancer immunotherapy. The other tumour associated antigen that is overexpressed in tumour cells is preferentially expressed antigen of melanoma (PRAME) which has been detected in a variety of cancers including breast cancer, but its expression is absent or low in normal tissues [8]. The protein PRAME was first detected in cells isolated from a melanoma as a tumour antigen with high expression of the gene detected in approximately (88–95%) of primary melanomas [8]. In breast cancer, the function of PRAME is still elusive [9]. Although many studies reported the detection of PRAME mRNA transcripts, only few studies linked the gene expression data to clinical outcomes. It has been reported that the expression of

PRAME is associated with poor prognosis in neuroblastoma, with more advanced tumour stage, poor clinical outcome, and older ages of patients at time of diagnosis [10].

Carbonic anhydrase IX (CA9) is one of the genes that are over expressed in tumour cells, this gene, as a member that belong to carbonic anhydrase family, is a cell membrane associated protein that responsible for regulation of cell proliferation in response to hypoxia [11,12].CA9 is expressed in tissues of many types of cancers including oesophagus, colon, kidney, bladder, breast, uterine, and cervix[13].CA9 is detected in approximately (80%) of primary and metastatic renal cell carcinoma (RCC) and approximately (95%) of clear cell renal cell carcinoma, while the normal renal tissues didn't show CA9expression [14]. Therefore, CA9 can be considered as a specific biomarker of RCC that serves as a potential target for RCC-specific immunotherapy. In this study, the influence of the expression levels of breast cancer- relevant TAAs on the breast cancer were investigated in an attempt to evaluate the diagnostic and prognostic value of CA9, WT1 and PRAMEgenes for early diagnosis and prediction of prognosis of breast cancer.

2. Materials and Methods:

blood samples from 55 patients with different stages of newly diagnosed Invasive Ductal Carcinoma were obtained from different Iraqi hospitals,after patients underwent cytopathological and histopathological examination. Two control groups were used in this study, 10 samples from patients with benign breast tumours, and 20 samples from healthy donors. The patient's informations (age and family history) and histological data (lymph node status) were obtained from the patients' files. The samples were preserved with TRIzolin the Genetic lab of National center for early detection of tumours in the medical city (Baghdad/ Iraq). Out of (2) ml of peripheral bloodthat drawn, 0.5 ml was preserved as whole blood after treating with TRIzol (sample were centrifuged at 1,000 xg for 5 minutes at 4Cº followed by removing the supernatant and adding phosphate buffer saline (PBS) containing 5% Triton X-100 and vortexed to be homogenized then a 0.75 ml of TRIzol added to each sample in a ratio of 3 TRIzol :1Sample volume then the samples were kept at -80Cº. Samples subjected to RNA extraction and molecular study by using Revers Transcription and Real Time PCR at Molecular Oncology Unit in Guy´s hospital – Kings College/London/ UK.

2.1. RNA extraction, reverse transcription and real-time -PCR assay:

The total RNA extractionfrom all groups of samples was performed using the TRIzol® LS Reagent(Life Technologies - Ambion. USA) following the manufacturer's protocol. Reverse transcription of total RNA was done using High-Capacity cDNA Reverse Transcription Kit (Life Technologies - Ambion. USA) in a reaction volume of 20 µl(2 µl RT buffer, 0.8µl dNTPs mix, 0.2 µl RT rundom primers,

1 µl reverse transcriptase, 1 µl RNase inhibitor and 15 µl total RNA) following the manufacturer's instructions. After that, cDNA was stored at -80 °C until being used. Expression of genes was analyzed using specific primers-designed with Primer3 (http://www.ncbi.nlm.nih.gov/tools/primer-blast/) (Table 1). Serial dilutions of cDNA were used for preparing of standard curve. The standard curves were generated for both target genes and endogenous control gene (ABL). Quantitative real-time PCR assays were performed in triplicate using the Applied Bio systems 7900 real time PCR machine. The 20 µl of reaction volume containing10 µl of SYBR Green master mix ,1 µl of primer mixes, 5µl of RNase free water and 4µl of cDNA template. Real-Time PCR protocol was as follows; stage 1 50ºC for 2 minutes, stage 2: 95ºC for 10 min, stage 3 in a two-step cycle procedure (95 ºC for 15 Sec. and 65ºC for 1 min) repeated for 6 cycles and stage 4 in a two-step cycle procedure (95 ºC for 15 Sec. and annealing 61ºC for 1 min) repeated for 40 cycles. The slope of a standard curves was used to estimate the PCR amplification efficiency of a real-time PCR reaction. A calculation for estimating the efficiency (E) of a real-time PCR assay was performed as following:

$E = (10 -1/slope-1) \times 100$

$E = (10 -1/3.35 -1) \times 100$

Assess the specificity of the amplified products was determined based on melting curve analysis. The studied genes expression levels were measured in cDNA samples by quantitative real-time PCR technique using the relative quantification method (2-ΔΔCt method). The housekeeping gene ABL and relative to a calibrator sample used for normalization of fold-change in gene expression and relative to a calibrator sample. Calculation of relative fold change of the target gene performed as described below:

$\Delta\Delta CT = \Delta CT \text{ sample} - \Delta CT \text{ calibrator}$

$\text{Fold Change} = 2^{-\Delta\Delta Ct}$

Table (1): primers sequences

Primer	Sequence
CA9-F	'GTGGAAGGCCACCGTTTC -3 -'5
CA9-R	'CTCGTCAACTCTGGCAAAGG -3 -'5
WT1-F	5'- AGGCTTTGCTGCTGAGGAC -3'
WT1-R	5'- CAGGTCATGCATTCAAGCTG ٣-'
PRAME-F	5'- CTTTCCTCGAAGGCCACCT -3'
PRAME-R	5'- GTTATTGTGAGGACCTTTAACGA-3'
ABL-F	5'-TGGAGATAACACTCTAAGCATAACTAAAGGT-3'
ABL-R	5'-GATGTAGTTGCTTGGGACCCA-3'

2.2. Statistical analysis

The Statistical Analysis System-SAS (2012) program was used to assessthe difference in the factors in study parameters. Chi Square was used to assess the significance of changes in the statistical parameters and least significant difference –LSD test was used to significant compare between meansin this study.

3. Results

The patients' age range was ranging between 20-70 years and the median age was 49 years with high frequency of patients in the range of 40-59 years. According to the family history, 50(90.91%) of breast cancer patients had a negative family history withstatistically significance differences (X2 =13.473 **, p<0.01) in comparison with patients that have positive family history. Regarding the lymph node status, the percentage of patients with multiple lymph nodes was significantly higher than those with few or no lymph nodes in the tested cohort (p value 0.0017**p<0.001). In regard to tumour size the highest percentage of patients showed atumour size of 2.0-2.9 cm. which showed statistically significant differences (p value 0.0014**p<0.001).

Relation between genes expression and clinicopathologic parameters are listed in Table 2. Out of55 breast cancer samples, 50 (91%) samples were CA9-positive which showed statistically significant differences (p<0.0001) with the percentage of CA9-negative breast cancer samples 5 (9%).For other two genes, the negative samples showed statistically significant differences (p<0.0001) with the 8(14.54%) WT1-positive samples and 5(9.09%) PRAME-positive samples. According to malignancy status the percentage of patients with CA9-positive gene expression was significantly higher (p value= 0.0477p<0.05) compared to benign tumoursand healthy controls samples, while for other two genes none of benign tumour and healthy controls samples showed positive expression for both WT1 and PRAME genes. Concerning the distribution of patients according to age groups, the present study showed that there is nostatistically significant differences in the levels of genes expression with age. Regarding the lymph node status, the results of all three genes showed that the highest percentage of positive samples 25(50%), 5(60%) and 4(80%) for CA9, WT1 and PRAME genes respectively, were multiple for lymph node status that significantly different from percentage of samples with no or few lymph node status (p value =0.0144, 0.0174, 0.0317p<0.05) for CA9, WT1 and PRAME genes respectively. For the tumour size, the results showed that there was statistically significant association between the increasedCA918(36%) and WT1 5(62.5%) genes expression withtumour size 2.0-2.9 cm(p value= 0.0136, 0.0127 p<0.05) for CA9, and WT1 genes respectively, while for the PRAME gene the highest percentage of positive samples 3(60%) were with tumour size 1.0-1.9 cm.(p value= 0.0114 p<0.05).

Table (2): Effect of clinic pathological features on genes expression in breast cancer patients.

Variable		*CA9-positive* (%) .No	*CA9-Negative* (%) .No	*WT1-positive* (%) .No	*WT1-Negative* (%) .No	*PRAME-positive* (%) .No	*PRAME-Negative* (%) .No
Study groups	**NO. of cases**						
Breast cancer	**55**	(90.9)50	(9.09)5	(14.54)8	(85.5)47	(9.09)5	(90.9)50
Benign tumour	**10**	(100)10	0	0	(100)10	0	(100)10
Healthy control	**20**	(50)10	(50)10	0	(100)20	0	(100)20
P value		**05 .0>* 0.0477**		**No Significance**			
Age groups	**NO. of cases**	(100)2	0	(50)1	(50)1	0	(100)2
20-29	**2**						
30-39	**11**	(100)11	0	0	(100)11	(9.1)1	(9 .90)10
40-49	**15**	(80)12	(20)3	(20)3	(80)12	(13.33)2	(86.66)13
50-50	**15**	(93.33)14	(6.66)1	(6.66)1	(93.33)14	(0)0	(100)15
60-70	**12**	(91.66)11	(8.33)1	(25)3	(75)9	(16.66)2	(83.33)10
P value		**No Significance**					
Lymph node status	**NO. of cases**	(77.77)7	(22.22)2	(22.22)2	(77.77)7	0	(100)9
Negative	**9**						
Few	**19**	(94.7)18	(5.2)1	(5.2) 1	(94.7)18	(5.2)1	(94.7)18
Multiple	**27**	(92.6)25	(7.4)2	(18.5)5	(81.4)22	(14.8)4	(85.2)23
P value		05 .0>					
Tumour size/cm	**NO. of cases**	(78.5)11	(21.42)3	(14.2)2	(85.7)12	(21.4)3	(78.5)11
1.0-1.9	**14**						
2-2.9	**19**	(7 .94)18	(5.2)1	(26.3)5	(73.68)14	0	(100)19
3-3.9	**18**	(94.44)17	(5.55)1	(5.55)1	(94.44)17	(5.55)1	(94.44)17
4-4.9	**4**	(100)4	0	0	(100)4	(25)1	(75)3

4. Discussion

The chances of breast cancer treatment and recovery can be improved by cancer early detection. Although detecting of breast cancer is highly effective, but to date it's still has significant limitations in asymptomatic patients, which in turn reflect the requirement of more sensitive, specific, convenient, accurate, and objective detection methods [15]. There were many attempts that based on identifying of specific antigenic markers that can be used as abiomarkers for breast cancer detection, however, the studies revealed that the combined use of those biomarkers with the available clinical information is still insufficient for early cancer diagnosis, predicting outcomes, and for guiding cancer therapeutic decisions. The previous results confirmed the necessity for the development of innovative diagnostic and prognostic markers that can effectively used for the management of human cancers such as tumour-associated antigens (TAAs) and their autoantibodies [16,17].

The present study examined the possibility of detecting mRNA of three tumour associated antigens (CA9, WT1, and PRAME) in peripheral blood of breast cancer patients using qRT-PCR technique. The present study showed that the percentage of CA9-positive breast cancer samples 50(91%) was significantly higher comparing with the percentage of CA9-negative breast cancer samples 5(9%), while for the other two genes the percentage of negative breast cancer samples was significantly higher comparing with the percentage of WT1-positive and PRAME-positive samples [8(14.54%),5(9.09%)] respectively. The present study results have some similarity to that reported by other studies includingChiaet alwho detected the expression of CA9in 49 (48%) of 103 cases with invasive breast carcinoma [18], Eom et al. who found that 191 cases (60.8%) of 314 cases with invasive breast carcinoma showed CA9 expression in tumour cells[19]. On the other hand, the present study results were different from results that reported by Trastour et al. that detected CA9 positive immunoreactivity only in 38(29%) of 132 patients with invasive breast carcinoma using immunohistochemistery technique[20].

For WT1 genethe present study results incompatible with most previous studies that detected mRNA expression of this gene in most of their samples, Loebet al. reported that WT1 expression was easily detectable in 27(87%) of 31 primary breast carcinomas using Western blotting technique[21]. Gillmore et al. who detected that WT1 was overexpressed in approximately)90%(of breast cancers samples[22], and Camc et al. who investigated WT1 mAb staining in 32(48.4%) of 66 samples with breast cancer using immunohistochemistery technique[23].

For PRAME gene Epping et al. showed that all breast cancer samples were PRAME-positive, but the highest proportion of those samples 197 samples (67%) expressed low levels of gene[24], Doolan et al.reported that PRAME mRNA was detected in)53%(of tumour specimens and (37%) of normal breast

specimens[25].In correlation to the clinicopathological features (tumour size and lymph node status) the results of the present study showed that there was statistically significant association ($p < 0.05$) of genes expression with lymph node status since the highest percentage of positive samples 25(50%), 5(60%) and 4(80%) for CA9, WT1 and PRAME genes respectively, were multiple for lymph node status. The analysis of the relationship between genes expression and tum our size demonstrated that there was statistically no significant association of genes expression with increasing of tum our size since the highest percentage of positive samples for CA9 18(36%) and WT1 5(62.5%) genes accossiated with tum our size 2.0-2.9 cm, and with tum our size 1.0-1.9 cm. for PRAME gene 3(60%).Several studies observed different results, Span et al. reported that CA9 levels did not differ statistically significant with age, nodal status, menopausal status, tum our size, type of surgery, radiotherapy or adjuvant systemic treatment [26]. Camc et al. showed a significant correlation between WT1 mAb staining and tumour grade, stage, and lymph node status [23]. Epping et al. demonstrated that the lymph node status of patients was not directly associated with PRAME [24].Doolan et al.indicated that expression of PRAME associated significantly with relapse-free survival, tumour grade and size, and lymph node status[25].Our study demonstrated that there was no expression of WT1 and PRAME genes in most of breast cancer samples (85.5% and 90.9%(for WT1 and PRAME respectively). These results may be due to facts that the exact function of WT1 and PRAME in the breast cancer tumourogenesis remains controversial. Some of the previous studies demonstrated that WT1 was strongly expressed in breast cancer, while other studies provide the evidences that WT1 have a tumour suppressor role in the tumourogenesis of breast cancer. For example Zhang et al. reported the association between the transformation of MDA-MB-231 phenotypes and constitutive expression of WT1 in breast cancer cells, which supporting the thought of suppressor functions of WT1 in breast cancer tumourigenesis[27]. However, Loeb et al. demonstrated the strongly expression of WT1 in primary carcinoma but not in normal breast epithelium, leading to the conclusion that the WT1 may not have a tumour suppressor role in the tumourigenesis of breast cancer[28].Zapata-Benavides et al.provide evidences supporting the growth-promoting role of WT1[30].Alteration of the PRAME gene expression have been also reported in different types of cancer including breast cancer, Sun et al.demonstrates that PRAME functions as a tumour suppressor in breast cancer[31]. Huang et al. found that PRAME expression is down-regulated in lung adenocarcinomas leading to the suggestion that PRAME has inhibitory roles in lung cancer[32]. Wadelin et al. reported that the precise molecular functions of PRAME and its role in oncogenesis remain to be add ressed [33]. In summary, our results demonstrated that CA9 gene can be a

useful tool for discriminating malignant breast tumours from non-malignant ones since gene expression was elevated in breast cancer samples, compare with healthy control and benign tumour, and the results may also indicate the diagnostic and prognostic values for this gene. On the other h and further studies WT1 and PRAMEmolecular mechanisms are required that may provide important information about the function and regulating pathways of these tow genes in tumourogenesis of breast cancer.

Acknowledgments

The authors thanks Dr. Khalid Tobal and the members of the molecular oncology unit/ Guys hospital / London, for their cooperation in part of the study related with molecular analysis. The authors would like to thank alsoDr. Mohammed Ghanim (Baghdad Medical City) for his support and assistance.

REFERENCES

[1] Winter J., Jung S., Keller S., Gregory R.I. and Diederichs S. Many roads to maturity: microRNA biogenesis pathways and their regulation. Nat Cell Biol.; 11:228-34, (2009).

[2] Jäger E, Jäger D and Knuth A. Antigen-specific immunotherapy and cancer vaccines. Int J Cancer 106: 817-820, (2003).

[3] Heber W, Sharma S and Chang HR. Development and preclinical evaluation of a Bacillus Calmette-Guerin-MUC1-based novel breast cancer vaccine. Cancer Res; 63:1280–1287, (2003).

[4] Stauss HJ, Thomas S, Cesco-Gaspere M, Hart DP, Xue SA, Holler A, King J, Wright G, Perro M and Pospori C. WT1-specific T cell receptor gene therapy: improving TCR function in transduced T cells. Blood Cells Mol Dis;40: 113–116, (2008).

[5] Pelletier J, Bruening W, Li FP, Haber DA, Glaser T and Housman DE.WT1 mutations contribute to abnormal genital system development and hereditary Wilms' tumour. Nature; 353:431–434, (1991).

[6] Wagner KD, Wagner N, Schley G, Theres H and Scholz H. The Wilms' tumour suppressor Wt1 encodes a transcriptional activator of the class IV POU-domain factor Pou4f2 (Brn-3b). Gene; 305:217–223, (2003).

[7] Algar E: A review of the Wilms' tumour 1 gene (WT1) and its role in hematopoiesis and leukemia.J Hematother Stem Cell Res;11:589–599, (2002).

[8] Ikeda H, Lethe B, Lehmann F, van Baren N, Baurain JF, de Smet C, Chambost H, Vitale M, Moretta A, Boon T and Coulie PG. Characterization of an antigen that is recognized on a melanoma showing partial HLA loss by CTL expressing an NK inhibitory receptor. Immunity 6: 199–208, (1997).

[9] Epping MT and Bernards R. A causal role for the human tumour antigen preferentially expressed antigen of melanoma in cancer. Cancer Res 66:10639–10642, (2006).

[10] Oberthuer A, Hero B, Spitz R, Berthold F and Fischer M. The tumourassociated antigen PRAME is universally expressed in high-stage neuroblastoma and associated with poor outcome. Clin Cancer Res 10:4307– 4313, (2004).

[11] Thiry A, Dogné JM, Masereel B and Supuran CT. Targeting tumour-associated carbonic anhydrase IX in cancer therapy. Trends Pharmacol Sci; 27:566–73, (2006).

[12] Wykoff CC, Beasley NJ and Watson PH. Hypoxia-inducible expression of tumour-associated carbonic anhydrases. Cancer Res.,60:7075–83, (2000).

[13] Driessen A, Landuyt W and Pastorekova S. Expression of carbonic anhydrase IX (CA IX), a hypoxia-related protein, rather than vascular

endothelial growth factor (VEGF), a pro-angiogenic factor, correlates with an extremely poor prognosis in esophageal and gastric adenocarcinomas. Ann Surg; 243:334–40, (2006).

[14] Grabmaier K, Vissers JL and De Weijert MC. Molecular cloning and immunogenicity of renal cell carcinoma-associated antigen G250. Int J Cancer; 85:865–70, (2000).

[15] Praveen Sharma P., Sahni N.S, Robert Tibshirani R., Per Skaane P. Early detection of breast cancer based on gene-expression patterns in peripheral blood cells. Breast Cancer Research, 57: R634, (2005).

[16] Sorlie, T. Charles M. Peroua, Robert Tibshiranie, Turid Aasf, Stephanie Geislerg, Hilde Johnsenb, Trevor Hastiee,Michael B. Eisenh, Matt van de Rijni, Stefanie S. Jeffreyj, Thor Thorsenk, Hanne Quistl, John C. Matesec,Patrick O. Brownm, David Botsteinc, Per Eystein Lønningg, and Anne-Lise Børresen-Dale. Gene expression patterns of breast carcinomas distinguish tumour subclasses with clinical implications. Proc. Natl Acad. Sci. USA 98, 10869-10874, (2001).

[17] van 't Veer L.J., Dai H., van de Vijver M.J., Yudong D and He Y.D.Gene expression profiling predicts clinical outcome of breast cancer. Nature 415, 530-536, (2001).

[18] Chia S.K., Wykoff C.C., Watson P.H., Han C., Leek R.D., Pastorek J., Gatter K.C., Ratcliffe P. and Harris A.L. Prognostic significance of a novel hypoxia-regulated marker, carbonic anhydrase IX, in invasive breast carcinoma. J Clin Oncol., 15;19(16):3660-8, (2001).

[19] Eom K-Y, Jang M.H., Park S.Y., Kang E.Y., Kim S.W., Kim J.H., Kim J-S. and Kim I.A. The Expression of Carbonic Anhydrase (CA) IX/XII and Lymph Node Metastasis in Early Breast Cancer. Cancer Res Treat.; 48(1):125-132, (2016).

[20] Cynthia Trastour, Emmanuel Benizri, Francette Ettore, Alain Ramaioli, Emmanuel Chamorey, Jacques Pouyssegur and Edurne Berra. HIF-1a and CA IX staining in invasive breast carcinomas: Prognosis and treatment outcome. Int. J. Cancer: 120, 1451–1458, (2007).

[21] Loeb D.M., Evron E.,Patel C.B., Sharma P.M., Niranjan B., Buluwela L., Weitzman S.A., Korz D. and Sukumar S. Wilms' Tumour Suppressor Gene (WT1) Is Expressed in Primary Breast Tumours Despite Tumour-specific Promoter Methylation. Cancer Research 61, 921–925, (2001).

[22] Gillmore R, Xue SA, Holler A, Kaeda J, Hadjiminas D and Healy V. Detection of Wilms' tumour antigen--specific CTL in tumour-draining lymph nodes of patients with early breast cancer. Clin Cancer Res; 12(1):34-42, (2006).

[23] Camc C. , Kalender M.E. , Paydaş S. , Sevinç A. , Zorludemir S. and Suner A. Prognostic significance of Wilms Tumour 1 (WT1) protein expression in breast cancer. Gaziantep Med J;17(2): 67-72, (2011).

[24] Epping M.T., Hart A.A.M., AM Glas A.M., Krijgsman O. and Bernards R. PRAME expression and clinical outcome of breast cancer. British Journal of Cancer: 99, 398 – 403 ,(2008).

[25] Doolan P., Clynes M., Kennedy S., Mehta J.P., Crown J. and O'Driscoll L. Prevalence and prognostic and predictive relevance of PRAME in breast cancer.Breast Cancer Research and Treatment.109 (2):359–365, (2008).

[26] Span P.N., Bussink J., Manders P. Beex L. and Sweep C.G. Carbonic anhydrase-9 expression levels and prognosis in human breast cancer: association with treatment outcome. British Journal of Cancer 89: 271 – 276, . (2003).

[27] Zhang TF, Yu SQ, Guan LS and Wang ZY. Inhibition of breast cancer cell growth by the Wilms' tumour suppressor WT1 is associated with a destabilization of β-Catenin. Anticancer Res; 3:35785– 35874, (2003).

[28] Loeb DM, Evron E, Patel CB, Sharma PM, Niranjan B, Buluwela L, Weitzman SA, Korz D and Sukumar S. Wilms tumour suppressor (WT1)

is expressed in primary breast tumours despite tumour-specific promoter methylation. Cancer Res; 76:921–925, (2001).

[29] Miyoshi Y, Ando A, Egawa C, Taguchi T, Tamaki Y, Tamaki H, Sugiyama H and Noguchi S. High expression of Wilms' tumour suppressor gene predicts poor prognosis in breast cancer patients. Clin Cancer Res; 8:1167–1171, (2002).

[30] Zapata-Benavides P, Tuna M, Lopez-Berestein G and Tari AM. Downregulation of Wilms' tumour 1 protein inhibits breast cancer proliferation. Biochem Biophys Res Commun; 295:784–790, (2002).

[31] Sun Z, Wu Z, Zhang F, Guo Q, Li L, Li K, Chen H, Zhao J, Song D, Huang Q, Li L and Xiao J. PRAME is critical for breast cancer growth and metastasis. Gene.12: S0378-1119(16)30732-6, (2016).

[32] Huang Q, Li L, Lin Z, Xu W, Han S, Zhao C, Li L, Cao W, Yang X, Wei H and Xiao J. Identification of Preferentially Expressed Antigen of Melanoma as a Potential Tumour Suppressor in Lung Adenocarcinoma. Med Sci Monit. 31; 22:1837-42, (2016).

[33] Frances Wadelin, Joel Fulton, Paul A McEwan, Keith A Spriggs, Jonas Emsley and David M Heery. Leucine-rich repeat protein PRAME: expression, potential functions and clinical implications for leukaemia. Mol Cancer; 9: 226, (2010).

Asymptotic Fitting Shadowing Property

Iftichar M.T. AL-Shara`a and Raad Safah AL- Joboury
Department of Mathematic, College of Education for Pure Sciences, University of Babylon, Iraq.

Received Date: 16 / 8 / 2015
Accepted Date: 10 / 2 / 2017

الخلاصة

ليكن(M,d) فضاء متري وليكن ϕ دالة من الفضاء المتري (M,d) الى نفسه وتحقق خاصية مقارب التظليل المناسب (Asymptotic Fitting Shadowing Property) (AFSB) فأن النتائج التالية متحققة: ϕ^m تمتلك خاصيـة مقـارب التظـليل المنـاسب لكل $m\in N$، وخاصية سلسلة متعدية (chain transitive)، وايضاً، اذا كانت ψ تمتلك حالة مقـارب التظـليل المنـاسب فأن$\phi\times\psi$ تمتلك خاصية مقـارب التظـليل المنـاسب. بالإضافة الى نتائج اخرى حول خاصية مقارب التظليل المناسب.

الكلمات المفتاحية

فضاء متري، خاصية مقارب التظـليل المناسب، سلسلة متعدية.

Abstract

Let (M,d) be a metric space, ϕ be a map from a metric space (M,d) to itself and satisfy the Asymptotic Fitting Shadowing property(AFSP) then these results are satisfy: For every $m\in N,\phi^m$ has asymptotic fitting shadowing property and ϕ is chain transitive, also, if ψ has the asymptotic fitting shadowing property then $\phi\times\psi$ has the asymptotic fitting shadowing property. In addition to the other results on the asymptotic fitting shadowing property.

Keywords

Metric space, Asymptotic Fitting Shadowing property, chain transitive.

1. Introduction

In dynamical systems the pseudo-orbit tracing property (POTP) is the most main ideas [1]. Blank defined the average shadowing property in studyingchaotic dynamical systems [2]. Yang conversed the relationship between topological ergodicity and the POTP for maps, and proved that the POTP with a chain transitive map is topologically ergodic [3].

Guo and Gu conversed the relationship topological ergodicity with the average shadowing property (ASP) for flows, and proved that the ASP with

Gu introduced the notion of the AASP, which is less power than the asymptotic POTP in the shadowing method, and achieved the relation transitivity with the AASP. He also proved for a compact metric space M, if a map ϕ has the AASP and continues on M, then ϕ is chain transitive[5].

In this paper we try to discuss the concept of the Asymptotic Fitting Shadowing property (AFSP) is topologically ergodic, We get that asymptotic fitting shadowing case with Lyapunov stable map from a compact metric space to itself, is topologically ergodic but not topologically weakly mixing, it is not also topologically mixing.

2. Preliminaries

Let N symbolize the set of natural numbers and Z symbolize the set of integer numbers, Z_+ symbolize the set of nonnegative integer numbers. In this section, we introduce some definitions that we will use in this search, we recall some fundamental definitions. Let (M,d) be a metric space and $\phi: M\to M$ is a continuous map. For every positive integer m , We define ϕ^m inductively by $\phi^m = \phi\circ\phi^{m-1}$ and $\phi^{-m} = \phi^{-1}\circ\phi^{-m+1}$, If A and B are two nonempty open subsets of M after that we let $N(A\cap B) = \{m\in Z_+ : \phi^m(A)\cap B\neq\emptyset\}$, for $A,B\subset M$, $\omega\in M$, we write $N(A, B)=\{ m\in Z_+ : A\cap\phi^{-m}(B)\neq\emptyset \}$,

$N(\omega,B)=\{n\in Z_+ : \phi^m(\omega)\in B\}$. Symbolize by $N_\varepsilon(B)$ the open ball with center ω and radius ε.

2.1. Definition

[6] Let $\phi: M\to M$ be a map and (M,d) be a compact metric space. A sequence $\{\omega_i\}_{i\in Z}$ is named orbit of ϕ if $\forall i\in Z$ we have $\omega_{i+1}=\phi(\omega_i)$ and we called it a $\propto$ - pseudo-orbit of ϕ $\forall i\in Z$, we have $d(\phi(\omega_i),\omega_{i+1}) \leq \propto$. The map ϕ is reminded to have the shadowing property, if $\forall \varepsilon>0$, $\exists \propto >0$, so $\forall\delta$ - pseudoorbit $\{\omega_i\}_{i\in Z}$ is ε - shadowed by the orbit $\{\phi^i(\omega), i\in Z\}$, $\exists z\in M$, it means, $\forall i\in Z$ we have $d(\phi^i(z),\omega_i)\leq\varepsilon$.

2.2. Definition

[6] Let $\{\omega_i\}i=0^\infty$ be a sequence in M, if $\exists$ $\alpha>0$ and a positive integer $N=N(\alpha)$ such that $\forall m\in N$ and $n\geq N$, we have

$$\frac{1}{n}\sum_{i=0}^{n-1} d(\phi(\omega_{i+m}),\ \omega_{i+m+1}) < \propto.$$

then a sequence $\{\omega_i\}_{i=0}^{\infty}$ is named a $\propto$ - average pseudo orbit of ϕ .

A map ϕ is reminded to have average shadowing property, if $\forall \varepsilon>0$, $\exists \propto >0$, so $\forall \propto$ - average pseudo orbit $\{\omega_i\}_{i\in Z}$ is ε - shadowed in average by the point $y\in M$, it means ,

$$\limsup_{n\to\infty} \frac{1}{n}\sum_{i=0}^{n-1} d(\phi^i(y), \omega_i) < \varepsilon.$$

We introduce a new definition as the following:

2.3. Definition

Let $\{\omega_i\}_{i=0}^{\infty}$ be a sequence in M, if ∃ α>0 and a positive integer N=N(α) such that ∀m∈N and n≥N, we have

$$\sum_{i=0}^{n-1} d(\phi(\omega_{i+m}), \omega_{i+m+1}) < \alpha .$$

then $\{\omega_i\}_{i=0}^{\infty}$ is named a α - fitting pseudo-orbit of ϕ.

A map ϕ is reminded to have fitting shadowing property (FSP) if ∀ε>0, ∃ α>0 so ∀ α - fitting pseudo orbit is ε - shadowed in fitting by the point y∈M , it means

$$\limsup_{n\to\infty} \sum_{i=0}^{n-1} d(\phi^i(y), \omega_i) < \varepsilon.$$

2.4. Definition

Let $\{\omega_i\}_{i=0}^{\infty}$ be a sequence in M is named the asymptotic

fitting pseudo-orbit of ϕ. if

$$\lim_{n\to\infty} \sum_{i=0}^{n-1} d(\phi (\omega_i), \omega_{i+1}) = 0.$$

A sequence $\{\omega_i\}_{i=0}^{\infty}$ in M is reminded to be asymptotically shadowed in fitting by the point y ∈ M if

$$\lim_{n\to\infty} \sum_{i=0}^{n-1} d (\phi^i(y), \omega_i) = 0$$

We say that ϕ has asymptotic fitting shadowing property (AFSP) if any asymptotic fitting pseudo-orbit of ϕ is asymptotically shadowed in fitting by the point z ∈ M.

2.5. Definition

[7] A map $\phi : Z+ \times (0, \varepsilon_0] \longrightarrow N$ such that ε_0>0 , then ϕ is called mistake map if ∀ ε∈ (0, ε_0] and ∀ m∈Z +, we have ϕ (m ,ε) ≤ ϕ (m+1 ,ε) and

$$\lim_{n\to\infty} \frac{\phi (m , \varepsilon)}{m} = 0 .$$

Supposed a mistake map ϕ , if ε>ε_0 , then we know ϕ (m ,ε)= ϕ (m ,ε_0) .

2.6. Definition

[7] A continuous map ϕ:M→M has the almost specification property if there is a mistake map $\phi^{\vee}$ and a function $k_{\phi^{\vee}}$:(0, ∞)⟶N so for any m≥1 , any ε_1 ,……,ε_m >0 any point y_1 ,…,y_m ∈M, and any integers

$n_1 > k_{\phi^{\vee}}(\varepsilon_1)$,……..,$n_m > k_{\phi^{\vee}}(\varepsilon_m)$ setting n_0=0 and $l_j=\sum_{(s=0)}^{(j-1)} n_s$,for j=1,…,m .We can find a point z∈M so for each j=1,…,m, we have $\phi^{\gamma(l_j)}(z)\in B_{nj}$ (ϕ : z_j ,ε_j).

2.7. Definition

[6] Let $\{\omega_i\}_{i=0}^{\infty}$ be a sequence in M is named asymptotic average pseudo-orbit of ϕ if

$$\lim_{n\to\infty} \frac{1}{n}\sum_{i=0}^{n-1} d(\phi (\omega_i), \omega_{i+1}) = 0.$$

A sequence $\{\omega_i\}_{i=0}^{\infty}$ in M is called an asymptotically shadowed in average by the point y ∈ M if

$$\lim_{n\to\infty} \frac{1}{n}\sum_{i=0}^{n-1} d(\phi^i(y), \omega_i) = 0$$

We say that ϕ has asymptotic average shadowing case if any asymptotic average pseudo-orbit of ϕ is asymptotically shadowed in average by the point $y \in M$.

2.8. Definition

[8] A map ϕ is called topologically transitive if for A, B$\subset$ M where A , B$\neq\emptyset$,N(A$\cap$B)$\neq\emptyset$. y$\in$M is named a transitive point if orbit y is dense in M.

2.9. Definition

[9] Let ϕ:M$\to$M be a continuous map, (M,d) be a compact metric space. For $\propto \in R$, so $\propto > 0$, a sequence $\{y_i\}_{i=0}^{\infty}$ in M is named an δ - chain if $d(\phi(y_i), y_{i+1}) \leq \propto$, $\forall i=0,1,2,\ldots$, the map ϕ is said to be chain transitive if $\forall$ z,y$\in$M and each $\propto > 0$, there is a finite $\propto$-chain $\{y_0,y_1,\ldots,y_n\}$ such that $y_0=z$ and $y_n=y$.

2.10. Definition

[8] A map ϕ is called topologically mixing A, B, $\exists m\in Z+$, $N(A\cap B) \supset \{m, m+1, \ldots\}$A map is named topologically weak mixing if $\phi\times\phi$ topologically transitive.

2.11. Definition

[8] A map ϕ is named chain mixing if for all z,y$\in$M and every $\delta>0$, there exists N$\in$N such that for any n$\geq$N there is δ - chain from x to y with length n.

2.12. Definition

[10] Let ϕ:M$\to$M be a continuous map and Let (M,d) be a compact metric space with metric d . We say that ϕ be topologically ergodic if for any A, B$\subset$M and A, B are open sets, A, B$\neq\emptyset$, then N(A ,B) has positive upper density, that is,

$$\bar{D}(N(A,B)) = \limsup_{m\to\infty} \frac{\text{Card}\,(N(A,B)\cap\{0,1,\ldots,m-1\})}{m} > 0\,.$$

q$\subset Z_+$ is called syndetic if $\exists$N$\in$N, where [m,m+N]$\cap$q$\neq\emptyset$ for every n$\in$N. ϕ is called strongly ergodic if for any pair of nonempty open subset A, B$\subset$M, N(A ,B) is syndetic set. If $\forall k\in N$, ϕ^k is strongly ergodic, we call ϕ totally strongly ergodic. We observe that

totally strongly ergodic $\Longrightarrow$ strongly ergodic $\Longrightarrow$ topologically ergodic $\Longrightarrow$

topologically transitivity.

If each y$\in$M is transitive point, then we say ϕ is minimal. y$\in$M is said to be minimal, if for every neighborhood B of y, N(y,B) is syndetic. Let AP(ϕ) symbolize of the set minimal point of ϕ.

2.13. Definition

[10] Let (M,d) be a compact metric space with metric d and ϕ:M$\to$M be a map, a point y$\in$M is named stable point of ϕ if $\forall$ $\varepsilon>0$,$\exists$ $\gamma>0$, where $d(\phi^n(y), \phi^n(\omega)) < \varepsilon$ for all $\omega\in M$ with $d(y,\omega) < \gamma$ and $\forall$ n$\in Z_+$. A map ϕ is named Lyapunov stable if each point of M is stable point of ϕ.

3.Main result and proof.

Let ϕ:M$\to$M be a map and (M,d) be a metric space. we prove some results of the asymptotic fitting shadowing property, also we show that if ϕ has the asymptotic fitting

shadowing property then ϕ^m has the asymptotic fitting shadowing property for every positive integer m.

We also prove if (M,d) be a compact and a map ϕ has the asymptotic fitting shadowing property on M, then ϕ is chain transitive. We get that a Lyapunov stable map with the AFSP from a compact metric space onto itself is topologically ergodic.

3.1. Lemma

[7] If $\{a_n\}_{n=0}^{\infty}$ be a bounded sequence of non-negative real numbers, then

the following conditions are equivalent:

(1) $\lim_{n\to\infty} \frac{1}{n}\sum_{i=0}^{n-1} a_n = 0$,

(2) There is a subset $J \subset N$ of density zero, that is,

$\lim_{n\to\infty} \frac{\mathbf{Card}(J \cap \{0,1,2,\ldots,n-1\})}{n} = 0$ such that $\lim_{n\notin J} a_n = 0$.

3.2. Theorem

Let ϕ:M→M be a map and (M,d) be a compact metric space. If $\{y_k\}_{k=0}^{\infty}$ is an asymptotic fitting pseudo-orbit of ϕ and ϕ is chain mixing, then there is an asymptotic pseudoorbit $\{z_k\}_{k=0}^{\infty}$ of ϕ so the set $\{k: y_k \neq z_k\}$

has asymptotic density zero.

proof: By chain mixing of ϕ:M→M, for every j there exists an integer L_j so that for any points y,z∈M there exists a $1/2^j$ - chain of length L_j+1 from y to z. we may suppose that L_j+1 is a multiple of L_j for every j. Assume that $\{y_k\}_{k=0}^{\infty}$ is an asymptotic fitting pseudo-orbit. By Lemma 3.1 there exists a set k so d(k)=0 and $(\lim)_{\top}(k\notin K)\ d(\phi(y_i), y_{i+1})=0$. (3.1)

Since d(k)=0, there exists a strictly increasing sequence $\{n_j\}_{j=1}^{\infty}$ such that for every j we have L_j+1 divides n_j and $L_j \cdot \text{card}(k \mid n) < 1/2^j$, for every $n>n_k$. By (3.1) we may assume that if $k\notin k$ and $k\geq n_j$ then $d(\phi(y_i), y_{i+1}) < 1/2^j$. Now we define a set k' and sequence $\{z_k\}_{(k\notin k')}$ in the following way: for every j and for every t such that $[sL_j, (t+1)L_j) \subset [n_j, n_{j+1})$ if $k \cap [sL_j, (t+1)L_j) \neq \emptyset$ then we include the set $[tL_j, (t+1)L_j) \cap N$ in k'. We define $\{z_k\}_{(k=tLj)}^{((t+1)L\_j)}$ as a $1/2^j$ - chain from to $y_{((t+1)Lj)}$ of length L_j+1. Note that $z\_(tL_j) = y_{(tLj)}$ and $z_{((t+1)Lj)} = y_{((t+1)Lj)}$. Let k' and $\{z_k\}_{(k\in k')}$ be obtained by the above procedure . For $k\notin k$ we put $y_k = x_k$. First note that for $k\geq n_j$ we have $(d(\phi(z_k), z_{k+1}) < 1)/2^k$ and hence $\{z_k\}_{k=0}^{\infty}$ is an asymptotic pseudo- orbit. Furthermore, if we fix any $n> n_1$ then there is $n_j < n \leq n_{j+1}$ so j>0 and

$$\text{card}(k' \mid n) = \text{card}(k' \mid n_1) + \sum_{(t=1)}^{j} \text{card}((k' \cap [n_t, n_{t+1}) \mid n)$$

$$\leq \text{card}(k' \mid n_1) + \sum_{s=1}^{k} \text{card}\ L_t((k \cap [n_t, n_{t+1}) \mid n)$$

$$\leq \text{card}(k' \mid n1) + L_j\ \text{card}(k \mid n) < \text{card}(k' \mid n_1) + 1/2^j$$

This shows that d(k')=0.

The proof is completed by noting that $\{k: y_k \neq z_{(k)}\} \subset k'$. ■

3.3. Lemma

[7] Let ϕ:M⟶M be continuous map and (M,d) be a compact metric space, If ϕ has the almost specification property and surjective, then ϕ is chain mixing.

3.4. Theorem

[7] Let ϕ:M⟶M be surjective map and (M,d) be a compact metric space, if ϕ has almost specification property, then ϕ has the asymptotically average shadowing property.

3.5. Remark

The Theorem 3.4 does not give the asymptotic fitting shadowing property ϕ because: let $\{y_i\}_{i=0}^{\infty}$ be an asymptotic fitting pseudo-orbit of ϕ. By Lemma 3.3 is chain mixing, and therefore we may use Theorem 3.2 to obtain an asymptotic pseudo-orbit of ϕ, denoted $\{z_i\}_{i=0}^{\infty}$,such that d({i:$y_i \neq z_i$})=0.

So we cannot to show that $\{z_i\}_{i=0}^{\infty}$ can be asymptotically shadowed on fitting by point ω ∈Y, then ϕ does not satisfy the asymptotically fitting shadowing property. ■

3.6. Proposition

Let ϕ:M⟶M be continuous map and (M,d) be a compact metric space, if for every positive integer m, ϕ has the asymptotic fitting shadowing property then ϕ^m has the asymptotic fitting shadowing property .

Proof:

Suppose ϕ has the asymptotic fitting shadowing property and m is positive integer. Let $\{y_i\}_{i=0}^{\infty}$ be an asymptotic fitting pseudo- orbit of ϕ^m, that is,

$$\lim_{n\to\infty} \sum_{i=0}^{n-1} d(\phi^k(y_i), y_{i+1}) = 0. \qquad (3.2)$$

Let $z_{tm+k} = \phi^m(y_i)$, for all $0 \le k < m$ and all $t \ge 0$.

Since $$\lim_{n\to\infty} \sum_{i=0}^{n-1} d(\phi(z_i), z_{i+1}) \le \frac{n}{tm+k} \lim_{n\to\infty} \sum_{i=0}^{t} d(\phi^m(y_i), y_{i+1}),$$

we get from (3.2)that $$\lim_{n\to\infty} \sum_{i=0}^{n-1} d(\phi(z_i), z_{i+1}) = 0$$

That is , the sequence {z_i }_(i=0)^∞ is an asymptotic fitting pseudo orbit of ϕ. So , there is point ω∈Ysuch that

$$\lim_{n\to\infty} \sum_{i=0}^{n-1} d(\phi^i(\omega), z_i) = 0, \qquad (3.3)$$

note that $$\lim_{n\to\infty} \sum_{i=0}^{t-1} d(\phi^{mi}(\omega), y_i) \le \lim_{n\to\infty} \sum_{s=0}^{t-1} \sum_{k=0}^{m-1} d(\phi^{sm+k}(\omega), z_{sm+k})$$

$$= \lim_{n\to\infty} \sum_{i=0}^{tm-1} d(\phi^i(\omega), z_i).$$

From (3.3)that $$\lim_{n\to\infty} \sum_{i=0}^{t-1} d(\phi^{mi}(\omega), y_i) = 0.$$

Thus ϕ^m has the asymptotic fitting shadowing property . ■

3.7. Remark

There are difference between the asymptotic average shadowing and the asymptotic fitting shadowing case for example : if ϕ^m has the asymptotic average shadowing for some m∈Z_+, then so does ϕ, but if ϕ^m has the asymptotic fitting shadowing property for some m∈Z_+, then does not ϕ.

3.8. Theorem

Let ϕ:M⟶M be continuous map and (M,d) be a compact metric space, if ϕ has the asymptotic fitting shadowing property then ϕ is chain transitive.

Proof:

Assume that y, z∈M such that y ≠z and γ>0. It is enough to prove that exists a γ- chain from y to z.

we defined a sequence $\{U_0\}_{i=0}^{\infty}$ as follows.

Let U_0= y, z= U_1

U_2=y, z= U_3

U_4=y, ϕ (y), z-1, z= U_7

…….

U_2^m =y, ϕ (y),…,$ϕ^{2^{m-1}-1}$ (y), z-2^{m-1}+1,…,z-1, z= $U_{2^{m+1}-1}$

……..

where ϕ (z-k)=z-k+1 for each k>0 and z_0=z. It is clear that for $2^m \le n < 2^{m-1}$, and

$$\sum_{i=0}^{n-1} d(\phi(\mathcal{U}_i), \mathcal{U}_{i+1}) < \frac{2(m+1)\times D}{2^m} \quad ,$$

where D is the diameter of M , that is , D= max {d(y ,z) :y,z∈Y} .

Thus $\lim_{n\to\infty} \sum_{i=0}^{n-1} d(\phi(\mathcal{U}_i), \mathcal{U}_{i+1}) = 0$.

It means $\{y_i\}_{i=0}^{\infty}$ is an asymptotic fitting pseudo-orbit of ϕ. Since ϕ has the asymptotic fitting shadowing property , there is a point ω in M so,

$$\lim_{n\to\infty} \sum_{i=0}^{n-1} d(\phi^i(\omega), \mathcal{U}_i) = 0 \qquad (3.4)$$

Since γ>0 and ϕ is continuous map, ∃ μ∈(0,γ) such that d(s,t)<μ

implies d(ϕ (s), ϕ(t))<γ for all s,t∈M .

Claim. (1) There is no limits of integers number k>0 , so

U_{nk}∈{y, ϕ(y),…,$ϕ^{2^{k-1}-1}$ (y)} and d($ϕ^{nk}$ (ω), U_{nk}<μ .

(2) There is no limits integers number r>0 , so U_{nr}∈{$z_{-2^{r+1}}$, …, z-1, z} and d($ϕ^{nr}$ (ω), U_{nr})<μ .

Proof (1) Assume on conversely that ∃N∈Z_+, so ∀m∈Z, m>N, so that U_i∈{y, ϕ(y),…,$ϕ^{2^{m-1}}$ (y)}, it is got that d($ϕ^i$ (ω), U_i)>μ. Then it would be got that

$$\lim_{n\to\infty} \inf \sum_{i=0}^{n-1} d(\phi^i(\omega), \mathcal{U}_i) \ge \frac{\mu}{2}$$

This contradiction with (3 .4) and the proof (1) is complete.

Proof (2) is similar to the Proof (1).

From this Claim , we pick ⟦ k⟧_0 ⟦ ,r⟧_0 are positive integers and so

$n_{k_0} > n_{r_0}$ and

$U_{n_{k_0}}$∈{y, ϕ(y),…,$ϕ^{2k_0-1}$ (y)} and d($ϕ^{n_{k_0}}$ (ω), $U_{n_{k_0}}$ <μ .

$U_{n_{r_0}}$∈{$z_{-2r_{0+1}}$,…, z-1, z } and d($ϕ^{n_{r_0}}$ (ω),$U_{n_{r_0}}$ <μ

It may be assumed $U_{n_{k_0}}$ = g^{k_1} (x) for some k_1>0 ;

$U_{n_{r_0}}$ = y-r_1 for some r_1>0 .

That is, γ- chain from y to z:

y ,ϕ(y),…,$ϕ^{k_1}$ (y) = U_{nk_0}, $ϕ^{nk_0+1)}$ (ω), $ϕ^{nk_0+2}$(ω),…,$ϕ^{n_{r0}-1}$(ω),

$U_{n_{r0}}$ = z- r_1, z- r_1+1, …, z .

Thus, ϕ is chain transitive. ■

3.9. Proposition

Let ϕ:M⟶M and ψ:T⟶T be maps ,(M,d) and (T,d') be metric spaces,. Then, ϕ× ψ has the asymptotic fitting shadowing property if and only if ϕ and ψ have the asymptotic fitting shadowing property.

Proof: ⟸)

we choose the metric d'' on ϕ× ψ as following : For m=(m_1,t_1), t= (m_2, t_2) ∈ ϕ×ψ, d'' (m,t)= max {d(m_1, m_2), d' (t_1, t_2)}, Assume that ϕ and ψ have the asymptotic fitting shadowing property and $\{(m_i, t_i)\}_{i=0}^{\infty}$ be asymptotic fitting pseudo-orbit of ϕ× ψ , that is ,

$\lim_{n\to\infty} \sum_{i=0}^{n-1} d''((\phi\times\psi)(m_i,t_i),(m_{i+1},t_{i+1})) = 0$.(3.5)

It means

$$\lim_{n\to\infty}\sum_{i=0}^{n-1} d(\phi(m_i), m_{i+1}) = 0 \qquad (3.6)$$

$$\lim_{n\to\infty}\sum_{i=0}^{n-1} d(\psi(t_i), t_{i+1}) = 0,$$

such that $\{m_i\}_{i=0}^{\infty}$ and $\{t_i\}_{i=0}^{\infty}$ are asymptotic fitting pseudo orbit of ϕ and ψ ,respectively, thus there is $r_1, r_2 \in M$ such that

$$\lim_{n\to\infty}\sum_{i=0}^{n-1} d(\phi^i(r_1), m_i) = 0, \qquad (3.7)$$

$$\lim_{n\to\infty}\sum_{i=0}^{n-1} d(\psi^i(r_2), t_i) = 0. \qquad (3.8)$$

By Lemma (3.1) and (3. 7), $\exists J_0 \subset Z_+$ of zero density so

$$\lim_{j\to\infty} d(\phi^i(r_1), m_j) = 0 \qquad (3.9)$$

so $j \notin J_0$.Similarly, $\exists J_1 \subset Z_+$ of zero density so

$$\lim_{j\to\infty} d(\psi^i(r_2), t_j) = 0 \qquad (3.10)$$

so $j \notin J_1$. Let $J = J_0 \cap J_1$. Then, $J \subset Z_+$ subset of zero density and $\lim_{j\to\infty} d''((\phi\times\psi)^i(r_1,r_2),(m_j,t_j)) = 0$ (3.11)

so $j \notin J$. so that, by Lemma 3 .1 we have

$$\lim_{n\to\infty}\sum_{i=0}^{n-1} d''((\phi\times\psi)^i(r_1,r_2),(m_j,t_j)) = 0. \qquad (3.12)$$

Thus $\phi\times\psi$ has the asymptotic fitting shadowing property.

$\Longrightarrow$) Similarly ,we can show that if $\phi\times\psi$ has the asymptotic fitting shadowing property then ϕ and ψ have the asymptotic fitting shadowing property. ■

3.10. Theorem

Let $\phi: M\to M$ be a Lyapunov stable map and (M,d) be a compact metric space, If ϕ has the asymptotic fitting shadowing case, then ϕ is topologically ergodic.

Proof:

Let $S_1, S_2 \subset M$ and $S_1, S_2 \neq \emptyset$. We pick $m \in S_1$,$z \in S_2$ and $\varepsilon > 0$ such that $B(m,\varepsilon) \subset S_1$ and $B(z,\varepsilon) \subset S_2$. Since ϕ is Lyapunov stable and M is compact, $\exists \propto > 0$ so for any s, $t \in M, d(s,t) < \propto$ implies that $d(\phi^n(s), \phi^n(t)) < \varepsilon, \forall\, n \geq 0$.

Construct the sequence $\{u_i\}_{i=0}^{\infty}$ as shown:

$u_0 = m$, $z = u_1$

$u_2 = m$, $z = u_3$

$u_4 = m\text{-}1$,y ,z-1, $z = u_7$

$u_{2k} = m_{-2^{r-1}+1}, \ldots, m\text{-}2, m, z_{-2^{r-1}+1}, \ldots, z\text{-}2, z\text{-}1, z = u_{2^{r+1}-1}$

where $\phi(m_{-j}) = m_{-j+1}, \forall\, j > 0$, $z_0 = z$ and $\phi(z_l) = z_{-l+1} \forall\, l > 0$,

$z_0 = z$. It is clear for $2^r \leq n < 2^{r+1}$,

$$\sum_{i=0}^{n-1} d(\phi(u_i), u_{i+1}) < \frac{2(r+1)\times D}{2^r},$$

where $D = \max\{d(m,z): m,z \in M\}$ is the diameter of M. Hence

$\lim_{T}(n\to+\infty)\sum_{(i=0)}^{(n-1)} d(\phi(u_i), u_{(i+1)}) = 0$.

Hence $\{u_i\}_{i=0}^{\infty}$ is an asymptotic fitting pseudo-orbit of ϕ. Since ϕ has the asymptotic fitting shadowing case, $\exists\, u \in M$, so

$$\lim_{n\to+\infty}\sum_{i=0}^{n-1} d(\phi^i(u), u_i) = 0. \qquad (3.13)$$

Let $J_m = \{i: u_i \in \{m_{-2^{i-1}+1}, m_{-2^{i-1}}, \ldots, m_{-1}, m\}\}$,

$J_z = \{i: u_i \in \{z_{-2^{i-1}+1}, z_{-2^{i-1}}, \ldots, z_{-1}, z\}\}$ and $d(\phi^i(u), u_i) < \propto$.

Claim: J_m and J_z have positive upper density, that is , $\overline{D}(J_m) > 0$ and $\overline{D}(J_z) > 0$.

proof of Claim. Now, we will prove $\overline{D}(J_y) \geq 0$. assume conversely, $\overline{D}(J_m) = 0$ then we have

$$\lim_{n\to+\infty} \frac{\mathrm{Card}(J_m \cap \{0, 1, \ldots, n-1\})}{n} = 0.$$

Let $J'_m = \{i: u_i \in \{m_{-2^{i-1}+1}, m_{-2^{i-1}}, \ldots, m_{-1}, m\}$

and $d(\phi^i(u), u_i) < \propto\}$.

Then $\lim_{n\to+\infty} \frac{\text{Card}(J'_m \cap \{0,1,\dots,n-1\})}{n} = \frac{1}{2}$.

so $\forall\ \mu \in (0,1/2\backslash)$, $\exists\ N>0$ so

$$\text{so } \forall\ \mu \in \left(0, \tfrac{1}{2}\right), \exists\ N > 0 \text{ so}$$

$$\frac{\text{Card}(J'_m \cap \{0,\ 1,\ \dots,\ n-1\})}{n} > \frac{1}{2} - \mu, \quad \forall\ n \geq N.$$

$$\text{So}, \limsup_{n\to+\infty} \sum_{i=0}^{n-1} d(\phi^i(u),\ u_i) \geq \limsup_{n\to+\infty} \sum_{i\in J'_m \cap \{0,1,\dots,n-1\}} d(\phi^i(u),\ u_i)$$

$$\geq \propto \limsup_{n\to+\infty} \frac{\text{Card}(J'_m \cap \{0,\ 1,\ \dots, n-1\})}{n}$$

$$\geq \propto (\tfrac{1}{2} - \mu)$$

Since μ is arbitrary, we have

$$\limsup_{n\to+\infty} \sum_{i=0}^{n-1} d(\phi^i(u),\ u_i) \geq$$

This is a contradiction with (3.13). Hence $D^-(J_m)>0$.

Proof that $D^-(J_z)>0$ in the same way.

Now let $J_t(z)=\{l\in J_z: u_l=z_{-t}\}$, $\forall t\geq 0$. Then, by Claim, $\exists\ t_0 \geq 0$, so $D^-(J_{t_0}(z))>0$.

We pick $l_0 \geq 0$ and $0 \leq k_0 \leq 2^{l_0-1)}-1$, so $\phi^{l_0}(u)\in B(m_{-k_0}, \propto)$.

$\forall\ J\in J_{t_0}(z)$ with $J\geq l_0+k_0$, we have $\phi^j(u)\in B(z_{-t_0}, \propto)$. Because ϕ Lyapunov stable , we have $\phi^{l_0+k_0}(u)\in B(m,\varepsilon)$ and $\phi^{j+t_0}(u)\in B(z,\varepsilon)$.

Let $n_j=(j+t_0)-(l_0+k_0)$. We have $\phi^{n_j}(B(m,\varepsilon)\cap B(z,\varepsilon)) \neq \emptyset$. So, $\phi^{n_j}(S_1) \cap S_2 \neq \emptyset$. Thus $D^-(K(S_1),S_2) \geq D^-(J_{t_0}(z))>0$. Hence ϕ is topologically ergodic. ■

References

[1] Bowen R., Equilibrium States and The Ergodic Theory of Axiom a Diffeomorphisms, Springer, New York, (1975).

[2] Blank M.L., Small Perturbations of Chaotic Dynamical Systems, Russian Math. Surveys 44, 1–33, (1989).

[3] Yang R.S., Topologically Ergodic Map, Acta Math.Sin.44,:1063-1068(in Chinese), (2001).

[4] Gu R. B. and Guo W. J., The Average Shadowing Property and Topological Ergodicity for Flows, Chaos Solitons Fractals 25,: 387-392, (2005).

[5] Gu R.B., The Asymptotic Average Shadowing Property and Transitivity, Nonlinear Anal, 67(6),: 1680-1689, (2007).

[6] Park J. and Zhang Y., Average Shadowing Properties on Compact Metric Spaces, Commun. Korean Math. Soc. Vol. 21, Number 2,: 355–361, (2006).

[7] Kulczycki M., Kwietniak D. and Oprocha P., On Almost Specification and Average Shadowing Properties. Math, To appear in Fund.

[8] Gu R.B., Shadowing Techniques and Chaos, Journal of Anhui University 34,:1 – 9, (2010).

[9] Ruchi Das and Tarun Das, Topological Transitivity of Uniform Limit Functions on G-spaces, int. Journal of Math. Analysis, Vol.6, No.30,: 1491-1499, (2012).

[10] Niu Y., The Average Shadowing Property and Strong Ergodicity, J. Math. Anal. Appl. Vol. 376, Number 2,: 528-534, (2011).

Evaluation of an Industrial Product Quality Level by Using Demerit Control Chart

Salman Hussein Omran
Mechanical Dept. Institute of Technology, Baghdad, Iraq.

Received Date: 25 / 4 / 2017
Accepted Date: 3 / 9 / 2017

الخلاصة

يعتبر هذا البحث محاولة لتحسين مستوى جودة منتج صناعي (مدفأة عشتار النفطية) في شركة الصناعات الخفيفة، باستخدام لوحة السيطرة النوعية لرقم القصور (لوحة-U) تم حساب رقم القصور للوحدة المعيبة (U) لغرض تحديد حدي السيطرة لثلاثين عينة مختارة. أظهرت النتائج ان عملية الانتاج منضبطة نوعيا استنادا على بيانات مسجلة إحصائيا. كما ان العيوب من الصنفين AوB ليس لها تأثير على أداء المنتج. إضافة الى ذلك، لقد وجد أن النسبة المئوية لمستوى جودة المنتج تتراوح بين (80-100 %) مما يدل على أن جودة المنتج جيدة جداً.

الكلمات المفتاحية

مستوى النوعية، لوحة رقم القصور، مستوى النوعية القياسي، مخططات السيطرة النوعية.

Abstract

This paper is an attempt to improve the quality level of an industrial product (Ishtar Kerosene Heater) in Light Industries Company by using Demerit Control Chart (U-chart). Demerit per defected unit (U) was calculated to determine the control limits for selected thirty samples. The results showed that the production process was under controlled according to the statistical recorded data. Also, the defects classes A and B have no influence of the product performance. Additionally, it was found that the percentage of the quality level of product was ranging between (80-100%), indicating that this level is quite good.

Keywords

Quality level, Demerits control chart, Standard Quality level, Quality Control charts.

1. Introduction:

Quality improvement means increasing the efficiency and completion of the company and expanding its ability to grow and develop, by producing a product that meets the desire of the consumer with good quality and the right price with efficiency in performance, and therefore reducing the likelihood of failures. It also helps in raising the morale of the employees and motivate them to produce products with higher quality and at lower cost. This will lead to increase the ability of local production to compete in foreign markets, with economic returns of quality is in its contribution to the national economy and national income.

There are several definitions of quality, which are given as follows:

Juran [1] defined it as " Fitness for purpose or use ", Feigenbaum [2] defined it as "Quality means best for certain customer conditions. Montgomery [3] define it as "Quality is inversely proportional to variability. the American National Standards Institute (ANSI) and the American Tociety for Quality (ASQ) [4] defined quality as " the totality of features and characteristics of a product or service that bears on its ability to satisfy given needs ". Wheeler and Chambers [5] define quality as being "on – target with minimum variance ". From the previous definitions, researcher has adopted Juran definition, since it focuses on the quality of product or service which is fitting to the specifications or using.

Quality control is a process employed by the company to provide and maintain the final product with the desired features, properties and characteristics of identity, uniformity, potency and stability within established

levels. is an effective system for integration the quality development, quality maintenance and quality improvement effects of the various groups in an organization so as to enable production and service at the most economical levels extending full customers satisfaction [6]. Fig. (1) shows the quality control system in a production system.

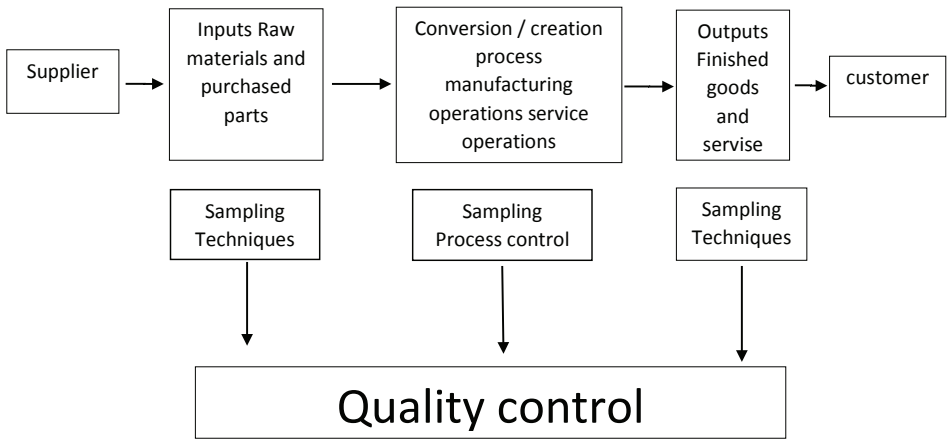

Fig. (1): Quality Control a production system [6]

1.2. Control charts:

Control charts are widely used for monitoring and examining a production process. The power of control charts lies in their ability to detect the process shifts and to identify the abnormal conditions in the process. This makes possible the diagnosis of many production problems and often reduces loses and brings substantial improvement in product quality. in 1924 (Walter She whart) designed the first control chart and proposed a general model for control charts [7, 8].

Control chart are the most important statistical process control (SPC) tools for monitoring the performance of products and services. They are classified in two parts according to their application, Variable and Attribute control charts [3]. Attribute control charts are often used to monitor services because they are based on quick diction of good or bad. C-Charts and U-charts are commonly used to render decisions on the statistical control status of products and services [9].

1.3. Demerit Control Chart:

A classical demerit control chart is used to monitor the counts of several different categories of defects simultaneously in a complex product. The traditional classical demerit control is used to plot the demerit statistic, a weighted sum of the number of defects in each category, on a control chart [10,11].

The demerit control chart was created by H. F. Dodge while working at Bell Laboratories as a means to chart product with more than one kind of possible defect. Some defects had very serious consequences on the performance of the product and some were not very serious [12]. The various types of defects were classified into four different categories, The different types of defects first need to be classified as either A, B, C or D. Once each defect is classified, a weight is given to each class depending on the impact of defect on performance or outward appearance , As well as the possibility of noting the defect or not noticed by the consumer [12] , as shown in Table (1) .

Table (1): Basic classification – definition of defects [13]

Defects class	Effect of defects on performance	Effect of defects on appearance	Effect of defects on complains	Numbers of demerits
A very important defects	Will certainly have a great influence on the function	Will certainly be noticed by customers and then cause complaints	Will certainly cause complaints	100
B Important defects	May have a great influence on the function	May be noticed by customers and will then cause complaints	Will possible cause complaints	50

C Less important defect	May to some extent have an influence on the function	May be noticed by customers but will then probably not cause complaints	Will probably not cause complaints	10
D Not important defects	Will not have influence on the function	Will not be noticed by customers	Will not cause complaints	1

1.4. Evaluation of the Degree of Product Quality:

The degree of product quality is to obtain information about the quality of the product extent of the acquisition and use of an appropriate degree of compliance with the specification as from the standpoint of the consumers, and use the audit result of a product quality in order to [14]:

provide production managers and officials with ongoing information about the levels of quality

know the defects, remove them, and continue to improve quality.

provide incentives for workers to do a good job and find an objective look at the quality of their output.

After the completion of the final inspection and packaging, then, the sample is randomly selected for examining and evaluating, depending on the characteristics and specifications, where the defect are recorded and classified according to the degree of importance, as was shown in Table (1) previously.

1.5. Used Methodology for Evaluating the Level of Product Quality by using Demirit:

This research aims to evaluate the final product quality by using Demerit Control Chart (U- chart) to determine the defects and its dangerous scope, in order to explain the Demerits from consumer point of view to improve the product quality.

The sample size is calculated every time by using the following equation [13, 14]

$$n = k\sqrt{2N} n = k\sqrt{2N} \quad \ldots\ldots (1)$$

where:

n: The sample size for ready product – examination

N: Total production volume – ready over a period of time (day, week, month)

k: A constant amount between (0.6 – 2.6) depending on the degree of complexity of product [13 ,14].

Examination of the sample. This is used most often in the same scales used in inspection during production stages.

Classification of four types of defect in relation to the degree of importance and the possibility of a complaint by the consumer which is given for each class demerit of points, which is shown in Table (1) previously.

Constructing a Demerit Control Chart.

Calculating the number of demerit per sample (U) through the following formula [15,16]:

$$U = \frac{d}{n} \ldots\ldots\ldots\ldots\ldots\ldots\ldots\ldots\ldots\ldots (2)$$

$d = (100d_A + 50d_B + 10d_D)$

U: Demerit per unit

n: The number of unit in the sample

where, d A is the no. of class A defects, dB is the no. of class B defects

dC is the no. of class C defects, dD is the no. of class D defects

ii-After calculating the number of demerit, it is compared with Table (2)

which shows the relationship between the level of quality and number of demerit.

Table (2): The relationship between the level of quality and number of demerit [16]

U(point of demerit)	Level of quality %
0 – 0.99	100 (Excellent)
1 – 1.99	90 (Excellent)
2 – 2.99	80 (very good)
3 – 3.99	70 (good)
4 – 4.99	60 (average)
5 – 5.99	50 (poor)
6 – 6.99	40 (very poor)
7 – 7.99	30 (very poor)
8 – 8.99	20 (very poor)
9 – 9.99	10 (very poor)

Table (2) shows when the value of level of the product quality is the range (60% -100%), this means that this level is acceptable by the company.

iii -Calculating the standard quality performance for the products (U) by following equation [10,15]:

$\bar{U} = 100\bar{U}_A + 50\bar{U}_B + 10\bar{U}_C + 1\bar{U}_D \dots\dots(3)$

$(\bar{U}_A, \bar{U}_B, \bar{U}_C, \bar{U}_D)$: The average number of each class of defect per unit (ex., $\bar{U}_A = \frac{\sum_{i=1}^{N} d_A}{\bar{n}}, \bar{U}_B = \frac{\sum_{i=1}^{N} d_B}{\bar{n}}, \bar{U}_C = \frac{\sum_{i=1}^{N} d_C}{\bar{n}}, \bar{U}_D = \frac{\sum_{i=1}^{N} d_D}{\bar{n}}$)

(dA, dB,dC , dD) = the total number of class (A,B,C,D)defects in the sample

$\bar{n}\bar{n}$: the total number of sample size.

Calculating the standard deviation through the following formula [13,16].

$$\sigma = \sqrt{\frac{(100)^2\bar{U}_A + 50^2\bar{U}_B + 10^2\bar{U}_C + 1^2\bar{U}_D}{\bar{n}}} \dots\dots\dots(4)$$

n- = Average Sample size

$$n^- = \frac{the\ total\ number\ of\ insfection\ unit}{sample\ number}$$

Calculate the control limits throw the following formulas [17]

Centre line =$\bar{U}\bar{U}$, as was shown in eq. (3) .

Upper control limit = $\bar{U} + 3\sigma \dots\dots\dots\dots(5)$

Lower control limit = $\bar{U} - 3\sigma \dots\dots\dots\dots(6)$

Plotting a demerit Control Chart (U-chart)

After drawing the center line and control limits, the values of(U) are pointed, if these values of (U) above the upper limit, this shows that the level of quality of the final product is less than the standard quality performance ($\bar{U}$ $\bar{U}$) . But, if it is near the centre line, this indicates the occurrence of a real improvement in the quality of the product. If the a value of (U) is between the upper and lower control limit, the quality of the product would be acceptable.

2. Practical Implementation:

In this section, a real application of industrial example, i. e, Ishtar Kerosene Heater product, Model (36) C, which is manufactured in the Light Industries Company, its geometry shape is described

in details in Fig. (2), and the manufacturing stages to produce the final product, are shown in Fig. (3).

Key No.	Part Name	Remarks	Key No.	Part Name	Remarks
1	CABINET COHPLETE				
1A	Top plate		4	PLNTE COVER	
1B	Screw for top plate	2 pcs.	4A	Plate cover	
1C	Grill		4B	Screw for plate cover	2 pcs.
1D	Cabinet				
1E	Carrying handle	2 pcs.	5	WICX ADJUSTER	
1F	Thumb screw for cabinet	3 pcs.	5A	Wick adjuster	
			5B	knob	3 pcs.
2	CHLMDEY COMPLETE		5C	wing nut	
2A	Heating coil		6	GLASS FIBER WICK	
2B	Chimney disc		7	RUSSER PACKING	
2C	Inner chimney		8	PUEL TANK	
2D	Middle chimney		8A	Main fuel tank	
2E	Outer chimney (glass)		8B	Fuel filler cap	
2F	Circular clip		8C	Fuel acceptance	
2G	Chimney supporter	2 pcs.	8D	Sub fuel tank	
2M	Cross pin	2 pcs.	9	DATSRY HOLDER	
3	LIGMING DEVICE		10	TRAY	4 pcs.
3A	Pilot heater		10A	Screw for tray	
3B	Lighting device				
3C	Screw for lighting device	2 pcs.			

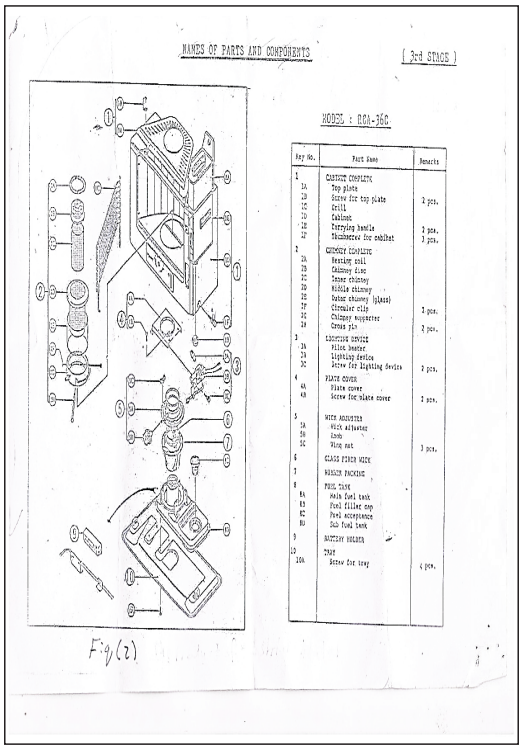

Fig. (2): Geometry Shape of Ishtar Heater

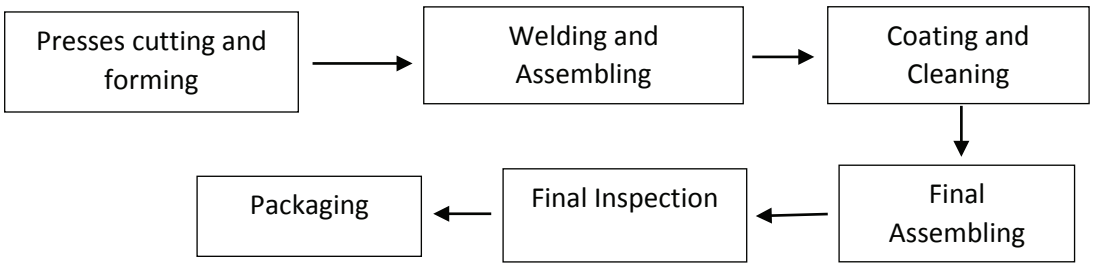

Fig (3): Manufacturing stages of Ishtar kerosene heater

To evaluate the quality of product, the following steps can be followed depending on the data given in Table (3):

(30) samples were selected randomly from the final products during (30) days.

The sample size was then calculated for each sample by eq. (1) taking the value of k=1 since the product is considered not a complex industrial one.

All the results of calculation are given in Table (3).

Table (3): Total production and sample size for Ishtar Heater product

No.	Date	Total production (N)	Sample size (n)	No.	Date	Total production (N)	Sample size (n)
1	12/1/ 2014	200	20	16	20/ 2	125	16
2	14/1	230	21	17	25/ 2	125	16
3	16/1	150	17	18	27 / 2	125	16
4	19 / 1	150	17	19	2 / 3	100	14
5	21 / 1	200	20	20	3 / 3	100	14
6	23 / 1	200	20	21	5 / 3	100	14
7	26 / 1	150	17	22	6 / 3	80	17
8	28 / 1	200	20	23	9 / 3	150	17
9	30 / 1	150	17	24	10 / 3	80	13
10	3 / 2	200	20	25	11 / 3	100	14
11	5 / 2	200	20	26	12 / 3	80	13
12	9/ 2	200	20	27	13 / 3	200	20
13	13 / 2	150	17	28	16 / 3	100	14
14	16 / 2	150	17	29	17 / 3	100	14
15	18 / 2	150	17	30	18 / 3	100	14
						∑ N=4345	∑ n=502

According to the form shown in Table (4) prepared by the researcher to find out the effective properties and classes of defects per property from the customer point of view regarding the product under the study, it was found that there are only effective properties. These are packaging, the performance

Of the product and appearance.

Table (4): The effective properties and classes of defects per property for the product under study.

Company		Batch size		Date	
Product name		Department		Issued	Issued date
No	Type of defect	Defect class			
		A	B	C	D
	Property (packaging)				
1	Install the product mark on the carton				X
2	Irregular striping found				X
	Property (The performance of the product)				
3	Main fuel tank	X			
4	Chimney completer	X			
5	Wick adjuster	X			
6	Knob	X			
7	Reflector		X		
8	Rubber packing	X			
9	Adjuster	X	X		
10	Tray	X			
	Property (Appearance)				
11	Top plate			X	X
12	Grill			X	X
13	Access			X	
14	Front panel			X	X
15	Decoration panel			X	
16	Cablnet			X	
17	Without the name of the product and model no.				X
18	Carrying handle			X	X

4- The results of classes of defects during the inspection period are given in Table (5).

5- The results of the calculated U for any day under study using eq. (2) are given below in Table (6).

Table (5): The numbers of classes defects (A, B. C. D)

No.	Date	Class of defects				No.	Date	Class of defects			
		A	B	C	D			A	B	C	D
1	12/ 1	-	-	-	3	16	20 / 2	-	-	1	-
2	14/ 1	-	-	2	-	17	25/ 2	-	-	1	1
3	16/ 1	-	-	-	1	18	27/ 2	-	-	-	1
4	19 / 1	-	-	-	1	19	2/ 3	-	-	-	2
5	21 / 1	-	-	-	-	20	3 / 3	-	-	-	1
6	23 / 1	-	-	1	-	21	5 / 3	-	-	4	-
7	26 / 1	-	-	-	-	22	6 / 3	-	-	1	-
8	28 / 1	-	-	1	2	23	9 / 3	-	-	-	-
9	30/ 1	-	-	2	-	24	10 / 3	-	-	1	-
10	3 / 2	-	-	-	-	25	11 / 3	-	-	1	-
11	5 / 2	-	-	-	5	26	12 / 3	-	-	-	-
12	9 / 2	-	-	4	-	27	13/ 3	-	-	-	2
13	13/ 2	-	-	-	2	28	16/ 3	-	-	1	1
14	16 / 2	-	-	-	3	29	17 / 3	-	-	-	3
15	19 / 2	-	-	3	-	30	18 / 3	-	-	-	1

$$\sum_{i=1}^{30} d_A = 0 \quad , \sum_{i=1}^{30} d_B = 0 \quad , \qquad \sum_{i=1}^{30} d_C = 23 \quad , \sum_{i=1}^{30} d_D = 29$$

Table (6): The number of demerit for (30) days

No	n	U	No	N	U	No	n	U
1	20	0.15	11	20	0.25	21	14	2.86
2	21	0.95	12	20	2	22	13	0.77
3	17	0.06	13	17	0.12	23	17	0
4	17	0.06	14	17	0.18	24	13	0.77
5	20	0	15	17	1.76	25	14	0.71
6	20	0.5	16	16	0.63	26	13	0
7	17	0	17	16	0.69	27	20	0.10
8	20	0.6	18	16	0.06	28	14	0.79
9	17	1.18	19	14	0.14	29	14	0.21
10	20	0	20	14	0.07	30	14	0.07

6- The percentage of quality level was in table (2) and values of U for 30 days, as computed depending on the data that given shown in Table (7).

Table (7): The percentage of quality and level number according to the no. of demerit (U) for product for 30 days

No	U(the number of demerit)	Level of quality	No	U(the number of demerit)	Level of quality
1	0.15	100	16	0.63	100
2	0.95	100	17	0.69	100
3	0.06	100	18	0.06	100
4	0.06	100	19	0.14	100
5	0	100	20	0.07	100
6	0.5	100	21	2.86	80
7	0	100	22	0.77	100
8	0.6	100	23	0	100
9	1.18	90	24	0.77	100
10	0	100	25	0.71	100
11	0.25	100	26	0	100
12	2	80	27	0.10	100
13	0.12	100	28	0.79	100
14	1.18	100	29	0.21	100
15	1.76	90	30	0.07	100

$$\sigma = \sqrt{\frac{(100)^2\bar{U}_A + 50^2\bar{U}_B + 10^2\bar{U}_C + 1^2\bar{U}_D}{\bar{n}}}$$

7-In order to construct the U- chart, one has to find the values of (U) according to eq. (3), standard deviation ( ) by eq .(4) ,and finally the upper and lower control limits . Therefore, the plot of demerit control chart (U- chart) is shown in Fig. (4).

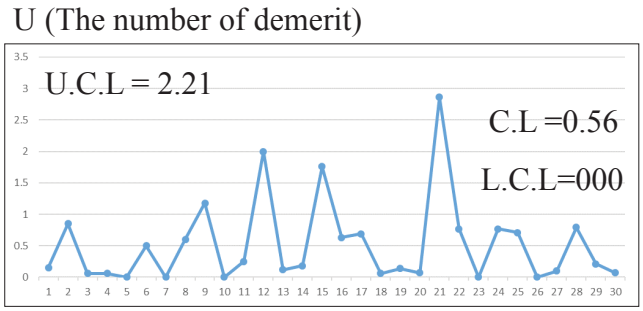

Fig. (4) Demerit Control Chart (U- Chart)

3. Results and Discussion:

The inspections of the selected sample (30 samples) showed that the sum of defects of class A and class B was Zero. Therefore, these types of defects had no effect on the product performance. But, the sum of defects of class C was (23) and class D (29), indicating that they had a slight influence on product function.

The percentage of quality level was found between (80 -100) Table (7), revealing that this quality was quite good, although that the (U) value for sample (21) is out the limit. And, this is attributed to insignificant assembling defects (class c defect), however these defects have no effect on the performance of product, there by no complaints have been not presented by any customer yet.

4.Conclusions:

From practical results, the following conclusions can be drawn:

The numbers of defect class (A, B) have zero percentage in comparison with the defects classes (C, D)

The defect class (D) has the larger (55.8 %) and these defects have no effect on the performance of a product which lead no complaints from the customers such as welding quality in grill less than the standard welding quality and the number of holes in top plate was less than the standard holes in holes.

The production process was statistically controlled because of the (U) value for samples is located between the upper and lower control limits.

The percentage quality for Ishtar Heaters in period (30) days was located

between (80%) and (100%.)

References

[1] Vinay, AKulkarni and Ananed Bewoor, " Quality Control", Wiley India Put. Ltd, New Delhi, (2009).

[2] Feigenbaum, A. V., "Total Quality Control", Third ed., New York, Mcgraw-Hill, p(15-16), (1986).

[3] Dowglas, C. Montogomery, "Introduction to statistical Quality Control " ,6thed, John Willey & Sons, Inc., p:3, (2009).

[4] James R. Evans, "Quality Management Organization and strategy " 6th ed, Suoth – Western, Cengage Learing, pp.5-6, (2011).

[5] Henderson,G. Robin , "Six Sigma quality Improvement with Minitab "2nd ed , John willey & Sons.Inc.,p:2, (2011).

[6] Zuher Hassan Abdullah, " Computer Aided Quality Control ", MSc Thesis , University of Technology , pp:1-4, (2003).

[7] V. Amirzadeh,M.Mashinchi and , M. A. Yaghoobi , Construction of Control Charts Using Fuzzy Multinomial quality "Journal Mathematics and Statistics ,Vol.4 , No.1 , pp .26-31, (2008).

[8] Vahid Amirzadeh, Mashaallah Mashinchi and , Abbas Porchami, "Construction of P-chart using degree of nonconformity " Information sciences 179 , pp.150 -160, (2009).

[9] Fikri Dweiri, Sharafuddin Ahmed Khan and M.Shamsauzzaman , "The Use of Statistical Quality Control Charts for the Acceptance and Sign – off Process for Web Application Products ", International Conference on Industrial Engineering and Operations Management , Istanbul , Turkey , July 3-6 , (2012).

[10] Long –Hui Chen , "A demerit Control Chart with Linguistic Weights "Journal of Intelligent with Linguistic Manufacturing , 16, pp. 349-359. WWW.IVSL, (2005).

[11] Chang, F. M, Chen,L .H,chen, Y. L and Haung , C.Y, 2008 ," Exact Properties of Demerit Control Chart", Journal of Computational Statistics & Data Analysis ,Vol.52, No.7, pp.3300 – 3309 ,WWW.IVSL.

[12] Mark Smallwood , "Quality Management " , WWW .Free quality . org., (2006).

[13] Magda khalid Ismail , "Design of a computer Aided Quality Rating Outgoing Products,MSc, Thesis, University of Baghdad, pp:29, (2006).

[14] AL-Mosawi,Niema Hafidh , "Building Quality Control Circles and their Applications in Industry ",MSc. Thesis, University of Technology, pp .8-9 [in Arabic], (1989).

[15] Daived A .Nembhard and Harriet Black Nembhord , " A demerits control Chart for Autocorrectlated Data "Quality Engineering , Vol .13 , pp :179 – 190,(2000).

[16] Salman Hussein Omran , "Development of Quality Rating Evaluation of Outgoing Product Case Study applied at the General Company for Vegetable Oils ",Journal of Engineering – Baghdad,Vol.19 , No.4 , pp:67-81 [in Arabic], (2013).

[17] Dale H. Besterfield, "Quality Control ", 8thed., Prentice – Hill, New Jersy, p:35, (2009).

Sol–Gel Processed Zinc Oxide Film Deposited on Equilateral Prism As Optoelectronic Humidity Sensor

Mustafa Shakir Hashim*, Reem Saadi Khaleel*, Hadi Ahmed Hussein*, Hussein Thamir Salloom**

Physics department, Education College, Al-Mustansiriya University, Iraq.
**Al-Nahrain nano renewable energy research center, Al-Nahrain University, Iraq.

Received Date: 20 / 12 / 2016
Accepted Date: 1 / 3 / 2017

الخلاصة

رسب غشاء اوكسيد الزنك على موشور متساوي الاوجه بطريقة الطلاء بالبرم. لُدنت العينة بعد ذلك بدرجة (400)م^0 لساعه واحدة. أكد حيود الاشعه السينية تكون التركيب المتعدد التبلور لأوكسيد الزنك وبمعلمات خلية وحدة a= (0.325) nm و c =(0.52) nm. قيست تغيرات النفاذية والامتصاصية مع الطول الموجي بالمدى من (300) nmالى (1100) nm. حسبت فجوة الطاقة البصرية للغشاء من تحليل الامتصاص البصري. اعتمادا على تغيير القدرة الخارجة لضوء الليزر المنعكس أستقصيت حساسية الغشاءالمرسب للرطوبة بمدى رطوبة نسبية مابين (10)الى (90) ٪. استعملت تلاث زوايا (45 ، 60 و80) درجة لاسقاط شعاع الليزر. بينت النتائج المستحصلة زيادة القدرة الخارجة للشعاع المنعكس مع الرطوبة. سجلت اعلى قيمة للرطوبة النسبية عند زاوية سقوط (80) درجة.

الكلمات المفتاحية

متحسس رطوبة، اوكسيد الزنك، الطلاء بالبرم، تغيير القدرة والرطوبة النتسبية.

Vol. 7, No. 13 and 14 P. (65-71)E, 2018

Abstract

Zinc oxide film has been deposited on an equilateral prism using spin coating method. The sample is then annealed at (400) 0C for one hour. X-ray diffraction (XRD) confirms the formation ZnO polycrystalline structure with the unit cell parameters of a= (0.325) nm and c= (0.52) nm .The variations of both the transmittance and absorbance with wavelength in the range from (300) to (1100) nm is measured. The optical energy gap of the film is calculated from analysis of optical absorption. Based on output power modulation of reflected laser light, the humidity sensing of the deposited film is investigated at relative humidity (%RH) in the range (10–90) %. Three angles (45, 60 and 80) degree are used to apply the laser beam. The obtained results showed that the output power of reflected beam is increased with humidity. Maximum relative humidity was recorded at incidence angle Θi = (80) degree.

Keywords

Humidity sensor, ZnO, Spin coating, power modulation and relative humidity.

1. Introduction:

Humidity is important a factor of environment drastically affects all organisms. For industrial applications and human life humidity sensors are becoming more important. Measurement of this parameter is needed in large applications such as, civil engineering, electronic processing, agriculture, air conditioning and meteorological services. In general humidity sensors can be classified to two types. The principle of first type is based on the measurement of electrical parameters like resistance, capacitance and impedance [1,2]. Second type measures the variations on optical parameters like frequency shift, refractive index and wavelength variation [3]. The second type is called optical (opto)-electronic humidity sensors. During the current work, attempts are done to measure the output power of reflected laser beam as many workers done [4,5].

Sol-gel spin coating technique has many advantageous over other frequent thin film techniques due to the following: it produces uniform thin film, it needs less equipment, it is relatively less expensive [6] Besides, uniformity of the deposited films and their microstructure can simply be controlled by arranging the preparation condition like fluid density, solution concentration, fluid viscosity, annealing temperature and speed of the spinner [7]. ZnO is a semiconductor material with direct wide band gap, a hexagonal wurtzite structure and binding energy of (60) meV. In fundamental research and due to its potential applications, this material has attracted much interest. ZnO is utilized in large scale of application like solar cells, violet/blue emission devices, acoustic devices and laser diodes [8].

In this contribution, an attempt is done to fabricate optoelectronic humidity sensor, the working principal is depend on measuring the variation of reflected laser output power from the base of prism located inside a cell with variable humidity circumstances.

2. Experimental part:

Microscope glass slide is used as substrate to deposit ZnO film. The dimensions of this substrate were (75) × (25) × (1) mm. The substrate is washed with ethanol and then distilled water. Sol solution was prepared by adding (3.1) g Zinc acetate dihydrate (Zn(CH3COO)2.2H2O) to isopropanol alcohol then (0.86) g mono ethanolamine (MEA) is added to yield a homogeneous and clear solution. The solution is then aged at room temperature for one day [9]. Home made spin coating machine is utilized with speed (2000) rpm. (100) micro liter from prepared sol solution is injected by using micropipette on substrate surface when the speed reaches the mentioned speed. After coating the substrate is heated to (400) 0C under ambient condition for one hour. The same procedure is repeated to deposit ZnO on one prism face and then heated at the same conditions. Shimadzu X-ray diffractometer is used to determine the orientations of ZnO. Bragg angle is ranged from (10) to (80) degree. To characterize the

optical properties of the samples UV-Visible 1800 spectrophotometer is used. Transmittance% and absorbance% are measured at ambient conditions " temperature = (30) degree and %RH = 35 ".

The output power of reflected laser beam from prism is measured by spectrometer type HR4000CG-UV-NIR as a function to %RH inside this chamber. The used laser has output power equals to (100) mW. Two saturated salts are used to increase and decrease humidity inside chamber, these salts is tabulated in Table (1).

Table (1): Humidifier and dehumidifier salts.

Salt	RH range%	Function
K_2SO_4	to 95 10	Humidifier
KOH	to 10 95	Dehumidifier

Illumination of the first face of prism is achieved by laser diode with wavelength (531) nm. After reflection from the second face (coated with ZnO and inserted inside the chamber); the laser beam exists from third face to be measured by spectrometer, as shown in Fig. (1).

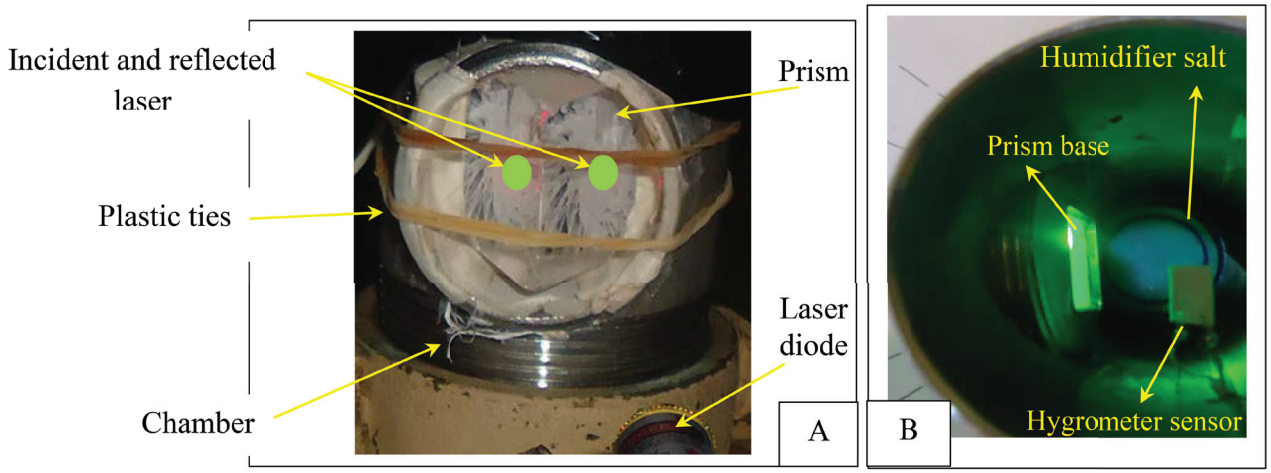

Fig. (1): A- The fixed prism on humidity chamber.
B-The details inside the chamber.

To measure the response and recovery time, humidity is stabilized at extreme %RH and then slowly exposed to atmosphere to achieve atmospheric %RH.

3. Results and discussion:

Fig. (2) shows the indexed XRD pattern of ZnO film. This pattern indicates that the film is polycrystalline. All appeared diffraction peaks are corresponded to the ZnO wurtzite structure (JCPDS Card, No. 36-1451). Fig. (2) illustrates enhanced intensities of the peaks corresponding to plane (002), indicating preferential orientation along the c-axis [10]. De-

bye Scherrer equation [11]:

Crystallite size(ξ) = 0.94λ / $\beta\cos\theta$

is used to calculate average crystallite size of the ZnO. Where λ is x-ray wavelength, β is the broadening of the hkl diffraction peak measured at half of its maximum intensity (in radians) and θ is Bragg diffraction angle. Table (2) illustrates some parameters calculated from Fig. (2).

Table (2): Calculated parameters from XRD pattern.

Crystallite size(nm)	Unit cell parameters (nm)	
	a	c
2.73	0.324982	0.52066

The peaks' sharpness indicates to a good crystallinity of the deposit. Lower intensities than that of (002) peak are observed for (102), (110), (103) and (112) peaks. The agglomeration of particles produces bigger crystallite size.

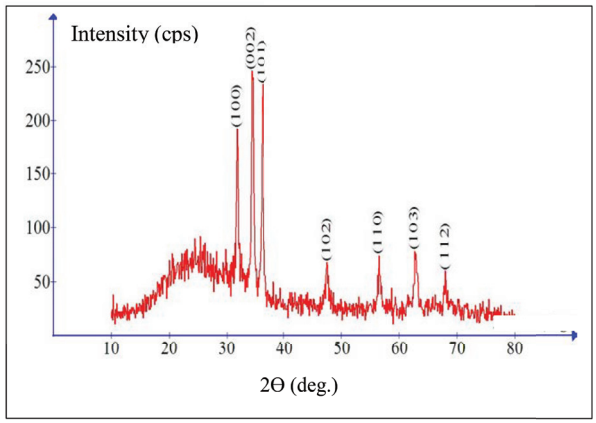

Fig. (2) : XRD pattern of ZnO film.

Fig. (3) illustrates the variations of both the transmittance% and absorbance with wavelength in the wavelength range from (300) to (1100) nm. Low relatively transmittance values of the film may be due to one or all the following: (1) increasing photons scattering due to crystal defects, (2) its comparatively high thickness (2) μm and (3) absorption of photons by free carriers [12].

From Fig. (3) it can be inferred that the reflection of the two used wavelengths (630.6) and (532) nm are more than the transmittance or absorption. This reflection's values are useful in current application because the variations of humidity inside the chamber are measured as a function to reflected laser from active ZnO layer.

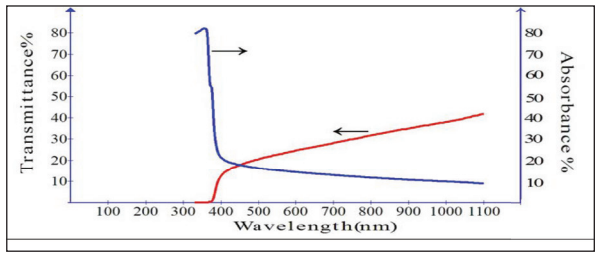

Fig. (3): Transmittance% and Absorbance versus wavelength.

By using extrapolation method the value of optical energy gap Eg is calculated. This method is done by plotting the square of ($\alpha h\nu$) versus photon energy, as Fig. (4) shows. Where α is absorption coefficient and ν is the frequency of the light. The Eg value is (3.26) eV in good agreement with others [13].

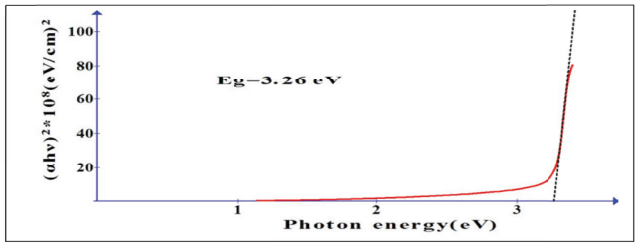

Fig. (4): Estimation of optical energy gap.

Fig. (5) shows the output power variations as a function to %RH. The sensitivities of the sensor are listed in Table (3) which it show slow increasing in reflected laser output powers for the three incident angles in the range (10-60) %RH and then the increasing becomes fast at high %RH. This Table shows also the increasing of average sensitivities with Θi. After the total internal reflection from ZnO layer at incident angles (45, 60 and 80) degree; the laser beam exist outside the surface of the prism. The variation of ZnO refraction index due to adsorption of water vapor (with increasing the humidity) produces output power changing of reflect laser. Inside the chamber humid air (water vapor) replaces dry air with increasing of humidity.

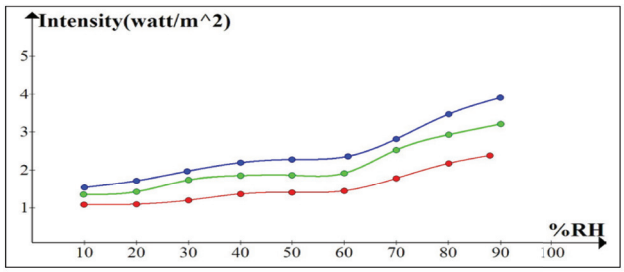

Fig. (5): Variation of reflected laser output power versus %RH.

Table (3): Sensitivity of the sensor as a function to incidence angle.

Incidence angle Θ_i (degree) at the prism-film interface	Average sensitivity (10-50%RH) ((Watt/m²/%RH	Average sensitivity (50-90%RH) (Watt/(m²/%RH
45	30	136
60	48	171
80	68	215

As a result, the pores of ZnO layer are filled with this humid air and water's condensation inside these pores increases the film refractive index [5]. ZnO layer density (5.67) g /cc will be changed as result to adsorption of water; its density (1.004) g/cc [14].

Response and recovery times are measured when %RH is stabilized at (10) and (90) respectively and then slowly subjected to room atmosphere. Fig. (6) shows the variation of output power with time for Θi = (60) degree. Recovery time and response time are (10 and 30) s. respectively. These values are close to that measured by Yadav et al [4] who fabricated opto-electronic humidity sensor from (Mg–Zn–Ti) oxide nanocomposite film.

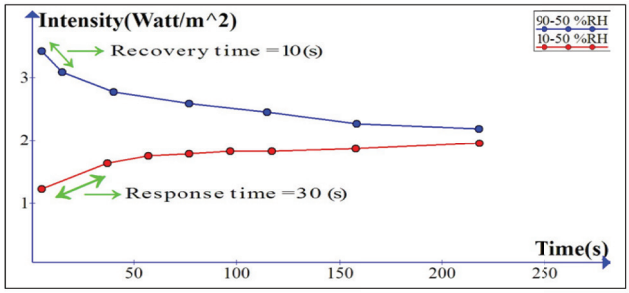

Fig. (6): Response and recovery times of the sensor for Θi = (60) degree.

4. Conclusions:

The obtained results allow us to draw the following conclusions:

1. Sol gel processed ZnO thin film is successfully deposited on an equilateral prism using spin coating technique.
2. Structural analysis indicates the formation of ZnO thin film with the average crystallite size about (2.73) nm.
3. The measured optical energy gap of thin film was in a good agreement with published values.
4. The present study explored utilizing ZnO thin film deposited on a prism as humidity sensor at room temperature, the output power of reflected laser light increases with increasing of water vapor adsorption.

References:

[1] Nahar RK, Khanna VK and Khokle WS. Journal of Physics D: Applied Physics 17,2087–2095, (1987).

[2] Basu S, Chatterjee S, Saha M, Bandyopadhay S, Mistry KK and Sengupta K. Sensors and Actuators B: Chemical .79,182–186, (2001).

[3] Bali LM, Srivastava Atul, Shukla RK and Srivastava Anchal. Optical Engineering 38,1715, (1999).

[4] B.C. Yadav, Ramesh C. Yadav and Prabhat K. Dwivedi. Sensors and Actuators B 148, 413–419, (2010).

[5] B.C. Yadav, Nidhi Verma and Satyendra Singh. Optics and Laser Technology. 44, 1681–1688, (2012).

[6] Rama Singh, Avadhesh Kumar Yadav and Chandkiram Gautam. Journal of Sensor Technology.1, 116-124, (2011).

[7] D. Meyerhofer. Journal of Applied Physics. 49(7), 3993-3997, (1978).

[8] M.F.A.Alias, H.Kh, Alamy and R.M. Shaker. J. Electron Dev. 14, 1178-1185, (2012).

[9] Mohammad H. Habibi and Mohammad Kh. Sardashti. Journal of Nanomaterials, Article ID 356765, 5 pages. doi:10.1155/2008/356765, Volume (2008).

[10] M. Sathya A. Claude, P. Govindasamy and K. Sudha. Advances in Applied Science Research. 3 (5),2591-2598, (2012).

[11] Kalyani Ghule, Anil Vithal Ghule, Bo-Jung Chena and Yong-Chien Ling. Green Chem. 8,1034–1041, (2006).

[12] Reem S. Khaleel . Ph.D. thesis, University of Al-Mustansiriyah , (2016).

[13] S. S. Shariffudin, M. Salina, S. H. Herman and M. Rusop. Transactions on electrical and electronic materials. 13(2),102-105, (2012).

[14] Shukla S. K., Anand B., Parashar G. K., Mishra A. P. and Dubey G. C. and Ashutosh T. Adv. Mat. Lett. 3(5), 365-370, (2012).

The Weighted Transmuted Pareto Distribution

Kareema Abed Al-kadim and Maysaa Hameed Mohammed
College of Education pure Sciences, University of Babylon, Iraq.

Received Date: 13 / 8 / 2015
Accepted Date: 4 / 7 / 2017

الخلاصة

ان توزيع الحياة يلعب دورا مهما في مجالات الحياة المختلفه كالأحصاءات الحياتية، تحليل المعولية او البقاء،... الخ. وفي هذا البحث حاولنا المساهمة في ايجاد توزيع حياة مقترح وهو توزيع باريتو المحول الموزون مع مناقشة بعض الخواص.

الكلمات المفتاحية

توزيع باريتو المعزول ، التوزيع الموزون ، دالة التوزيع التراكمي ، وظيفة الموثوقية.

Abstract

The lifetime distributions play important role in many real life fields such as the biostatistics, reliability and survival analysis, so we try to contribute infinding anew proposed lifetime distribution, weighted transmuted Pareto distribution, and discuss some of its statistical properties.

Keywords

Transmuted Pareto distribution, Weighted distribution, Cumulative distribution function, Reliability function.

1. Introduction

The statistical analysis depends on the statistical model, or distribution, represented the life phenomena under study. However, the models available do not fit data of many important and practical problems. So that a non-linear parametric model may be recommended. The weighted, transmuted, weighted transmuted distributions are from these non-linear parametric distributions.

Shaw & Buckley (2009) [3] used the rank transmutation map RTM, a tool for the construction of new families of non-Gaussian distributions. They used it to modulate a given base distribution for the purposes of modifying the moments, in particular the skew and kurtosis. They introduced the quadratic rank transmutation map (QRTM) that has been used by many authors to introduce different new important distributions. The transmuted Pareto was derived by F. Merovciaand L. Pukab

2.distribution:

The weighted distribution is considered as a good tool for modeling statistical data when these data can not fit the standard distributions because the damage, missing caused to the original observation resulting in a reduced value, or adoption of a sampling procedure which gives unequal chances to the units in the original. Fisher (1934) [1] introduced this concept and Rao (1965) [2] developed it.

Some recent searches of weighted distributions studied by many authors like:

K. K. Das and T. Deb Roy (2011) [4] who introduced the length-biased Weighted Generalized Rayleigh distribution and some of its properties,

X. Shi, B. O. Oluyede and M. Pararai (2012) [5] derived a new class of weighted generalization of the Rayleigh distribution, and discussion some of properties,

K. abed al-kadim and A.F. Hantoosh (2013) [6] constructed the Double weighted distribution, and Double weighted Exponential distribution.

K.A. Mir, A. Ahmed and J. A. Reshi (2013) [7] studied a new class of Length-biased beta distribution introduced the first kind, and estimation its parameters,

N. I. Rash wan (2013) [8] presented a new weighted distribution which is known as the double weighted rayleigh distribution and some of its properties,

A. Ahmad, S.P Ahmad and A. Ahmed (2014) [9] constructed a new weighted distribution which is known as the Double Weighted Rayleigh Distribution, and discussion statistical properties of this distribution ,

K Abed Al-Kadim and N. A. Hussein (2014) [10] introduce new class of length-biased of weighted exponential and Rayleigh distributions. And they studied some of its statistical properties with application.

P. Seenoi, T. Supapakorn and W. Bodhisuwan (2014) [11] introduce a length-biased of the exponentiated inverted Weibull distribution.

The aim of this paper is to propose and

study a generalization of the Pareto distribution using the weighted distribution, that is obtain a larger class of flexible parametric distribution. In this paper, the transmuted Pareto distribution derived by Faton M., Llukan P. (2014) [12], we study the a new proposed distribution, the weighted transmuted Pareto distribution, and discuss some of its statistical properties. It may use in applications of reliability, actuarial science, economics, finance and telecommunications. This paper is organized as follows. Section 1 contains introduction. The weighted transmuted Pareto distribution is introduced in section 2, including the cumulative distribution function (cd f), pdf, hazard and reverse hazard functions and some of its properties. In section 3, the conclusions are presented.

3. Mainresul:

3.1. The Weighted Transmuted Pareto Distribution(WTPD):

3.1.1. Definition (WTPD):

Let the weight function and the transmuted Pareto distribution be w(x)≥0 and $f_{TPD}(x)$ respectively. Then the weighted transmuted Pareto density function $g_{WTPD}(x)$ is obtained as:

$$g_{WTPD}(x) = \frac{w(x) f_{TPD}(x)}{w_D} \quad (1)$$

Where w(x)=x ,is called the weight , it is a normalizing factor obtained to make the total probability equal to unity that is chosen such that choosing

$0 < \omega = E[w(X,\beta)] < \infty$.

$$w_D = E[w(x)] = \int_{x_m}^{\infty} x \frac{\alpha x_m^{\alpha}\left(1-\lambda+2\lambda\left(\frac{x_m}{x}\right)^{\alpha}\right)}{x^{\alpha+1}} = \frac{\alpha x_m[2\alpha-1-\lambda]}{(\alpha-1)(2\alpha-1)} \quad (2)$$

where the pdf of transmuted Pareto distributionis:

$$f_{TPD}(x) = \frac{\alpha x_m^{\alpha}\left(1-\lambda+2\lambda\left(\frac{x_m}{x}\right)^{\alpha}\right)}{x^{\alpha+1}},\ x > 0\ ,|\lambda| \le 1, \alpha > 0 \quad (3)$$

So that

$$g_{WTPD}(x) = \frac{x_m^{\alpha-1}(\alpha-1)(2\alpha-1)\left(1-\lambda+2\lambda\left(\frac{x_m}{x}\right)^{\alpha}\right)}{x^{\alpha+1}(2\alpha-1-\lambda)}, x > 0, |\lambda| \le 1, \alpha > 0 \quad (4)$$

Which is similar to pdfof WTPD with weight (α-1)(2α-1)/((2α-1-λ)) for |λ|≤1,α>0

And with slightly difference.

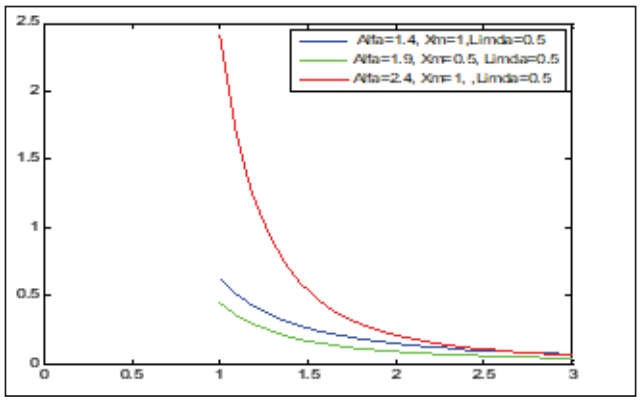

Fig. (1) The pdf of WTPD for different values of λ,α

In Fig. (1)we note as the shape of the pdf of WTPD, it is decreasing function along the increasing x and at different values of λ,α .

3.1.2. Remark

In this remark we prove that $g_{WTPD}(x)$ is a pdf as follows:

$\int_{x_m}^{\infty} g_{WTPD}(x)dx = \int_{x_m}^{\infty} (x_m^{\alpha-1})\ x^{-\alpha}(\alpha-1)(2\alpha-1)(1-\lambda+2\lambda(x_m/x)^{\alpha})/((2\alpha-1-\lambda))\ dx$

$$= \frac{(\alpha-1)(2\alpha-1)}{(2\alpha-1-\lambda)}\left[(1-\lambda)x_m^{\alpha-1}\int_{x_m}^{\infty} x^{-\alpha}dx + 2\lambda x_m^{\alpha-1}\int_{x_m}^{\infty} x^{-\alpha}\left(\frac{x_m}{x}\right)^{\alpha}dx\right]$$

$$= -\frac{(\alpha-1)(2\alpha-1)}{(2\alpha-1-\lambda)}\left(\frac{-2\alpha+1+2\alpha\lambda-\lambda-2\alpha\lambda+2\lambda}{(\alpha-1)(2\alpha-1)}\right)$$

$$= -\frac{(\alpha-1)(2\alpha-1)}{(2\alpha-1-\lambda)}\left(\frac{-2\alpha+1+\lambda}{(\alpha-1)(2\alpha-1)}\right) = 1 \ \blacksquare$$

Acumulative distribution function (cd f)

of weighted transmuted Pareto distribution is given as:

$$G_{WTPD}(x) = 1 - \frac{(\alpha-1)(2\alpha-1)}{(2\alpha-1-\lambda)} x_m^{\alpha-1} x^{-\alpha+1}\left[\frac{(1-\lambda)}{(\alpha-1)} + \frac{2\lambda}{(2\alpha-1)}\left(\frac{x_m}{x}\right)^{\alpha}\right] (5)$$

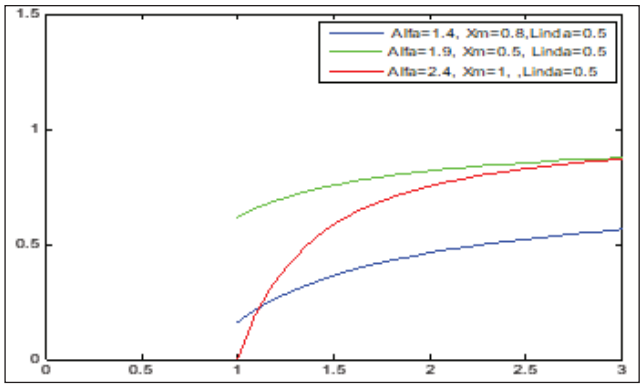

Fig. (2) The cdf of WTPD for different values of λ,α

Fig. (2) shows as the shape of the cdf of WTPD, it is increasing function along increasing x and at different values of λ,α

3.2. Reliability Analysis:

3.2.1. The Reliability Function (RF):

The reliability function of weighted transmuted Pareto distribution is given as:

$$R_{WTPD}(x;\alpha,\lambda) = \frac{(\alpha-1)(2\alpha-1)x_m^{\alpha-1}}{(2\alpha-1-\lambda)x^{\alpha-1}}\left[\frac{(1-\lambda)}{(\alpha-1)} + \frac{2\lambda}{(2\alpha-1)}\left(\frac{x_m}{x}\right)^{\alpha}\right] (6)$$

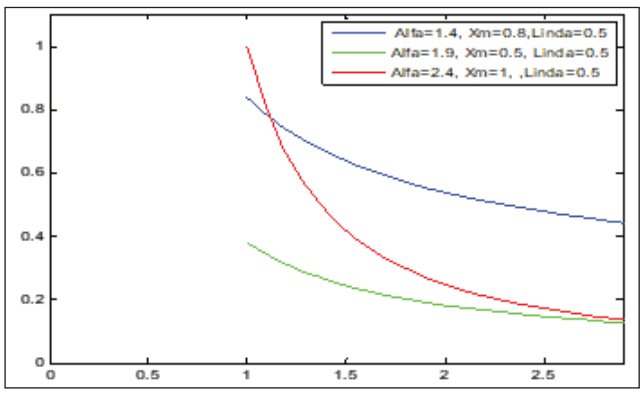

Fig. (3) The RF of WTPD for different values of λ,α

In Fig. (3)we note that the shape of the RF of WTPD, it is the inverted of the shape of cd f function along increasing x and at different values of λ,α

3.2.2. The Hazard Rate Function (HF):

The hazard rate function of (WTPD) is

$$h_{WTPD}(x;\alpha,\lambda) = \frac{g_{WTPD}(x;\alpha,\lambda)}{R_{WTPD}(x;\alpha,\lambda)} = \frac{\left(1-\lambda+2\lambda\left(\frac{x_m}{x}\right)^{\alpha}\right)}{x\left[\frac{(1-\lambda)}{(\alpha-1)}+\frac{2\lambda}{(2\alpha-1)}\left(\frac{x_m}{x}\right)^{\alpha}\right]} (7)$$

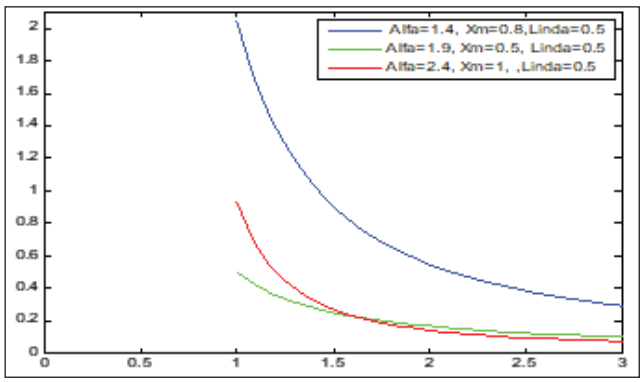

Fig. (4) The HF of WTPD for different values of λ,α

In Fig. (4)we note that the shape of the HF of WTPD, it is the similar to the shape of pdf function along increasing x and at different values of λ,α but with some differences.

3.2.3. The Reverse Hazard Function:

The reverse hazard function of WTPD(x;α,λ), is defined as

$$H_{WTPD}(x;\alpha,\lambda) = \frac{g_{WTPD}(x;\alpha,\lambda)}{G_{WTPD}(x;\alpha,\lambda)}$$

$$= \frac{x_m^{\alpha-1}x^{-\alpha}(\alpha-1)(2\alpha-1)\left(1-\lambda+2\lambda\left(\frac{x_m}{x}\right)^{\alpha}\right)}{\left[(2\alpha-1-\lambda)-x_m^{\alpha-1}x^{-\alpha+1}\left((1-\lambda)(\alpha-1)+2\lambda(2\alpha-1)\left(\frac{x_m}{x}\right)^{\alpha}\right)\right]} (8)$$

3.2.4. The Limit:

Proposition (1)

The limits of the pdf and its hazard func-

tion of WTPD as x→x_m and as →∞ , respectively, are equal.

Proof

$$\lim_{x\to x_m} g_{WTPD}(x,x_m,\alpha,\lambda)=\lim_{x\to x_m}\frac{x_m^{\alpha-1}x^{-\alpha}(\alpha-1)(2\alpha-1)\left(1-\lambda+2\lambda\left(\frac{x_m}{x}\right)^{\alpha}\right)}{(2\alpha-1-\lambda)}$$

$$=\frac{x_m^{-1}(\alpha-1)(2\alpha-1)(1+\lambda)}{(2\alpha-1-\lambda)}$$

The limit of weighted transmuted density function of Pareto distribution when x→∞ is

$$\lim_{x\to\infty} g_{WTPD}(x,x_m,\alpha,\lambda)=\lim_{x\to\infty}\frac{x_m^{\alpha-1}x^{-\alpha}(\alpha-1)(2\alpha-1)\left(1-\lambda+2\lambda\left(\frac{x_m}{x}\right)^{\alpha}\right)}{(2\alpha-1-\lambda)}$$

$$=\frac{x_m^{\alpha-1}\infty^{-\alpha}(\alpha-1)(2\alpha-1)\left(1-\lambda+2\lambda\left(\frac{x_m}{\infty}\right)^{\alpha}\right)}{(2\alpha-1-\lambda)}=0$$

The limit of weighted transmuted hazard rate function of Pareto distribution when x→x_m is:

$$\lim_{x\to x_m} h_w(x,x_m,\alpha,\lambda)=\frac{\left(1-\lambda+2\lambda\left(\frac{x_m}{x_m}\right)^{\alpha}\right)}{x_m\left[\frac{(1-\lambda)}{(\alpha-1)}+\frac{2\lambda}{(2\alpha-1)}\left(\frac{x_m}{x_m}\right)^{\alpha}\right]}$$

$$=\frac{(1+\lambda)(\alpha-1)(2\alpha-1)}{x_m(2\alpha-1-\lambda)}$$

$$=\lim_{x\to x_m} g_{WTPD}(x,x_m,\alpha,\lambda)$$

The limit of hazard rate function of weighted transmuted Pareto distribution when x→∞ is:

$$\lim_{x\to\infty} g_w(x,x_m,\alpha,\lambda)=\frac{\left(1-\lambda+2\lambda\left(\frac{x_m}{\infty}\right)^{\alpha}\right)}{\infty\left[\frac{(1-\lambda)}{(\alpha-1)}+\frac{2\lambda}{(2\alpha-1)}\left(\frac{x_m}{\infty}\right)^{\alpha}\right]}$$

$$=0=\lim_{x\to\infty} g_{WTPD}(x,x_m,\alpha,\lambda)\ \blacksquare$$

3.2.5. The mode:

Take the natural logarithm to two sides of the pdf of the WTPD

$$lng_{WTPD}(x)=ln\frac{x_m^{\alpha-1}x^{-\alpha}(\alpha-1)(2\alpha-1)\left(1-\lambda+2\lambda\left(\frac{x_m}{x}\right)^{\alpha}\right)}{(2\alpha-1-\lambda)}$$

$$lng_w(x)=(\alpha-1)lnx_m-\alpha lnx+ln(\alpha-1)+ln(2\alpha-1)+ln\left(1-\lambda+2\lambda\left(\frac{x_m}{x}\right)^{\alpha}\right)-ln(2\alpha-1-\lambda)$$

$$\frac{\partial lng_w(x)}{\partial x}=\frac{-\alpha}{x}-\frac{2\alpha\lambda x_m^{\alpha}x^{-\alpha-1}}{\left(1-\lambda+2\lambda\left(\frac{x_m}{x}\right)^{\alpha}\right)}$$

$$\frac{-\alpha}{x}-\frac{2\alpha\lambda x_m^{\alpha}x^{-\alpha-1}}{\left(1-\lambda+2\lambda\left(\frac{x_m}{x}\right)^{\alpha}\right)}=0$$

$$x_{mode}=\left(\frac{\lambda-1}{4\lambda x_m^{\alpha}}\right)^{-1/\alpha}\quad(9)$$

3.3. Moment and Moment Generated Function:

3.3.1. The Moments:

Proposition(2) If X has the WTPD(x;α,λ) with |λ| ≤ 1,then the rth moment of X is

$$E(X^r)=\frac{(\alpha-1)(2\alpha-1)(2\alpha-(1+\lambda)(1+r))}{(2\alpha-1-\lambda)(\alpha-r-1)(2\alpha-r-1)}x_m^r\quad(10)$$

For $\alpha>\frac{1+\lambda}{2},\alpha>r+1,\alpha>\frac{1+r}{2}$.

Especially, $\mu=\frac{(2\alpha-1)(\alpha-1-\lambda)}{(2\alpha-1-\lambda)(\alpha-2)}x_m$

$$\sigma^2=\frac{(2\alpha-1)}{(2\alpha-1-\lambda)}x_m^2\left(\frac{(\alpha-1)(2\alpha-3(1+\lambda))}{(\alpha-3)(2\alpha-3)}-\frac{(2\alpha-1)(\alpha-1-\lambda)^2}{(2\alpha-1-\lambda)(\alpha-2)^2}\right)(11)$$

Proof

$$E(X^r)=\int_{x_m}^{\infty}x^r\frac{x_m^{\alpha-1}x^{-\alpha}(\alpha-1)(2\alpha-1)\left(1-\lambda+2\lambda\left(\frac{x_m}{x}\right)^{\alpha}\right)}{(2\alpha-1-\lambda)}dx$$

$$=\frac{(\alpha-1)(2\alpha-1)(2\alpha-(1+\lambda)(1+r))}{(\alpha-r-1)(2\alpha-\lambda-1)(2\alpha-r-1)}x_m^r$$

We note that

$E(X^r)\to\infty$ as $x\to\infty$ and at $\alpha\le\frac{1+\lambda}{2}$, or $\alpha\le(r+1)$, or $\alpha\le\frac{1+r}{2}$ for $r\epsilon Z^+$.

Therefor $E(X^r)$ does not exist for $\alpha\le\frac{1+\lambda}{2}$, or $\alpha\le(r+1)$, or $\alpha\le\frac{1+r}{2}$ for $r\epsilon Z^+$,only.

Now ifr=1,then the mean

$$\mu = E(X) = \frac{(\alpha-1)(2\alpha-1)\big(2\alpha-2(1+\lambda)\big)}{(2\alpha-1-\lambda)(\alpha-2)(2\alpha-2)}x_m = \frac{(2\alpha-1)(\alpha-1-\lambda)}{(2\alpha-1-\lambda)(\alpha-2)}x_m$$

$$E(X^2) = \frac{(\alpha-1)(2\alpha-1)\big(2\alpha-3(1+\lambda)\big)}{(2\alpha-1-\lambda)(\alpha-3)(2\alpha-3)}x_m^2$$

$$\sigma^2 = E(X^2) - [E(X)]^2$$

$$= \frac{(2\alpha-1)}{(2\alpha-1-\lambda)}x_m^2\left(\frac{(\alpha-1)\big(2\alpha-3(1+\lambda)\big)}{(\alpha-3)(2\alpha-3)} - \frac{(2\alpha-1)(\alpha-1-\lambda)^2}{(2\alpha-1-\lambda)(\alpha-2)^2}\right) \blacksquare$$

Proposition (3)

If X has the WTPD(x;α,λ) with $|\lambda|\leq 1$, then the rth central moment about the mean μ is defined as

$$\mathrm{E}(X-\mu)^r = \sum_{j=0}^{r} \mathrm{C}_j^r\,(-\mu)^{r-j}\,\frac{(\alpha-1)(2\alpha-1)\big(2\alpha-(1+\lambda)(1+j)\big)}{(2\alpha-1-\lambda)(\alpha-j-1)(2\alpha-j-1)}x_m^j \quad (12)$$

And the coefficients of variation, skewness, kurtosis are as respectively

$$CV. = \frac{\sqrt{\frac{(2\alpha-1)}{(2\alpha-1-\lambda)}\left(\frac{(\alpha-1)(2\alpha-3(1+\lambda))}{(\alpha-3)(2\alpha-3)} - \frac{(2\alpha-1)(\alpha-1-\lambda)^2}{(2\alpha-1-\lambda)(\alpha-2)^2}\right)}}{\frac{(2\alpha-1)(\alpha-1-\lambda)}{(2\alpha-1-\lambda)(\alpha-2)}} \quad (13)$$

$$CS. = \frac{\frac{1}{(\alpha-2)}\left[\frac{(\alpha-1)(\alpha-2(1+r))}{(\alpha-4)} - 3\frac{(\alpha-1)(2\alpha-3(1+\lambda))(2\alpha-1)(\alpha-1-\lambda)}{(\alpha-3)(2\alpha-3)(2\alpha-1-\lambda)} + 4\frac{(2\alpha-1)^2(\alpha-1-\lambda)^3}{\big((2\alpha-1-\lambda)(\alpha-2)\big)^2}\right]}{\left(\frac{(2\alpha-1)}{(2\alpha-1-\lambda)}\right)^2\left[\frac{(\alpha-1)(2\alpha-3(1+\lambda))}{(\alpha-3)(2\alpha-3)} - \frac{(2\alpha-1)(\alpha-1-\lambda)^2}{(2\alpha-1-\lambda)(\alpha-2)^2}\right]^{3/2}} \quad (14)$$

$$CK. = \frac{\frac{w_2x_m^4}{w_3}\left[\frac{w_1(2\alpha-5(1+\lambda))}{(\alpha-5)(2\alpha-5)} - 4\frac{w_1w_2(\alpha-2(1+r))w_4}{w_3(\alpha-4)(\alpha-2)^2} + 6\left(\frac{w_2w_4}{w_3(\alpha-2)}\right)^2\frac{w_1(2\alpha-3(1+\lambda))}{(\alpha-3)(2\alpha-3)} - 3\frac{(w_2)^3(w_4)^4}{(w_3)^3(\alpha-2)^4}\right]}{\left[\frac{w_2}{w_3}\left(\frac{w_1(2\alpha-3(1+\lambda))}{(\alpha-3)(2\alpha-3)} - \frac{w_2(w_4)^2}{w_3(\alpha-2)^2}\right)x_m^2\right]^2} \quad (15)$$

Where

$$w_1 = (\alpha-1), w_2 = (2\alpha-1), w_3 = (2\alpha-1-\lambda), w_4 = (\alpha-1-\lambda)$$

Proof

$$E(X-\mu)^r = \int_{x_m}^{\infty}(x-\mu)^r\,\frac{x_m^{\alpha-1}x^{-\alpha}(\alpha-1)(2\alpha-1)\left[1-\lambda+2\lambda\left(\frac{x_m}{x}\right)^{\alpha}\right]}{(2\alpha-1-\lambda)}dx$$

$$= \frac{(\alpha-1)(2\alpha-1)}{(2\alpha-1-\lambda)}\left[(1-\lambda)x_m^{\alpha-1}\int_{x_m}^{\infty}(x-\mu)^r x^{-\alpha}dx + 2\lambda x_m^{2\alpha-1}\int_{x_m}^{\infty}(x-\mu)^r x^{-2\alpha}dx\right]$$

$$= \sum_{j=0}^{r}\mathrm{C}_j^r\,(-\mu)^{r-j}\,\frac{(\alpha-1)(2\alpha-1)\big(2\alpha-(1+\lambda)(1+j)\big)}{(2\alpha-1-\lambda)(\alpha-j-1)(2\alpha-j-1)}x_m^j$$

Then 1st ,2nd, 3rdcentral moments about the mean μ are defined as

$$\mathrm{E}(X-\mu)^2 = \frac{(2\alpha-1)}{(2\alpha-1-\lambda)}\left(\frac{(\alpha-1)\big(2\alpha-3(1+\lambda)\big)}{(\alpha-3)(2\alpha-3)} - \frac{(2\alpha-1)(\alpha-1-\lambda)^2}{(2\alpha-1-\lambda)(\alpha-2)^2}\right)x_m^2 = \sigma^2$$

$$E(X-\mu)^3 = E(X^3 - 3X^2\mu + 3X\mu^2 + \mu^3)$$

$$= \frac{(2\alpha-1)x_m^3}{(2\alpha-1-\lambda)(\alpha-2)}\left[\frac{(\alpha-1)\big(\alpha-2(1+r)\big)}{(\alpha-4)} - 3\frac{(\alpha-1)\big(2\alpha-3(1+\lambda)\big)(2\alpha-1)(\alpha-1-\lambda)}{(\alpha-3)(2\alpha-3)(2\alpha-1-\lambda)} + 4\frac{(2\alpha-1)^2(\alpha-1-\lambda)^3}{\big((2\alpha-1-\lambda)(\alpha-2)\big)^2}\right]$$

$$E(X-\mu)^4 = E(X^4 - 4\mu X^3 + 6\mu^2X^2 - 4\mu^3X + \mu^4)$$

$$= \frac{(2\alpha-1)x_m^4}{(2\alpha-1-\lambda)}\left[\frac{(\alpha-1)\big(2\alpha-5(1+\lambda)\big)}{(\alpha-5)(2\alpha-5)} - 4\frac{(\alpha-1)(2\alpha-1)\big(\alpha-2(1+r)\big)(\alpha-1-\lambda)}{(2\alpha-1-\lambda)(\alpha-4)(\alpha-2)^2} + 6\left(\frac{(2\alpha-1)(\alpha-1-\lambda)}{(2\alpha-1-\lambda)(\alpha-2)}\right)^2\frac{(\alpha-1)\big(2\alpha-3(1+\lambda)\big)}{(\alpha-3)(2\alpha-3)} - 3\frac{(2\alpha-1)^3(\alpha-1-\lambda)^4}{(2\alpha-1-\lambda)^3(\alpha-2)^4}\right]$$

So that

CV=σ/μ

$$= \frac{\sqrt{\frac{(2\alpha-1)}{(2\alpha-1-\lambda)}\left(\frac{(\alpha-1)\big(2\alpha-3(1+\lambda)\big)}{(\alpha-3)(2\alpha-3)} - \frac{(2\alpha-1)(\alpha-1-\lambda)^2}{(2\alpha-1-\lambda)(\alpha-2)^2}\right)}}{\frac{(2\alpha-1)(\alpha-1-\lambda)}{(2\alpha-1-\lambda)(\alpha-2)}}$$

$$CS = \frac{E(X-\mu)^3}{\sigma^3}$$

$$= \frac{\frac{1}{(\alpha-2)}\left[\frac{(\alpha-1)\big(\alpha-2(1+r)\big)}{(\alpha-4)} - 3\frac{(\alpha-1)(2\alpha-3(1+\lambda))(2\alpha-1)(\alpha-1-\lambda)}{(\alpha-3)(2\alpha-3)(2\alpha-1-\lambda)} + 4\frac{(2\alpha-1)^2(\alpha-1-\lambda)^3}{\big((2\alpha-1-\lambda)(\alpha-2)\big)^2}\right]}{\left(\frac{(2\alpha-1)}{(2\alpha-1-\lambda)}\right)^2\left[\frac{(\alpha-1)(2\alpha-3(1+\lambda))}{(\alpha-3)(2\alpha-3)} - \frac{(2\alpha-1)(\alpha-1-\lambda)^2}{(2\alpha-1-\lambda)(\alpha-2)^2}\right]^{3/2}}$$

$$CK = \frac{E(X-\mu)^4}{\sigma^4}$$

$$= \frac{\frac{w_2x_m^4}{w_3}\left[\frac{w_1(2\alpha-5(1+\lambda))}{(\alpha-5)(2\alpha-5)} - 4\frac{w_1w_2(\alpha-2(1+r))w_4}{w_3(\alpha-4)(\alpha-2)^2} + 6\left(\frac{w_2w_4}{w_3(\alpha-2)}\right)^2\frac{w_1(2\alpha-3(1+\lambda))}{(\alpha-3)(2\alpha-3)} - 3\frac{(w_2)^3(w_4)^4}{(w_3)^3(\alpha-2)^4}\right]}{\left[\frac{w_2}{w_3}\left(\frac{w_1(2\alpha-3(1+\lambda))}{(\alpha-3)(2\alpha-3)} - \frac{w_2(w_4)^2}{w_3(\alpha-2)^2}\right)x_m^2\right]^2}$$

We suppose that:

$$w_1 = (\alpha - 1), w_2 = (2\alpha - 1), w_3 = (2\alpha - 1 - \lambda), w_4 = (\alpha - 1 - \lambda)$$

3.3.2. Moment Generating Function:

Proposition (4)

If a X random variable is distributed WTPD(x;α,λ) with $|\lambda| \leq 1$, then the moment generating function of X is

$$M_x(t) = \sum_{r=0}^{\infty} \frac{t^r}{r!} \frac{(\alpha-1)(2\alpha-1)(2\alpha-(1+\lambda)(1+r))}{(2\alpha-1-\lambda)(\alpha-r-1)(2\alpha-r-1)} x_m^r \quad (16)$$

Proof: Using the moment generating function, then

$$M_x(t) = \int_{x_m}^{\infty} e^{tx} g_{WTPD}(x;\alpha,\lambda)\, dx$$

$$= \int_{x_m}^{\infty} e^{tx} \frac{x_m^{\alpha-1} x^{-\alpha} (\alpha-1)(2\alpha-1)\left(1-\lambda+2\lambda\left(\frac{x_m}{x}\right)^{\alpha}\right)}{(2\alpha-1-\lambda)} dx$$

$$= \int_{x_m}^{\infty} \sum_{r=0}^{\infty} \frac{(tx)^r}{r!} g_{WTPD}(x;\alpha,\lambda)\, dx$$

Since $e^{tx} = \sum_{r=0}^{\infty} \frac{(tx)^r}{r!}$

$$M_x(t) = \frac{(\alpha-1)(2\alpha-1)}{(2\alpha-1-\lambda)} \sum_{r=0}^{\infty} \frac{t^r}{r!} \left[\int_{x_m}^{\infty} x_m^{\alpha-1} x^{r-\alpha} \left(1-\lambda+2\lambda\left(\frac{x_m}{x}\right)^{\alpha}\right) dx \right]$$

$$= \frac{(\alpha-1)(2\alpha-1)}{(2\alpha-1-\lambda)} \sum_{r=0}^{\infty} \frac{t^r}{r!} \left[(1-\lambda) \int_{x_m}^{\infty} x_m^{\alpha-1} x^{r-\alpha} dx + 2\lambda \int_{0}^{\infty} x_m^{2\alpha-1} x^{r-2\alpha} dx \right]$$

$$= \frac{(\alpha-1)(2\alpha-1)}{(2\alpha-1-\lambda)} \sum_{r=0}^{\infty} \frac{t^r}{r!} \left[(1-\lambda) \frac{x_m^r}{\alpha-r-1} + 2\lambda \frac{x_m^r}{2\alpha-r-1} \right]$$

$$= \sum_{r=0}^{\infty} \frac{t^r}{r!} \frac{(\alpha-1)(2\alpha-1)(2\alpha-(1+\lambda)(1+r))}{(2\alpha-1-\lambda)(\alpha-r-1)(2\alpha-r-1)} x_m^r \blacksquare$$

3.4. Order Statistic:

Proposition (5)

Let $X_1,\ldots,X_n$ denote a random sample from a WTPD distribution, then the pdf of the rth order statistic is given by

$$f_{i,n}(x) = \frac{n!}{(i-1)!(n-i)!} g_{WTPD}(x;\alpha,\lambda) (G_{WTPD}(x;\alpha,\lambda))^{i-1} [1 - G_{WTPD}(x;\alpha,\lambda)]^{n-i} \quad ()$$

And the pdfs of the minimum, the maximum and the median respectively are defined as follows

If i=1we have the pdf of the minimum

$$f_{1,n}(x) = n \frac{x_m^{\alpha-1} x^{-\alpha} (\alpha-1)(2\alpha-1)\left(1-\lambda+2\lambda\left(\frac{x_m}{x}\right)^{\alpha}\right)}{(2\alpha-1-\lambda)} \left[\frac{(\alpha-1)(2\alpha-1)}{(2\alpha-1-\lambda)} x_m^{\alpha-1} x^{-\alpha+1} \left(\frac{(1-\lambda)}{(\alpha-1)} + \frac{2\lambda}{(2\alpha-1)} \left(\frac{x_m}{x}\right)^{\alpha} \right) \right]^{n-1}$$

If i=n we have the pdf of the maximum

$$f_{n,n}(x) = n \frac{x_m^{\alpha-1} x^{-\alpha} (\alpha-1)(2\alpha-1)\left(1-\lambda+2\lambda\left(\frac{x_m}{x}\right)^{\alpha}\right)}{(2\alpha-1-\lambda)} \left(1 - \frac{(\alpha-1)(2\alpha-1)}{(2\alpha-1-\lambda)} x_m^{\alpha-1} x^{-\alpha+1} \left(\frac{(1-\lambda)}{(\alpha-1)} + \frac{2\lambda}{(2\alpha-1)} \left(\frac{x_m}{x}\right)^{\alpha} \right) \right)^{n-1}$$

And if i=m+1we have the pdf of the median

$$f_{m+1,n}(x) = \frac{n!}{m!\,(n-m-1)!} \frac{x_m^{\alpha-1} x^{-\alpha} (\alpha-1)(2\alpha-1)\left(1-\lambda+2\lambda\left(\frac{x_m}{x}\right)^{\alpha}\right)}{(2\alpha-1-\lambda)} \left(1 - \frac{(\alpha-1)(2\alpha-1)}{(2\alpha-1-\lambda)} x_m^{\alpha-1} x^{-\alpha+1} \left(\frac{(1-\lambda)}{(\alpha-1)} + \frac{2\lambda}{(2\alpha-1)} \left(\frac{x_m}{x}\right)^{\alpha} \right) \right)^{m} \left(\frac{(\alpha-1)(2\alpha-1)}{(2\alpha-1-\lambda)} x_m^{\alpha-1} x^{-\alpha+1} \left[\frac{(1-\lambda)}{(\alpha-1)} + \frac{2\lambda}{(2\alpha-1)} \left(\frac{x_m}{x}\right)^{\alpha} \right] \right)^{n-m-1}$$

4. Conclusions:

We has found new lifetime distribution, weighted transmuted Pareto, which is similar to pdf of WTPD with weight $\frac{(\alpha-1)(2\alpha-1)}{(2\alpha-1-\lambda)}$ for $|\lambda| \leq 1, \alpha > 0$; and with slightly difference.

The limit of hazard rate function of weighted transmuted Pareto distribution equal to the limit of the pdf of WTPD as x→x_m and as x→∞ respectively. It has single mode. And we can find its variance using the central moments about the origin, and about the mean directly. Also we can find its the central moments about the origin using the moment generating function.

References:

[1] Fisher, R.A. The effects of methods of ascertainment upon the estimation of frequencies, The Annals of Eugenics 6, 13–25, (1934).

[2] Rao, C.R. Stat istics And Truth Putting Chance to Work, World Scientific Publishing Co. Pte.Ltd. Singapore, (1997).

[3] Shaw, W.T. and Buckley, I. R. C. The Alchemy of Probability Distributions: beyond Gram-Charlier Expansions, and a Skew-Kurtotic-Normal Distribution from a Rank Transmutation Map, (2009).
Available at http://arxiv.org/pdf/0901.0434.pdf.

[4] Das, K. K and Deb Roy, T. On Some Length-Biased Weighted Weibull Distribution, Pelagia Research Library Advances in Applied Science Research, Vol.2 ,No.5, pp: 465-475, (2011).

[5] Shi, X.; Oluyede, B. O and Pararai, M. Theoretical Properties of Weighted Generalized Rayleigh and Related Distributions, Theoretical Mathematics & Applications, Vol.2, No.2, pp: 45-62, ISSN: 1792-9687 (print), 1792-9709 ,(online) International Scientific Press, (2012).

[6] AbedAl-Kadim, K. and Hantoosh, A. F. Double Weighted Distribution and Double Weighted Exponential Distribution, Mathematical Theory and Modeling, Vol.3, No.5, ISSN 2224-5804 (Paper), ISSN 2225-0522 (Online), (2013).

[7] Mir, K. A.; Ahmed, A. and Reshi, J. A. Structural Properties of length biased Beta distribution of first kind, American Journal of Engineering Research (AJER), Vol.2, Issue-2, pp: 1-6, e-ISSN: 2320-0847, p-ISSN: 2320-0936, (2013).

[8] Rash wan, N. I. The Double Weighted Rayleigh Distribution Properties and Estimation, International Journal of Scientific & Engineering Research Vol.4, Issue 12, ISSN 2229-5518, (2013).

[9] Ahmad, A., Ahmad, S.P and Ahmed, A. Characterization and Estimation of Double Weighted Rayleigh Distribution, Journal of Agriculture and Life Sciences, Vol.1, No. 2 , ISSN 2375-4214 (Print), 2375-4222 (Online), (2014).

[10] Abed Al-Kadim, K. and Hussein, N. A. New Proposed Length-Biased Weighted Exponential and Rayleigh Distribution with Application, Mathematical Theory and Modeling, Vol.4, No.7, ISSN 2224-5804 (Paper), ISSN 2225-0522 (Online), (2014).

[11] Seenoi, P., Supapakorn, T. and Bodhisuwan, W. The length-biased exponentiated inverted Weibull distribution, International Journal of Pure and Applied Mathematics Vol. 92, No. 2, pp: 191-206, (2014).

[12] Merovcia F.,and Pukab L., Transmuted Pareto distribution, ProbStat Forum, Volume 07, January, Pages 1–11, (2014).

Influence of Number of Blows and Water Content onE Engineering Properties of Compacted gypseous Soi

Israa Saleh Hussein
Civil Engineering Department, Engineering Collage, Tikrit University, Iraq.

Received Date: 21 / 1 / 2016
Accepted Date: 10 / 1 / 2017

الخلاصة

ان المشكلة الرئيسية في إعادة تمثيل التربة الجبسية مختبرياً تعود إلى كون الجبس يعمل كمادة رابطة بين جزيئات التربة مما يمنح التربة الجبسية تماسكاً قوياً. إلا ان هذه الرابطة تنكسر ويكون من الصعب إعادتها إلى وضعها الحقيقي عند إعادة رص التربة بالطرق الاعتيادية حيث تنخفض قيمتي التماسك وزاوية الاحتكاك الداخلي للنماذج المعاد رصها بشكل واضح عن قيمها الحقلية. لذلك تم اقتراح دراسة إمكانية إعادة نمذجة التربة الجبسية ومحاولة معرفة مدى تأثير عدد الضربات لكل طبقة رص وتأثير قيمة المحتوى الرطوبي على قيمة كل من التماسك وزاوية الاحتكاك الداخلي من اجل تسهيل اعادة نمذجة التربة الجبسية مختبرياً ومحاكاة تصرفها حقلياً. تم اجراء فحص الحدل على التربة بعدد ضربات (30,25,15) ضربة لكل طبقة حدل ولقيم مختلفة للمحتوى الرطوبي لكل حالة لمعرفة تأثير عدد الضربات لكل طبقة حدل وكذلك معرفة تأثير المحتوى الرطوبي على قيمتي التماسك وزاوية الاحتكاك الداخلي للتربة. تم استخدام ثلاث قيم مختلفة من المحتوى ألجبسي (18.9, ,60%) حيث اخذت من ثلاث اماكن مختلفة في مدينة تكريت والواقعة في محافظة صلاح الدين وسط العراق . وتم التوصل في هذا البحث الى ان الزيادة في عدد الضربات والمحتوى الرطوبي تؤدي الى زيادة كل من قيمتي التماسك وزاوية الاحتكاك الداخلي. كما أن العدد الأمثل للضربات كان (30) ضربة لثلاث نسب مختلفة من المحتوى ألجبسي ولكن المحتوى الرطوبي الأمثل يزداد بزيادة نسبة الجبس حيث كان (7, 12, 15) ٪ لثلاث نسب جبس مختلفة (18.9, 32.4 ,60)٪ بالتتابع من اجل إعادة قولبة التربة المستخدمة في البحث. لذا يمكن القول ان تغيير نسبة الجبس في التربة لم يؤثر تأثيراً واضحاً على عدد الضربات الأمثل ولكن زيادة نسبة الجبس أدت إلى زيادة ملحوظة في المحتوى الرطوبي الأمثل لإعادة القولبة..

الكلمات المفتاحية

التربة الجبسية، إعادة النمذجة مختبريا، عدد الضربات، المحتوى الرطوبي.

Abstract

The main problem in laboratory re-molded gypseous soil is that, gypsum material in soil do as bounded material between soil particles which increases soil strength. But these bounding between soil particles would be broken when attempts to re-compact soil and made it difficult to return to its origin state. As a results, the value of cohesion and angle of internal friction would be changed for samples which that re-compacted using the ordinary compaction method comparing with the field values. In this study, compaction test was used with different blows number (15, 25, 30) for each layer. Different value of water content are used for each case to record the effect of numbers of blows and water content on thecohesion and angle of internal friction. Three different gypsum content samples (18.9%, 32.4%, 60%) are used in this study which taken from three different locations in Tikrit city - Salah-Aldeen Governorate, in the middle of Iraq. The results of laboratory tests for re-molded gypseous soil show that increasing number of blows and water content leads to increase cohesion and angle of internal friction. Also, the optimum blows number per layer was (30) for the three percent of gypsum content. But the optimum water content increased with increasing gypsum content to (7%, 12%, 15%) for the three values of gypsum content (18.9%, 32.4%, 60%) respectively, to obtain laboratory value of cohesion and angle of internal friction close to the field value. So it could be notice that, changing gypsum content in soil had no effect on the optimum number of blow for laboratory re-molded gypseous soil. But increasing gypsum content leads to increase optimum water content.

Keywords

Gypseous Soil, Laboratory Re-Sampling, Number of Blows, Water Content

1. Introduction

Gypseous soil is that soil which contains enough gypsum(CaSO4.2H2O) which effected onengineering construction. I t is the worst among the problematic soils as it contains soluble salt and its chemical reactions. Gypseous soil in Iraq covers (11 to 15) % of the area of Iraq [1].

One of the most complicatedengineering problems isthe presence of gypsum in the soils due to its detrimental behavior, especially when accompanied by environmental changes in temperature, water content and presence of certain types of salts. Therefore, some teqniques are needed to improve these soils before constructing on it [2].

Many studies have been made to investigate the effect of gypsum content on the physical and mechanical properties of gypseous soils. These soils arecharacterized by high void ratios and low dry densities. Accor dingly, upon wetting gypseous soil is renowned for being highly compressible material with low bearingcapacity and hence considered among the poorest of foundation material [3,4].

In the last decades many attempts have been made to understand the behavior of these soils. Most of these attempts were laboratory and field investigations. Obtaining undisturbed samples of gypseous soils is in many cases very difficult. This leds many researchers to prepare the gypseous soils in the laboratory. The behavior of gypseous soils in the laboratory is highly complicated and different behaviors were noted. This caused a conflict in understanding the phenomena related to the gypseous soils [5].

Compaction is one of the methods are used to improve the engineering properties of the soil mass which occurs through increasing strength, reducing compressibility, volume change and permeability, and increasing the stability of structures [6,7].

This study deals with the effect of number of compaction blows (N) and water content (w c) on the engineering properties of gepyseous soil that re-compacted in the laboratory specially (c) and (φ) for different values of gypsum content.

2. Experimental Work:

2.1. Sampling:

Three types of natural gypsuous soils taken from three different locations in Tikrit city - Salah-Aldeen Governorate, in the middle of Iraqwhich used in this study . Samples (S1), (S2) and (S3) with three different values of gypsum content (18.9%, 32.4%, 60%) respectively, were taken from depth of (1.5-2) m below the natural ground surface. Two types of samples, disturbed and undisturbed packed and transported to the soil mechanics laboratory, Civil Eng. Dept., College of Engineering, Tikrit University. Samples prepared for the testing program and tested according to the American Society for Testing and Materials Specifications (ASTM) [8] and British Standards (BS) [9].

2.2. Laboratory Testing Program:

2.2.1. Classification and Engineering Tests:

The grain size distribution for the three soils (distributed sample) are shown in Fig. (1). Also the physical and chemical properties are shown in Tables (1) and (2).

Table (1): Physical properties of the soils

Property	S1	S2	S3
Natural Water Content (wc)%	5.7	4.3	2.9
Specific Gravity	2.35	2.64	2.42
Liquid Limit (L.L)	28	24	N.L
Plastic Limit (P.L)	N.P	N.P	N.P
Plasticity Index (P.I)	N.P	N.P	N.P
Dry Unit Weight(γ_d) kN/m^3	13.8	14	14.8

Table (2): Chemical properties of the soils

Property	S1	S2	S3
PH	8.9	7.4	8.1
Gypsum Content (Gyp.)%	18.9	32.4	60
Total Soulble Salt (T.S.S)%	32.7	38	67.4

The three soils were classified as poorly graded sand (SP) according to the Unified Soil Classification System (USCS). The angle of internal friction (φ) and apparent cohesion (c) for undisturbed sample taken from the field-shown in Table (3) and for disturbed samples shown in Tables (4), (5) and (6). Direct shear test were conducted according to the ASTM (D3080-72) [10], under normal pressures of 50, 100 and 200kPato determine the shear strength parameters cohesion and angle of internal friction.

A calibrated proving ring at (2.5kN) capacity and (2mm) precision dial gage, for vertical deformation (0.01 mm) precision dial gage was used while for horizontal deformation (0.01 mm) dial gage was used. The rate of strain was (0.6 mm/min). The shear stress and vertical displacement were plotted against horizontal displacement for each test. From which, the shear stress versus normal stress was obtained and the strength parameters, the

cohesion intercept (c) and the angle of internal friction (φ) determined.

Table (3): Engineering properties of the soils

Property	S1	S2	S3
Apparent Cohesion (c) kN/m2	29	39	54.1
Angle of Internal Friction (ϕº)	24.6	40	30.7

2.2.2. Re-mouded of Gypseous Soil:

The main problem in laboratory re-molded gypseous soil is a great difference in field and laboratory values of both (c) and (φ). The gypsum works as a binding agent between soil particles. Therefore, it has a significant effect on the cohesion and strength of gypseous soil. In case of refraction this binding and try to re-compaction soil in the laboratory, the distribution of gypsum in soil would be differ and would not works as a binding agent to soil particles which leading to a significant reduction in laboratory value of (c) and (φ). So, it is important to study the possibility of re-molded gypseous soil tofind how many blows numbers per layer (N) and water content (w c) values effected on (c) and (φ), reach to the field values of (c) and (φ) and to facilitate the formation models in laboratory studies and scientific research to simulate the disposal field gypseous soil. In this study, compaction test for disturbing soil samples with number of blows(N) (15, 25, 30) for each layer and different values of water content (w c) are prepared. Then re-molded soil ret urn to the value of its field moisture by drying it with percent of error not exceed (3%). Compaction test was performed for each case in order to investigate the effect different number of blows and water content on the fundamental characteristics of soil.

2.2.3 Compaction Test:

Compaction tests are carried out for the gypseous soil to determine the moisture-unit weight relationship. Samples are compacted in three equal layers each hammered by (15, 25, 30) blows using (2.5) kg hammer dropped from (30.5) mm height. These samples are compacted in a mold of(101.6) mm in diameter and (115.5)mm in height.

3. Results and Discussion:

3.1 Effect of Number of Blows:

The effect of number of blows (N) on engineering properties of gypseous soil (c, φ) was investigated. Number of blows (15, 25, 30) per layer for each value of water content (wc) with three percent of gypsum content (18.9%, 32.4%, 60%) were studied and the results are shown in Tables (4), (5) and (6).

Table (4): Engineering properties for re-representation soil (gypsum content 18.9%)

Water Content (%)	Number ofBlows (N)	c (kN/m2)	φ (deg)	γd (kN/m3)
7	15	16	20.3	13.1
7	25	21	22	13.4
7	30	27.4	26.2	13.5
10	15	19	26	13.8
10	25	24	27	14
10	30	33	35	14.6
12	15	20.4	29.2	12.9
12	25	28.6	30.1	13.2
12	30	35.4	39.6	14.0

Table (5): Engineering properties for re-representation soil (gypsum content 32.4%)

(%) Water Content	(Number of Blows (N	(c (kN/m2	(ϕ (deg	(γd (kN/m3
10	15	21	27.2	11.1
10	25	27.2	32.5	12.2
10	30	34.1	36.86	13.0
12	15	26.3	32.8	13.4
12	25	33.5	37.62	13.85
12	30	40.3	41.8	14.3
15	15	32.52	37.04	12.12
15	25	38.7	42.27	13.3
15	30	44.69	43.97	14.0

Table (6): Engineering properties for re-representation soil (gypsum content 60%)

(%) Water Content	(Number of Blows (N	(c (kN/m2	(ϕ (deg	(γd (kN/m3
12	15	32	14	11.7
12	25	40	15	12.4

12	30	45	20	13.0
15	15	40	18	12.9
15	25	50	23	14.0
15	30	52.7	28.8	14.7
17	15	42	20.3	13.0
17	25	51	26.4	14.3
17	30	54	31.7	15.0

3.1.1. Effect of number of blows on the cohesion of gypseous soil:

The results show that the cohesion of gypseous soil (c) increased with increasing the number of blows for each value of water content (wc) and gypsum content as shown in Figs. (2), (3) and (4) due to increasing convergence between soil particle with increasing number of blows. Also there was a significant increasing in cohesion (c) with increasing water content (w c) by remaining numbers of blows (N) constant due to increasing binding agent between gypsum and soil particle when it reaches to optimum moisture content which was (7%, 12%, 15%) for the three percent of gypsum content (18.9%, 32.4%, 60%) respectively. But this increasing in cohesion (c) would be disappear when excessiveincreasing in water content (wc) occurs because soil particle would be diverging and sliding each other. Also gypsum would be dissolving which led to decreasing binding agent between soil particle and decreasing the cohesion of the gypseous soil (c).

3.1.2. Effect of number of blows on the angle of internal friction of gypseous soil:

The results show that the angle of internal friction (φ) of the gypseous soil increased with increasing the number of blows for each value of water content (wc) and gypsum content as shown in Figs. (5), (6) and (7) due to increasing convergence between soil particle with increasing number of blows. Also there was a significant increasing in value of (φ) with increasing water content (wc) by remaining the value of (N) constant due to increasing binding agent between gypsum and soil particle when it reaches to optimum moisture content which was (7%, 12%, 15%) for the three percent of gypsum content (18.9%, 32.4%, 60%) respectively. But this increasing in angle of internal friction (φ) would be disappear when excessive increasing in water content (wc) occurs because soil particle would be diverging and sliding each other. Also amount of gypsum would be dissolving which led to decreasing binding agent between soil particle and decreasing the angle of internal friction (φ).

3.2. Optimum number of blow (n) and water content (wc) for re-moldedgypseous soil:

As it clear from the previous figures which describe relationship between number of blows (N) for different value of water content (wc) with each of cohesion (c) and angle of internal friction (φ) that, the optimum number of blows (N) for each layer was (30) for different values of gypsum content. But the optimum values of water content (w c) differed with each value of gypsum content. It was (7%) when the gypsum content (18.9%), (12%) when the gypsum content (32.4%) and (15%) when the gypsum content (60%) due to the convergence of laboratory values of (c, φ) with the field values. Hence, these values of number of blows (N) which was (30) blows and water content (w c) which was (7%, 12%, 15%) for the three percent of gypsum content (18.9%, 32.4%, 60%) respectively was the best value for laboratory re-representation gypseous soil. Also, the value of (γ d) was maintained to remain within the range of its field value during re-representation gypsum soil as shown in Figs. (8), (9) and (10) due to the effect of (γd) on the engineering properties of re-representation soil.

3.3. Effect of gypsum content on optimum number of blows (n) and water content (w c):

Figs. (11) and (12) show the effect of gypsum content on each optimum number of blows (N) and optimum water content (w c). As it clear from these figures, the optimum value of number of blows (N) was (30) for the three percent of gypsum content. But optimum percent of water content (w c) increases with increasing gypsum content. From that, it could bededuced that the number of blows is working on reconnecting power ionic between molecules gypsum, so the optimal number of blows remains constant with different values of gypsum content. While the value of the moisture content optimal, increases with the proportion of gypsum, because increasing the proportion of gypsum need to more amount of water to re-melt salts and configured to re-link with soil particles.

4. Conclusion:

In re-molding gypseous soil, increasing number of blow (N) leads to increase cohesion of the soil (c) and angle of internal friction (φ) within optimum limits of number of blow (N).

In re-molding gypseous soil, increasing water content (wc) leads to increase cohesion (c) and angle of internal friction (φ) of the soil within optimum limits of water content (wc). In other words, when water content (wc) exceeds optimum percent, this would be lead to collapse of infrastructure and melting association gypsum between soil particle.

In re-molding gypseous soil, increasing gypsum content had no effect on optimum numbers of blows (N) which was (30) blow per layer, but optimum water content increases with increasing gypsum content.

References

[1] Jawad, Y., Abd Al-Jabbar, M.: " Effect of Compaction on the Behaviour of Kirkuk Gypseous Soil" Journal of Engineering, N.4. V. 13, P.P1-20, (2006).

[2] Aziz, H.Y.: "Gypseous Soil Improvement using Fuel Oil", World Academy of Science, Engineering and Technology 51, (2011).

[3] Aiban, S.A. and Al-Ahmadi, H.M.: ''Effect of geotextile and cement on the performance of Sabkha sub grade ''Building and Environment 41,PP.440-447, (2006).

[4] Al-Amoudi,O.S.,andSahel,N.A.:"Compressibility and collapse characteristics ofarid saline Sabkha soils'' Eng. Geology,Vol.39,PP.185-202, (1995).

[5] Al- Mufty, A.A.: "Effect of Gypsum Dissolution on the Mechanical Behavior of Gypseous Soils", Ph.D. thesis, Dept. Civil Eng., Baghdad University, (1997).

[6] Lambe, T.W., Whitman, R.V., Soil Mechanics) Inc., John Wiley and sons (New York, (1979).

[7] Holtz, R.D., Kovacs, W.D., An Introduction to Geotechnical Engineering (Printice-Hall) Inc., Englewood Cliffs, New Jersey, (1982).

[8] ASTM Standers, Soil and Rock (I), Volume 04.08, 2003.

[9] BS 1377 British Standard Institution, Method of Testing Soil for Civil Engineering Purposes, London, (1975).

[10] Head K.H.: "Manual of Soil Lab. Testing", Vol.2, Pentech Press, London, (1982).

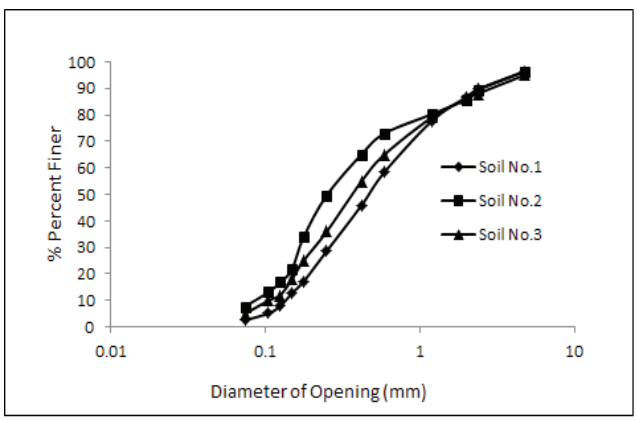

Fig. (1): Grain size distribution for the soils

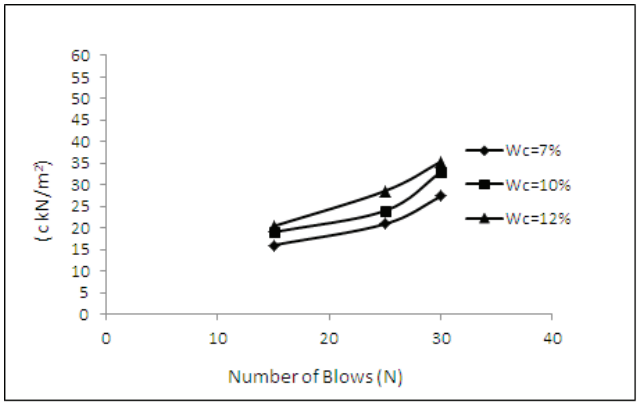

Fig. (2): Effect of number of blows (N) on the cohesion (gypsum content 18.9%)

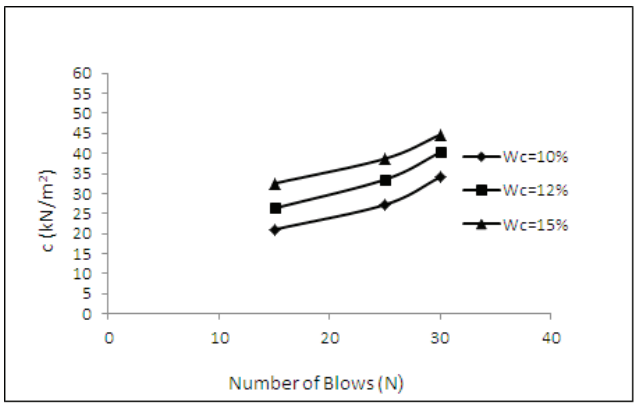

Fig. (3): Effect of number of blows (N) on the cohesion (gypsum content 32.4%)

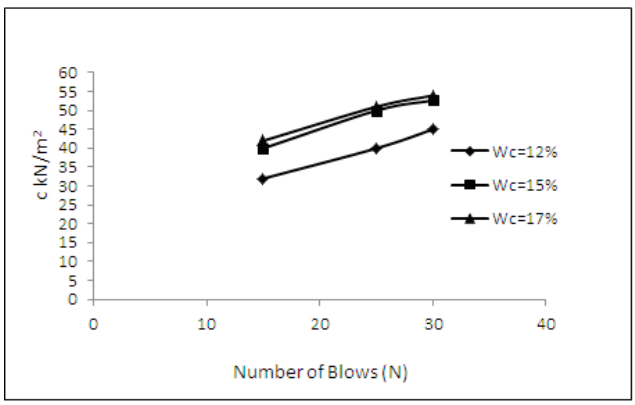

Fig. (4): Effect of number of blows (N) on the cohesion (gypsum content 60%)

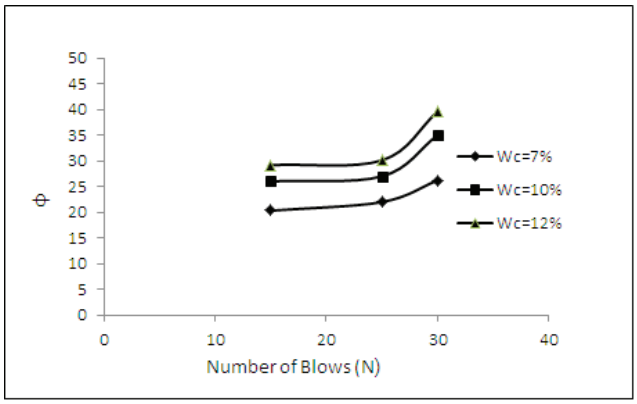

Fig. (5): Effect of number of blows (N) on the angle of internal friction (gypsum content 18.9%)

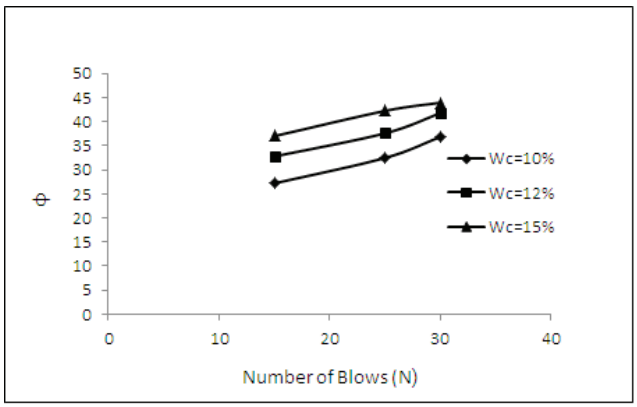

Fig. (6): Effect of number of blows (N) on the angle of internal friction (gypsum content 32.4%)

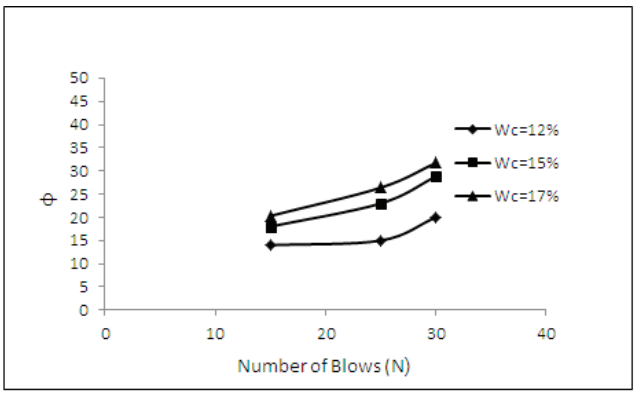

Fig. (7): Effect of number of blows (N) on the angle of internal friction (gypsum content 60%)

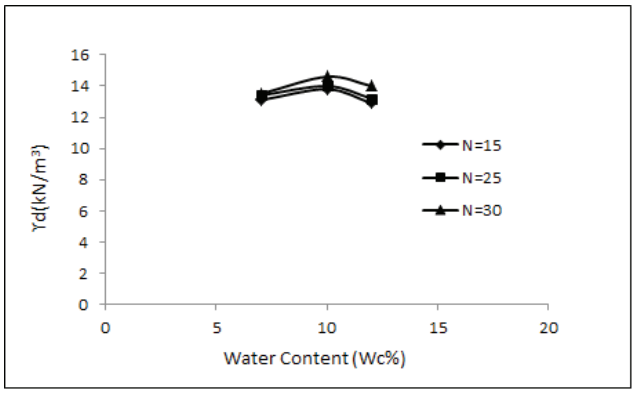

Fig. (8): Water content and dry density relationship (gypsum content 18.9%)

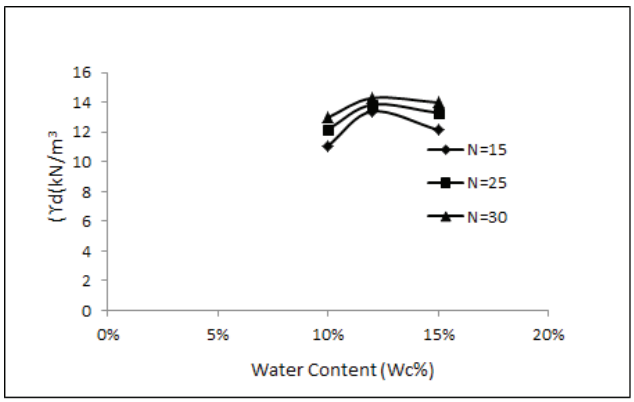

Fig. (9): Water content and dry density relationship (gypsum content 32.4%)

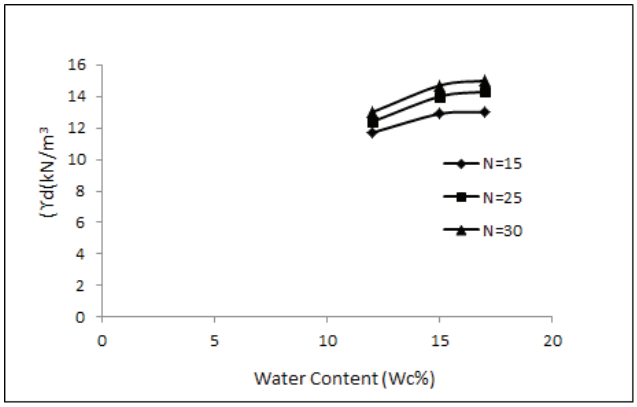

Fig. (10): Water content and dry density relationship (gypsum content 60%)

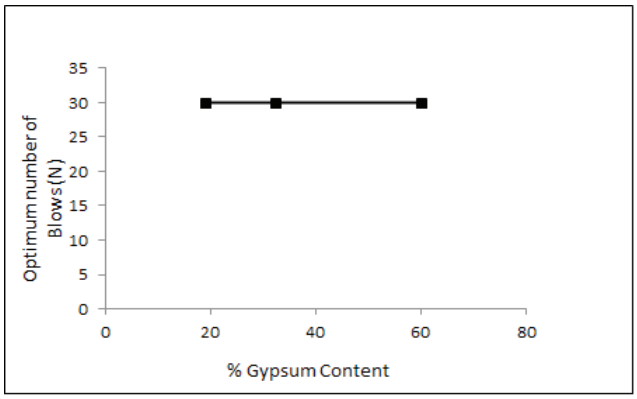

Fig. (11): Effect of gypsum content on optimum number of blows (N)

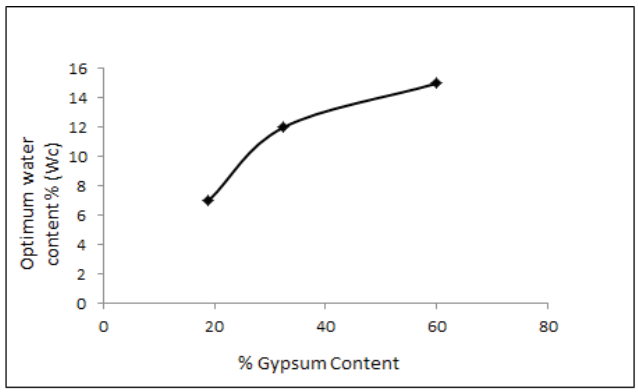

Fig. (12): Effect of gypsum content on optimum water content (wc)

Molecular Docking of Some Peptides to Varicella Zoster Virus Drug Targets

Abo Almaali, H. M.
Branch of Clinical Laboratory Sciences, College of Pharmacy, Kerbala University, Iraq.

Received Date: 1 / 9 / 2016
Accepted Date: 31 / 7 / 2017

الخلاصة

يعد فيروس الحماق النطاقي (جدري الماء)، فيروس الهربس الموجه للعصب، هو العامل المسبب لكلاً من الحماق (جدري الماء) والنطاقي (القوباء المنطقية). كما هو الحال مع فيروسات الهربس الاخرى، جدري الماء يسبب كلا الأمراض الحادة والامراض الكامنة مدى الحياة. وان فيروس النطاقي الحماقي هو فايروس شائع خلال مرحلة الطفولة وخاصة في المناخات المعتدلة. الحماق عادة هو مرض حميد ويشفى من تلقاء نفسه، ولكن يمكن أن يكون أكثر شدة عند البالغين والأشخاص ذوي المناعة القليلة. وان الهدف من هذه الدراسة هو التنبؤ او انتخاب أفضل الببتيدات بطريقة حاسوبية لكي يتم اثباتها تجريبيا عن طريق المختبر وتوضيح قدرتها في معالجة فايروس النطاقي الحماقي. في هذه الدراسة تم استخدام العديد من الببتيدات المضادة للميكروبات والببتيدات المضادة للفيروسات لتوقع فعالية هذه الببتيدات ضد ثلاثة أهداف من فيروس النطاقي الحماقي وهذه الاهداف تشمل Thymidine kinase (PDBID: 1OSN), Envelope glycoprotein H (PDBID:4XHJ), Protease (PDBID: 1VZV)) باستخدام نهج المعلوماتية الحيوية.

ومن ثم تم التنبؤ بقابلية ارتباط الببتيدات مع الاهداف الفيروسية باستخدام برنامج (Hex 8.0.0)على شبكة الإنترنت. بالإضافة إلى ذلك تم حساب بعض الخصائص الفيزيائية والكيميائية للببتيدات بواسطة عدة برامج محددة بها في ذلك: T cell epitope Class I immunogenicity (ToxinPred, CellPPD hydropathicit، نقطة التعادل الكهربائي PI والوزن الجزيئي، Boman index values وبرنامج anti-cp . ومن مجموع 64 ببتيد مضاد للميكروبات التي تم جمعها من عدة أبحاث ظهر ان فقد تم اختيار 11 ببتيد وذلك لامتلاكهم

شدة ارتباط جيدة مع أهداف الفيروس النطاقي الحماقي وكانت الخصائص الفيزيائية والكيميائية لهذه الببتيدات جيدة. وتشمل هذه الببتيدات: (16-Polyphemusin 2، K4S4 (1 ، F، AVP 1092، MSI-78، 1074 AVP 5.6، Dahlein 1، Magainin GLK-19، Fv16، A. وأخيرا، هناك حاجة للمزيد من التجارب المختبرية لكي يثبت ان هذه الببتيدات المضادة للفايروس يمكن ان تستخدم كدواء مضاد لفيروس الحماق النطاقي.

الكلمات المفتاحية

الحماق النطاقي، فيروس الهربس، الببتيدات.

Abstract

Varicella-zoster virus (VZV), a neurotropic herpesvirus, is the causative agent of both varicella (chickenpox) and zoster (shingles). Like another herpes viruses, the VZV can cause both acute illness and latency lifelong. In other hand, the VZV common during childhood, especially in temperate climates. Moreover, Varicella is usually a benign and self-limiting illness. But may be more severe in adults, and in patients suffering from immunedeficiency. Because of the huge information available concerning inhibitors of this virus the current study spots light on them bypredicting the best peptides that can be a candidate to offer to wet laboratory experiments sufficient data about their ability to treat VZV. To acheve this aim several antimicrobial peptides and antiviral peptides used to predict their theoretical actions against three targets of VZV, Thymidine kinase (PDBID: 1OSN), Envelope glycoprotein H (PDBID: 4XHJ), Protease (PDBID: 1VZV) using Bioinformatics approach. And the binding potential of these peptides with the VZV drug targets was predicted using online program Hex 8.0.0., and some physical and chemical properites of peptides were predicted by specific programs, including T cell epitope Class I immunogenicity software, ToxinPred software, CellPPD software, isoelectric points (PI) and molecular weight, Boman index values software, and anti-cp software. The analysis of these data resulted with that from 64 antimicrobial peptide only 11 peptides have been found have favored binding affinities with VZV targets and good physical and chemical properties, these peptides were Polyphemusin 2, K4S4(1-16) a, F, AVP1092, MSI-78, A, Fv16, GLK-19, Magainin 1, Dahlen 5.6.

Keywords

Varicella, zoster, peptides.

1. Introduction

Varicella zoster virus (VZV) is an exclusively human virus that belongs to the α-herpes virus family. The VZV present worldwide and is highly infectious. Moreover, the primary infection leads to acute varicella or "chickenpox", usually from exposure either through direct contact with a skin lesion or through airborne spread from respiratory droplets [1, 2]. In addition, more than 90% of adults in the United States acquired the disease in childhood, while the majority of children and young adults have been vaccinated with the live virus vaccine [3]. The increasing incidence of VZV in patient aged 15 years or has resulted in an increase in severe forms and in mortality, also cases of resistance to classical antiviral treatment. Unusual forms of varicella and zoster are occasionally encountered even in non-immune compromised patients. Infections of VZV are a matter of concern in high-risk groups includes immune compromised children and adults [4].

The aim of this current study is to predict the best antimicrobial peptides (AMP) that can be a candidate to offer these peptides to the laboratory experiments, to show their ability to inhibit VZV. Consequently, this aim was done by picking about 64 short peptides by gathering these sequences from the web server, and entered them in specific computer programs to know their strength for binding to receptors of VZV by molecular docking, in addition calculating the probability of cell penetrating, physicochemical properties and other parameters.

Materials and Methods

2. Materials

2.1. Short Peptides

Sixty-four short peptides sequences used to predict their anti-VZV attachment and to study their physical and chemical properties. These peptides listed below in Table 1.

Table (1): Short peptides used in current study with their sequences

No	Peptide	Sequence	Reference
9	Brevinin-1BYa	FLPILASLAAKFGPKLFCLVTKKC	[10]
10	Brevinin-1BYb	FLPILASLAAKLGPKLFCLVTKKC	[10]
11	Brevinin-1BYc	FLPILASLAATLGPKLLCLITKKC	[10]
1	A	VVKKARKAAKKVAKK	[5]
2	Alloferon 1	HGVSGHGQHGVHG	[6]
3	Alloferon 2	GVSGHGQHGVHG	[6]
4	Androctonin	RSVCRQIKICRRRGGCYYKCTNRPY	[7]
13	C	TGKIGKLKKGTGKIA	[71]
16	D	AIRRLARRGGVKRISGLI	[71]
22	FV16	KKVGTSKVVAKTVTKK	[71]
54	F	KATKATITKKPVA	[71]
37	polyphemusin II	RRWCFRVCYKGFCYRKCR	[73]
38	Protegrin PG-1	RGGRLCYCRRRFCVCVGR	[73]

43	Tachyplesin I	KWCFRVCYRGICYRRCR	[73]
48	Citropin 1.1	GLFDVIKKVASVIGGL	[74]
14	CP11	ILKKWPWWPWRRK	[11]
15	Cp10A	ILAWKWAWWAWRR	[11]
26	Indolicidin	ILPWKWPWWPWRR	[11]
17	DET1	GWVKPAKLDG	[12]
18	DET2	PWLKPGDLDL	[12]
19	DET3	IGVRPGKLDL	[12]
20	DET4	AGVKDGKLDF	[12]
21	Dahlein 5.6	GLLASLGKVFGGYLAEKLKPK	[13]
32	Maculatin 1.1	GLFGVLAKVAAHVVPAIAEHF	[13]
40	Ranatuerin-6	FISAIASMLGKFL	[13]
44	Uperin 3.6	GVIDAAKKWNVLKNLF	[13]
45	Caerin 1.1	GLLSVLGSVAKHVLPHVVPVIAEHL	[13]
46	Caerin 1.9	GLFGVLGSIAKHVLPHVVPVIAEKL	[13]
47	Caerin 4.1	GLWQKIKSAAGDLASGIVEGIKS	[13]
5	Aurein 1.2	GLFDIIKKIAESF	[8]
23	HNP-1ΔC18	IAGERRYGTIYQGRLWAF	[14]
24	HNP-1ΔC18A	IAAERRYATIYQARLWAF	[14]
25	HNP-1ΔC	AYRIPAIAGERRYGTIYQGRLWAF	[14]
27	K4S4 (1–16)a	ALWKTLLKKVLKAA	[15]
41	S4 (6–28)	TLLKKVLKAAAKAALNAVLVG	[15]
28	LfcinB	FKCRRWQWRMKKLGAPSITCVRRAF	[16]
49	AVP 1093	RRKKALLALLAP	[16]
50	AVP 1074	RRKKAAVALLPAVLLA	[16]
51	AVP 1092	RRKKPAVLLALLAP	[16]
52	AVP 1072	RRKKAAVALLPAVLLALL	[16]
53	AVP 1070	RRKKAAVALLPAVLLALLLAP	[16]
29	Limandapleu-rocidin(LmPle)	GWKKWFKKATHVGKHVGKAALDAYL	[17]
30	MRP	AIGSILGALAKGLPTLISWIKNR	[18]
31	MSI-78	GIGKFLKKAKKFGKAFVKILKK	[19]
33	Magainin I	GIGKFLHSAGKFGKAFVGEIMKS	[20]
34	Magainin II	GIGKFLHSAKKFGKAFVGEIMNS	[20]
35	P1	WLVFFVIFYFFR	[21]
36	P2	WLVFFVIFYIFR	[21]
39	RTD1	GFCRCLCRRGVCRCICTR	[21]
42	TAT-C	GRKKRRQRRRC	[22]
55	STAT 1	CTAGACTTCAGACCACACAAC	[23]
56	STAT 2	GAGGAGAAGCAATGGGTCTTAG	[23]
57	GAPdH	CACATGGCCTCCAAGGAGTAA	[23]
58	Mx 1	AAGCCTGATCTGGTGGACAAAGGA	[23]
6	B	VPKFKAGKILKQKVEKG	[9]
7	BR-C	CKLKNFAKGVAQSLLNKASKLSGQC	[9]
8	BR-D	KLKNFAKGVAQSLLNKASCKLSGQC	[9]

12	Brevinin-2R	KLKNFAKGVAQSLLNKASCKLSGQC	**[9]**
59	GLK-19	GLKKLLGKLLKKLGKLLLK	**[24]**
60	GLR-19	GLRRLLGRLLRRLGRLLLR	**[24]**
61	GLRC-1	GCRRLLGRLLRRLGRLLCR	**[24]**
62	GLRC-2	GLRCRLGRLLRR LGRCLLR	**[24]**
63	GLRC-3	GLRRLCGRLGRRLCRLLLR	**[24]**
64	GLRC-4	GCRRLCGRLGRRLCRLLCR	**[24]**

2.2. Varicella Zoster Virus Targets

Three VZV molecules were taken from protein databank website (http://www.rcsb.org/pdb/home/home.do) used in molecular docking experiment as drug targets, these molecules listed in Table 2:

Table (2): Viral molecules target with their three-dimensional structure

No.	Viral molecules	Structure	Ref.
1	Envelope glycoprotein H target (PDBID: 4XHJ)	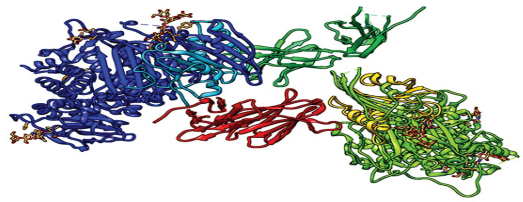	[25]
2	Thymidine kinase target (PDBID: 1OSN)	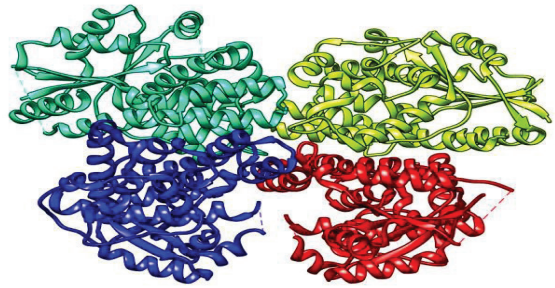	[26]
3	Protease target (PDBID: 1VZV)	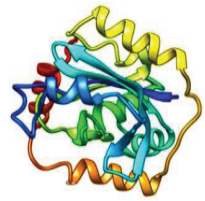	[27]

2.3. Methods

Several programs have been used to assess theoretical attachment of used short peptides against Varicella Zoster Virus, in addition to their physical and chemical properties. These programs are:

- Hex 8.0.0: Molecular docking of receptors and ligands, was done using this program [28].
- Pymol and Chimera software were used for results visualization [29].
- Pepstr server: Pepstr server predicts the tertiary structure of short peptides [30].
- T cell epitope: by which immunogenicity was predicted using T cell epitope (http://tools.immuneepitope.org/immunogenicity/)[31].
- ToxinPred: used for the estimation of peptides toxicity and chemical-physical properties (http://crdd.osdd.net/raghava/toxinpred/design.php) [32].
- CellPPD: was used to predict cell penetrating probability of peptides, it also predicts hydropathicity, isoelectric point (PI) and molecular weight. On the other hand, the hydrophobicity and hydrophilicity were directly related to the hydropathy index as reported by Kyte and Doolittle [33], CellPPD available at (http://crdd.osdd.net/raghava/cellppd/index.html)[34].
- The Boman index values test was performed; this test shows the ability of the peptide to bind with other proteins rather than the targets of protein it can be calculated according to the online Antimicrobial Peptide Database (http://aps.unmc.edu/AP/main.php) [35].

3. Results

Molecular docking for several peptides that set as AMP, these AMP collected from particular researches then investigated according to specific VZV targets including Thymidine kinase (PDBID: 1OSI), envelope glycoprotein H (PDPID: 4XHJ) and protease (PDBID: 1VZV) by a specific program Hex.

3.1. Molecular docking of selected peptides with Envelope glycoprotein H target (PDPID: 4XHJ)

Envelope glycoprotein H docked with AMP as shown in Table 3 the delta G values, or energy values (E-value) arranged from the lowest energy value to highest. From 64 peptides only 22 peptides are selected to be the lowest energy value, from the lowest one (MSI-78) its'E-value (-791.49 Kcal/mol) to the highest selected one (brevinin-1BYa) its'E-value (-507.62 Kcal/mol).

Table (3): Energy value of selected peptides attached with envelope glycoprotein H target (PDBID: 4XHJ)

No	Molecule Name	Sequence	E-value (Kcal/ (mol
1	MSI-78	GIGKFLKKAKKFGKAFVKILKK	-791.49
2	A	VVKKARKAAKKVAKK	-725.94
3	Androctonin	RSVCRQIKICRRRGGCYYKCTNRPY	-715.35
4	TAT-C	GRKKRRQRRRC	-653.67
5	GLRC-2	GLRCRLGRLLRR LGRCLLR	-648.08
6	Polyphemusin 2	RRWCFRVCYKGFCYRKCR	-597.55
7	K4S4(1-16)a	ALWKTLLKKVLKAA	-596.65
8	GLRC-1	GCRRLLGRLLRRLGRLLCR	-596.03
9	Lfcin B	FKCRRWQWRMKKLGAPSITCVRRAF	-594.88
10	GLRC-3	GLRRLCGRLGRRLCRLLLR	-592.09
11	GLK-19	GLKKLLGKLLKKLGKLLLK	-589.28
12	GLRC-4	GCRRLCGRLGRRLCRLLCR	-583.16
13	Fv16	KKVGTSKVVAKTVTKK	-582.14
14	Limandapleu-(rocidin(LmPle	GWKKWFKKATHVGKHVGKAALDAYL	-581.17
15	BR-C	CKLKNFAKGVAQSLLNKASKLSGQC	-549.89
16	D	AIRRLARRGGVKRISGLI	-545.19
17	B	VPKFKAGKILKQKVEKG	-543.06
18	GLR-19	GLRRLLGRLLRRLGRLLLR	-541.15
19	S4a	TLLKKVLKAAAKAALNAVLVG	-539.54
20	Tachyplesin 1	KWCFRVCYRGICYRRCR	-520.54
21	Brevinin-1BYb	FLPILASLAAKLGPKLFCLVTKKC	-513.22
22	Brevinin-1BYa	FLPILASLAAKFGPKLFCLVTKKC	-507.62
23	Brevinin-2R	KLKNFAKGVAQSLLNKASCKLSGQC	-495.28
24	C	TGKIGKLKKGTGKIA	-493.16
25	AVP 1070	RRKKAAVALLPAVLLALLLAP	-489.79
26	MRP	AIGSILGALAKGLPTLISWIKNR	-487.93
27	RTD 1	GFCRCLCRRGVCRCICTR	-482.88
28	Brevinin-1BYc	FLPILASLAATLGPKLLCLITKKC	-470.52
29	Protegrin PG-1	RGGRLCYCRRRFCVCVGR	-470.41
30	AVP 1072	RRKKAAVALLPAVLLALL	-457.49
31	CP11	ILKKWPWWPWRRK	-456.91
32	Magainin 2	GIGKFLHSAKKFGKAFVGEIMNS	-454.95
33	AVP 1093	RRKKALLALLAP	-451.36
34	Caerin 4.1	GLWQKIKSAAGDLASGIVEGIKS	-441.03
35	Vperin 3.6	GVIDAAKKWNVLKNLF	-433.25

36	Dahlein5.6	GLLASLGKVFGGYLAEKLKPK	-429.57
37	AVP 1092	RRKKPAVLLALLAP	-419.46
38	AVP 1074	RRKKAAVALLPAVLLA	-417.46
39	F	KATKATITKKPVA	-412.62
40	Magainin 1	GIGKFLHSAGKFGKAFVGEIMKS	-410.62
41	HNP-1C	AYRIPAIAGERRYGTIYQGRLWAF	-396.29
42	HNP-1C-18A	IAAERRYATIYQARLWAF	-386.45
43	CP10A	ILAWKWAWWAWRR	-368.96
44	Indolicidin	ILPWKWPWWPWRR	-358.66
45	Ranatuerin 6	FISAIASMLGKFL	-354.21
46	HNP-1C-18	IAGERRYGTIYQGRLWAF	-353.17
47	Aurein 1	GLFDIIKKIAESF	-351.63
48	Caerin 1.1	GLLSVLGSVAKHVLPHVVPVIAEHL	-344.07
49	Caerin 1.9	GLFGVLGSIAKHVLPHVVPVIAEKL	-341.62
50	Maculatin 1-1	GLFGVLAKVAAHVVPAIAEHF	-332.89
51	Citropin 1.1	GLFDVIKKVASVIGGL	-323.20
52	DET3	IGVRPGKLDL	-320.28
53	DET1	GWVKPAKLDG	-310.85
54	DET4	AGVKDGKLDF	-307.41
55	STAT 1	CTAGACTTCAGACCACACAAC	-302.93
56	Mx 1	AAGCCTGATCTGGTGGACAAAGGA	-298.40
57	BR-D	KLKNFAKGVAQSLLNKASCKLSGQC	-296.92
58	P1	WLVFFVIFYFFR	-285.42
59	P2	WLVFFVIFYIFR	-280.77
60	GAPdH	CACATGGCCTCCAAGGAGTAA	-274.34
61	Alloferon 2	GVSGHGQHGVHG	-273.30
62	STAT 2	GAGGAGAAGCAATGGGTCTTAG	-265.15
63	DET2	PWLKPGDLDL	-221.29
64	Alloferon 1	HGVSGHGQHGVHG	-214.73
Indicated to the lowest selected energy value of peptide			

Then these 22 AMP treated with other online programs to predict its characteristic, including cell penetration, PI, Boman index, hydropathicity, and molecular weight as shown in Table 4. The cell penetration test shows good penetration probability for some selected peptides, so from 22 peptides about 16 peptides could penetrate into the cell (The cell penetrated one, has a positivE-value of the SVM score (Yellowish color). In addition, this Table shows hydropathicity values, the peptide that has more hydpathicity value than 1or less than -1, it will be neglected, and so from 16 peptides 13 peptides pass the hydropathicity test.

Table (4): Predicted cell penetration, isoelectric point, Boman index, hydropathicity and molecular weight values for the selected AMP with envelope glycoprotein H target.

.No	Molecule\ Name	Cell penetration Prediction	SVM Score of cell penetration	PI	Boman index (kcal/ (mol	Hydropathicity (Kcal/mol)	Mol. wt (Dalton)
1	MSI-78	CPP	0.46	10.91	0.49	-0.16	2478.54
2	A	CPP	0.51	11.48	2.29	-0.80	1653.34
3	Androctonin	Non-CPP	-0.12	10.23	3.93	-1.06	3081.01
4	TAT-C	CPP	1.52	12.31	9.44	-3.29	1499.95
5	GLRC-2	CPP	0.47	12.13	3.4	-0.06	2281.17
6	K4S4(1-16)a	CPP	0.41	10.49	-0.47	0.54	1583.25
7	GLRC-1	CPP	0.35	12.13	3.4	-0.06	2281.17
8	Lfcin B	CPP	0.18	11.85	2.75	-0.58	3126.17
9	GLRC-3	CPP	0.32	12.13	3.4	-0.06	2281.17
10	GLK-19	CPP	0.41	10.78	-0.43	0.30	2105.16
11	GLRC-4	CPP	0.23	11.61	3.78	-0.19	2261.11
12	Fv16	CPP	0.02	10.71	1.59	-0.51	1702.35
13	Limandapleurocidin(LmPle)	Non-CPP	-0.18	10.13	0.73	-0.49	2840.75
14	Polyphemusin 2	CPP	0.27	10.11	3.75	-0.80	2431.19
15	BR-C	Non-CPP	-0.24	9.91	1.02	-0.16	2637.53
16	D	Non-CPP	-0.18	12.61	2.69	0.03	1992.72
17	B	Non-CPP	-0.18	10.31	1.23	-0.68	1898.63
18	GLR-19	CPP	0.47	12.78	3.01	0.08	2301.23
19	S4a	Non-CPP	-0.31	10.49	-0.81	1.06	2092.96
20	Tachyplesin 1	CPP	0.05	9.94	3.53	-0.52	2268.99
21	Brevinin-1BYb	CPP	0.02	9.72	-1.04	1.12	2575.66
22	Brevinin-1BYa	CPP	0.02	9.72	-0.96	1.08	2609.67

Indicated to the peptide that could perpetrated to cell.
Indicated to peptide excepted value for hydropathicity.

Furthermore, Table 5 shows the prediction of immunogenicity by class I immunogenicity test. From these 13 peptides only 6 peptides pass the immunogenicity test, and all these 6 peptides predicted to be non-toxic by toxicity prediction test. So these 6 peptides predicted to be effective against VZV.

Table (5): Predicted immunogenicity and toxicity of selected antimicrobial peptides with the envelope glycoprotein H target.

.No	Molecule Name	Score Class I Immunogenicity	Toxicity Prediction	SVM score of toxicity
1	MSI-78	-0.99548	Non-Toxin	-0.86
2	A	-0.80642	Non-Toxin	-0.65
3	GLRC-2	0.17076	Non-Toxin	-1.25
4	K4S4(1-16)a	-0.67828	Non-Toxin	-1.48
5	GLRC-1	0.23118	Non-Toxin	-1.35
6	Lfcin B	0.02174	Non-Toxin	-0.92
7	GLRC-3	0.1728	Non-Toxin	-1.35
8	GLK-19	-1.14128	Non-Toxin	-1.14
9	GLRC-4	0.14778	Non-Toxin	-1.41
10	Fv16	-0.39388	Non-Toxin	-1.31
11	Polyphemusin 2	-0.11773	Non-Toxin	-0.19
12	GLR-19	0.2562	Non-Toxin	-1.14
13	Tachyplesin 1	0.3526	Non-Toxin	-1.15

Indicated to non-immunogenic peptide.
Indicated to non-toxic peptide.

Then the selected 6 peptides sorted according to the lowest energy value to the highest one with the other properties of peptide as shown in Table 6. Furthermore the selected 6 peptide were sorted according to Boman index value and the molecular.

Table (6): Peptides with the lowest E-values of an envelope glycoprotein H target (PDBID: 4XHJ), and their prediction of cell penetration, immunogenicity, toxicity, isoelectric point, Bomam index, hydropathicity and molecular weight. Sorted according E-values.

.No	Molecule Name	E-value (kcal/mol)	Cell penetration Prediction	SVM Score of cell penetration	Class I Immunogenicity	Toxicity Prediction	SVM score of Toxicity	pI	Boman index (kcal/mol)	Hydropathicity(kcal/mol)	Molwt (Dalton)
1	MSI-78	-791.49	CPP	0.46	-0.99548	Non-Toxin	-0.86	10.91	0.49	-0.16	2478.54
2	A	-725.94	CPP	0.51	-0.80642	Non-Toxin	-0.65	11.48	2.29	-0.80	1653.34
3	Polyphemusin 2	-597.55	CPP	0.27	-0.11773	Non-Toxin	-0.19	10.11	3.75	-0.80	2431.19
4	K4S4(1-16)a	-596.65	CPP	0.41	-0.67828	Non-Toxin	-1.48	10.49	-0.47	0.54	1583.25
5	GLK-19	-589.28	CPP	0.41	-1.14128	Non-Toxin	-1.14	10.78	-0.43	0.30	2105.16
6	Fv16	-582.14	CPP	0.02	-0.39388	Non-Toxin	-1.31	10.71	1.59	-0.51	1702.35
Indicated to energy value from lowest to highest values.											

Finally, Table 7 shows the three-dimensional structures of these 6 selected peptides with their binding site to their proposed target; envelope glycoprotein H; and docking were done using Hex 8.0.0 software.

Table (7): The three-dimensional structures of selected antimicrobial peptides with their binding site on their proposed envelope glycoprotein H target (PBBID: 4XHJ), docking was done using Hex 8.0.0 software.

.NO	Molecule Name	Envelope glycoprotein H (4XHJ) - peptides complex	Focus docking
1	 MSI-78		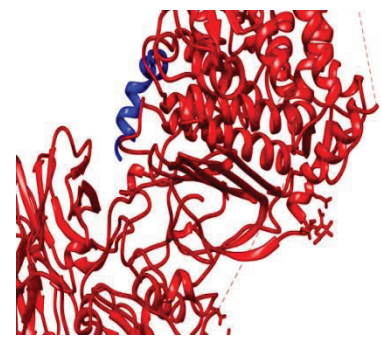

2	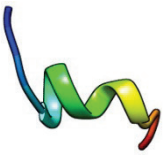 A	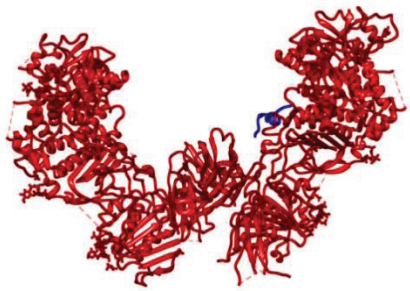	
3	Polyphemusin 2 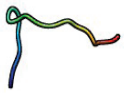	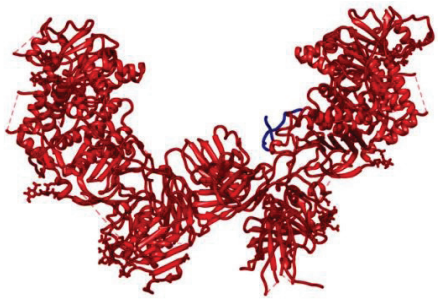	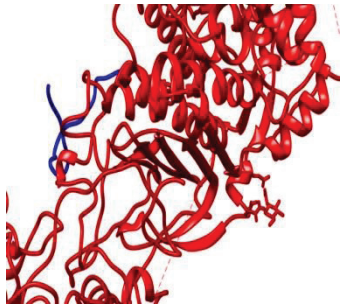
4	K4S4(1-16)a 	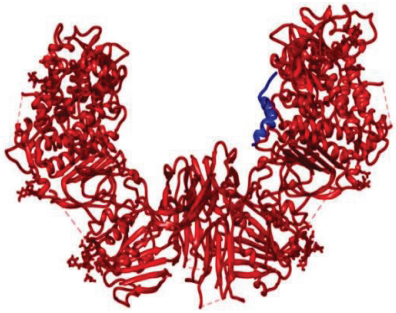	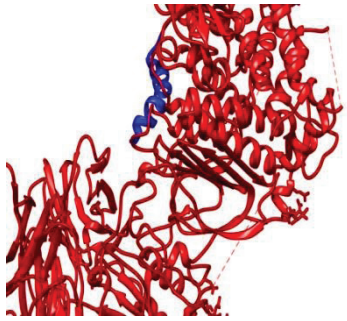
5	GLK-19 	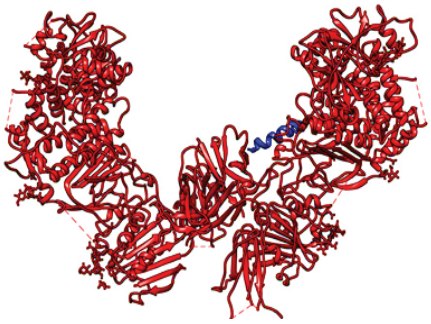	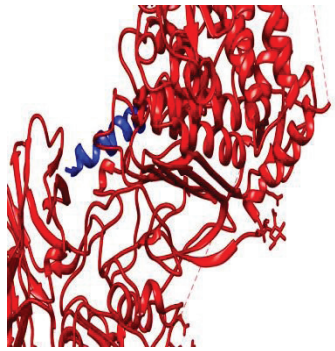
6	Fv16 	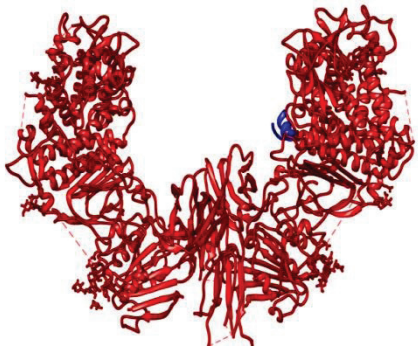	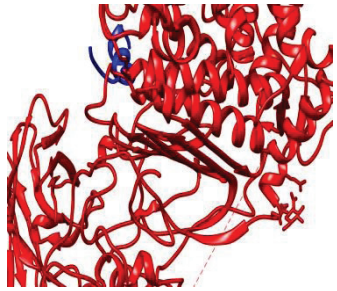

3.2 Molecular docking of selected antimicrobial peptides with thymidine kinase target (PDBID: 1OSN)

Thymidine kinase target docked with peptides as shown in Table 8 the E-value arranged in ascending order. From 64 peptides only 27 peptides were selected to be the lowest energy value, from the lowest one MSI-78 its' E-value -1027.32 Kcal/mol to the highest selected one AVP 1072 it is E-value -800.62 Kcal/mol.

Table (8): Energy value of selected antimicrobial peptides attached with thymidine kinase target (PDBID: 1OSN)

No	Molecule Name	Sequence	E-value (Kcal/mol)
1	MSI-78	GIGKFLKKAKKFGKAFVKILKK	-1027.32
2	A	VVKKARKAAKKVAKK	-967.51
3	GLRC-3	GLRRLCGRLGRRLCRLLLR	-905.46
4	GLRC-2	GLRCRLGRLLRR LGRCLLR	-902.08
5	Androctonin	RSVCRQIKICRRRGGCYYKCTNRPY	-886.84
6	GLK-19	GLKKLLGKLLKKLGKLLLK	-883.56
7	Fv16	KKVGTSKVVAKTVTKK	-882.43
8	Polyphemusin 2	RRWCFRVCYKGFCYRKCR	-876.07
9	GLRC-1	GCRRLLGRLLRRLGRLLCR	-869.31
10	AVP 1092	RRKKPAVLLALLAP	-860.48
11	Lfcin B	FKCRRWQWRMKKLGAPSITCVRRAF	-858.07
12	TAT-C	GRKKRRQRRRC	-855.35
13	AVP 1074	RRKKAAVALLPAVLLA	-848.62
14	BR-D	KLKNFAKGVAQSLLNKASCKLSGQC	-841.01
15	Brevinin-2R	KLKNFAKGVAQSLLNKASCKLSGQC	-841.01
16	Magainin 1	GIGKFLHSAGKFGKAFVGEIMKS	-840.59
17	F	KATKATITKKPVA	-837.74
18	Protegrin PG-1	RGGRLCYCRRRFCVCVGR	-832.00
19	K4S4(1-16)a	ALWKTLLKKVLKAA	-827.8
20	Limandapleu-(rocidin(LmPle	GWKKWFKKATHVGKHVGKAALDAYL	-822.71
21	AVP 1070	RRKKAAVALLPAVLLALLLAP	-815.91
22	C	TGKIGKLKKGTGKIA	-812.93
23	CP10A	ILAWKWAWWAWRR	-812.93
24	GLR-19	GLRRLLGRLLRRLGRLLLR	-812.27
25	Tachyplesin 1	KWCFRVCYRGICYRRCR	-809.53
26	Dahlein5.6	GLLASLGKVFGGYLAEKLKPK	-803.68
27	AVP 1072	RRKKAAVALLPAVLLALL	-800.62

28	D	AIRRLARRGGVKRISGLI	-798.49
29	S4a	TLLKKVLKAAAKAALNAVLVG	-795.68
30	CP11	ILKKWPWWPWRRK	-763.61
31	AVP 1093	RRKKALLALLAP	-747.25
32	Brevinin-1BYb	FLPILASLAAKLGPKLFCLVTKKC	-747.08
33	Caerin 1.9	GLFGVLGSIAKHVLPHVVPVIAEKL	-746.54
34	Brevinin-1BYc	FLPILASLAATLGPKLLCLITKKC	-741.05
35	Brevinin-1BYa	FLPILASLAAKFGPKLFCLVTKKC	-735.59
36	B	VPKFKAGKILKQKVEKG	-733.19
37	HNP-1C	AYRIPAIAGERRYGTIYQGRLWAF	-732.21
38	MRP	AIGSILGALAKGLPTLISWIKNR	-703.66
39	Magainin 2	GIGKFLHSAKKFGKAFVGEIMNS	-699.17
40	HNP-1C-18A	IAAERRYATIYQARLWAF	-698.07
41	RTD 1	GFCRCLCRRGVCRCICTR	-697.41
42	HNP-1C-18	IAGERRYGTIYQGRLWAF	-664.99
43	Citropin 1.1	GLFDVIKKVASVIGGL	-664.75
44	Ranatuerin 6	FISAIASMLGKFL	-659.47
45	Vperin 3.6	GVIDAAKKWNVLKNLF	-656.30
46	Maculatin 1-1	GLFGVLAKVAAHVVPAIAEHF	-649.71
47	Caerin 4.1	GLWQKIKSAAGDLASGIVEGIKS	-639.73
48	Indolicidin	ILPWKWPWWPWRR	-618.09
49	Caerin 1.1	GLLSVLGSVAKHVLPHVVPVIAEHL	-601.06
50	Aurein 1	GLFDIIKKIAESF	-561.93
51	GAPdH	CACATGGCCTCCAAGGAGTAA	-543.67
52	DET4	AGVKDGKLDF	-523.02
53	STAT 1	CTAGACTTCAGACCACACAAC	-521.32
54	P1	WLVFFVIFYFFR	-511.13
55	STAT 2	GAGGAGAAGCAATGGGTCTTAG	-502.79
56	DET2	PWLKPGDLDL	-493.49
57	DET3	IGVRPGKLDL	-491.53
58	DET1	GWVKPAKLDG	-484.01
59	Alloferon 1	HGVSGHGQHGVHG	-471.02
60	Alloferon 2	GVSGHGQHGVHG	-467.14
61	GLRC-4	GCRRLCGRLGRRLCRLLCR	-424.64
62	BR-C	CKLKNFAKGVAQSLLNKASKLSGQC	-353.71
63	Mx 1	AAGCCTGATCTGGTGGACAAAGGA	-226.49
64	P2	WLVFFVIFYIFR	543.98
Indicated to the lowest selected energy value of peptide			

Table (9): Predicted cell penetration, isoelectric point, Boman index, hydropathicity and molecular weight values for the selected peptides attached well with thymidine kinase target (PDBID: 1OSN).

.No	Molecule Name	Cell penetration Prediction	SVM Score of cell penetration	PI	Boman index ((kcal/mol	Hydropathicity (kcal/mol)	Molwt (Dalton)
1	MSI-78	CPP	0.46	10.91	0.49	-0.16	2478.54
2	A	CPP	0.51	11.48	2.29	-0.80	1653.34
3	GLRC-3	CPP	0.32	12.13	3.4	-0.06	2281.17
4	GLRC-2	CPP	0.47	12.13	3.4	-0.06	2281.17
5	Androctonin	Non-CPP	-0.12	10.23	3.93	-1.06	3081.01
6	GLK-19	CPP	0.41	10.78	-0.43	0.30	2105.16
7	Fv16	CPP	0.02	10.71	1.59	-0.51	1702.35
8	Polyphemusin 2	CPP	0.27	10.11	3.75	-0.80	2431.19
9	GLRC-1	CPP	0.35	12.13	3.4	-0.06	2281.17
10	AVP 1092	CPP	0.48	12.02	0.84	0.34	1546.18
11	Lfcin B	CPP	0.18	11.85	2.75	-0.58	3126.17
12	TAT-C	CPP	1.52	12.31	9.44	-3.29	1499.95
13	AVP 1074	CPP	0.03	12.02	0.25	0.89	1690.38
14	BR-D	Non-CPP	-0.14	9.91	1.02	-0.16	2637.53
15	Brevinin-2R	Non-CPP	-0.14	9.91	1.02	-0.16	2637.53
16	Magainin 1	CPP	0.25	10.01	0.08	0.22	2410.23
17	F	CPP	0.41	10.49	1.19	-0.40	1356.85
18	Protegrin PG-1	CPP	0.39	10.67	3.65	-0.25	2160.87
19	K4S4(1-16)a	CPP	0.41	10.49		0.54	1583.25
20	Limandapleu-rocidin(LmPle)	Non-CPP	-0.18	10.13	0.73	-0.49	2840.75
21	AVP 1070	CPP	0.09	12.02	-0.59	1.23	2198.14
22	C	Non-CPP	-0.18	10.61	0.83	-0.53	1500.10
23	CP10A	CPP	0.19	12.01	0.65	-0.28	1829.37
24	GLR-19	CPP	0.47	12.78	3.01	0.08	2301.23
25	Tachyplesin 1	CPP	0.05	9.94	3.53	-0.52	2268.99
26	Dahlein5.6	CPP	0.05	9.84	-0.3	0.25	2190.00
27	AVP 1072	Non-CPP	-0.20	12.02	-0.31	1.21	1916.74

.Indicated to the peptide that could perpetrated to cell

.Indicated to peptide excepted value for hydropathicity

After that, Table 10, shows the prediction of immunogenicity by class I immunogenicity test. From these 19 peptides; only 11 peptides were pass the immunogenicity test, and all these 11 peptides predicted to be non-toxic by toxicity prediction test. So these 11 peptides predicted to be effective against VZV.

Table (10): Predicted immunogenicity and toxicity of selected peptides attached well to thymidine kinase target (PDBID: 1OSN).

No.	Molecule Name	Score Class I Immunogenicity	Toxicity Prediction	SVM score of toxicity
1	MSI-78	-0.99548	Non-Toxin	-0.86
2	A	-0.80642	Non-Toxin	-0.65
3	GLRC-3	0.1728	Non-Toxin	-1.35
4	GLRC-2	0.17076	Non-Toxin	-1.25
5	GLK-19	-1.14128	Non-Toxin	-1.14
6	Fv16	-0.39388	Non-Toxin	-1.31
7	Polyphemusin 2	-0.11773	Non-Toxin	-0.19
8	GLRC-1	0.23118	Non-Toxin	-1.35
9	AVP 1092	-0.19994	Non-Toxin	-1.45
10	Lfcin B	0.02174	Non-Toxin	-0.92
11	AVP 1074	-0.10378	Non-Toxin	-1.62
12	Magainin 1	-0.26042	Non-Toxin	-1.03
13	F	-0.35934	Non-Toxin	-1.28
14	Protegrin PG-1	0.20047	Non-Toxin	-0.48
15	K4S4(1-16)a	-0.67828	Non-Toxin	-1.48
16	CP10A	0.9648	Non-Toxin	-0.82
17	GLR-19	0.2562	Non-Toxin	-1.14
18	Tachyplesin 1	0.3526	Non-Toxin	-1.15
19	Dahlein5.6	-0.38065	Non-Toxin	-1.39

.Indicated to non-immunogenic peptide
Indicated to non-toxic peptide

Then the selected 11 peptides sorted according to the lowest energy value to the highest one with the other properties of peptide as shown in Table 11. Furthermore the selected 11 peptides sorted according to Boman index value and according to the molecular weight.

Table (11): Peptides with the lowest E-values of binding to thymidine kinase target (PDBID: 1OSN), and their prediction of cell penetration, immunogenicity, toxicity, isoelectric point, Bomam index, hydropathicity and molecular weight. Sorted according E-values.

No	Molecule Name	E-value (kcal/mol)	Cell penetration Prediction	SVM Score of cell penetration	Score Class I Immunogenicity	Toxicity Prediction	SVM score of Toxicity	pI	Boman index (kcal/mol	Hydropathicity (kcal/mol)	Molwt (Dalton)
1	MSI-78	-1027.32	CPP	0.46	-0.99548	Non-Toxin	-0.86	10.91	0.49	-0.16	2478.54
2	A	-967.51	CPP	0.51	-0.80642	Non-Toxin	-0.65	11.48	2.29	-0.80	1653.34
3	GLK-19	-883.56	CPP	0.41	-1.14128	Non-Toxin	-1.14	10.78	-0.43	0.30	2105.16
4	Fv16	-882.43	CPP	0.02	-0.39388	Non-Toxin	-1.31	10.71	1.59	-0.51	1702.35
5	Polyphemusin 2	-876.07	CPP	0.27	-0.11773	Non-Toxin	-0.19	10.11	3.75	-0.80	2431.19
6	AVP 1092	-860.48	CPP	0.48	-0.19994	Non-Toxin	-1.45	12.02	0.84	0.34	1546.18
7	AVP 1074	-848.62	CPP	0.03	-0.10378	Non-Toxin	-1.62	12.02	0.25	0.89	1690.38
8	Magainin 1	-840.59	CPP	0.25	-0.26042	Non-Toxin	-1.03	10.01	0.08	0.22	2410.23
9	F	-837.74	CPP	0.41	-0.35934	Non-Toxin	-1.28	10.49	1.19	-0.40	1356.85
10	K4S4(1-16)a	-827.8	CPP	0.41	-0.67828	Non-Toxin	-1.48	10.49	-0.47	0.54	1583.25
11	Dahlein5.6	-803.68	CPP	0.05	-0.38065	Non-Toxin	-1.39	9.84	-0.3	0.25	2190.00
Indicated to energy value from lowest to highest values.											

Finally, a

Table (12): shows the three-dimensional structures (by Chimera software) of these 11 selected peptides with their binding site to their proposed target; thymidine kinase; and docking was done using Hex 8.0.0 software.

Table (12): The three-dimensional structures of selected peptides with their binding site on their predicted thymidine kinase target (PDBID: 1OSN), docking is done using Hex software

No.	Molecule Name	Thymidine kinase target (1OSN) – peptides complex	Focus docking
1	MSI-78		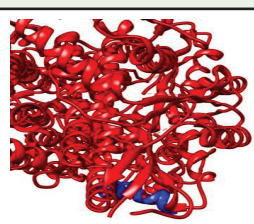

2	A 	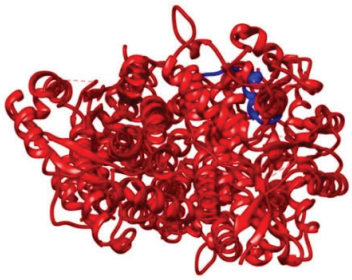	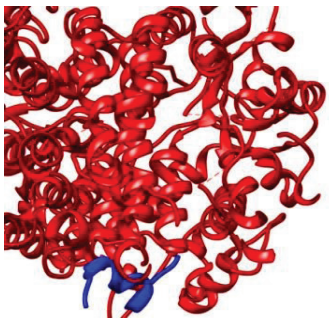
3	GLK-19 	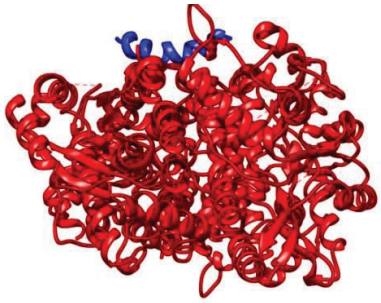	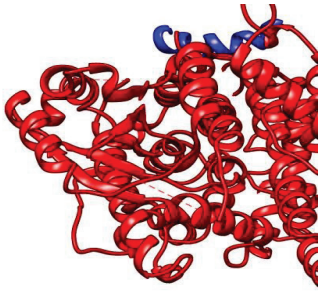
4	Fv16 	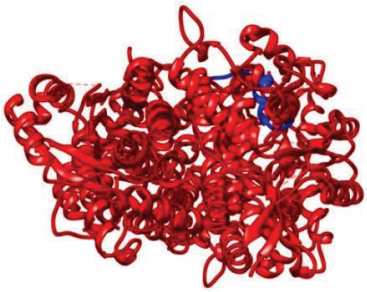	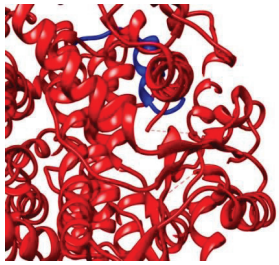
5	Polyphemusin 2 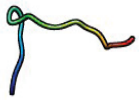	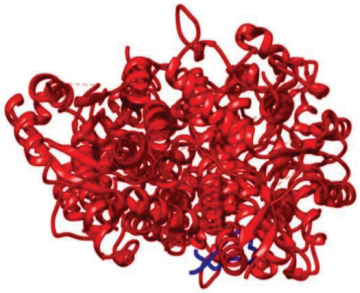	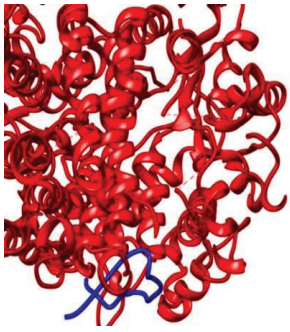
6	AVP 1092 		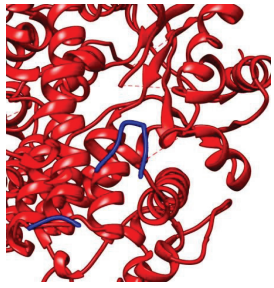

7	AVP 1074 		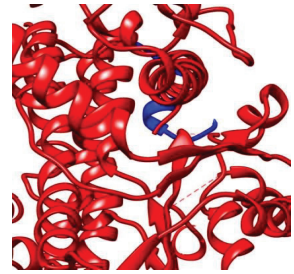
8	Magainin 1 	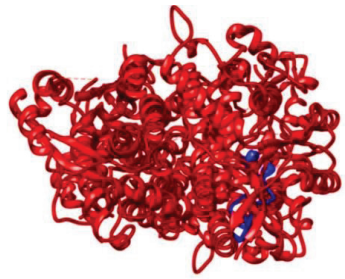	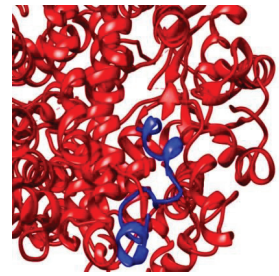
9	F 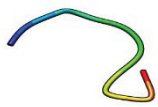	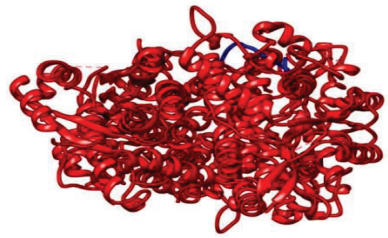	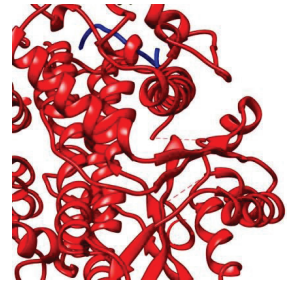
10	K4S4(1-16)a 	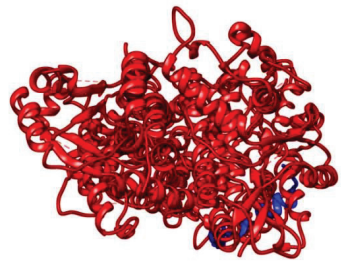	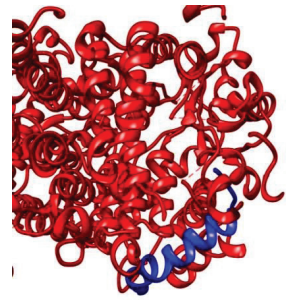
11	Dahlein5.6 	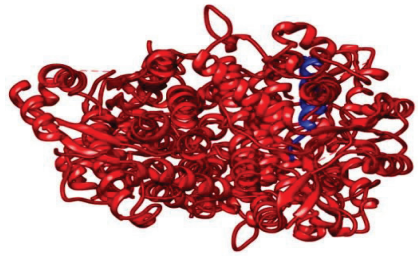	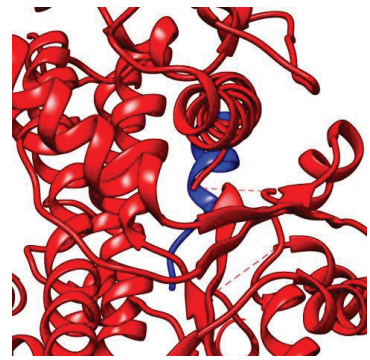

3.3. Molecular docking of selected peptides with Protease target (PDBID: 1VZV)

The VZV Protease docked with peptides as shown in Table 13 the E-value arranged from the lower energy value to highest. From 64 peptides only 20 peptides are selected to be the lowest energy value, from the lowest one (Lfcin B) its' E-value (-659.51Kcal/mol) to the highest selected one CP11 its' E-value -598.73Kcal/mol.

Table (13): Molecular docking of selected peptides with Protease target (PDBID: 1VZV)

No	Molecule Name	Sequence	E-value (Kcal/ (mol
1	Lfcin B	FKCRRWQWRMKKLGAPSITCVRRAF	-659.51
2	MSI-78	GIGKFLKKAKKFGKAFVKILKK	-643
3	BR-D	KLKNFAKGVAQSLLNKASCKLSGQC	-642.58
4	Brevinin-2R	KLKNFAKGVAQSLLNKASCKLSGQC	-642.58
5	GLRC-2	GLRCRLGRLLRR LGRCLLR	-635.92
6	K4S4(1-16)a	ALWKTLLKKVLKAA	-632.87
7	AVP 1070	RRKKAAVALLPAVLLALLLAP	-632.48
8	Caerin 1.9	GLFGVLGSIAKHVLPHVVPVIAEKL	-632.38
9	C	TGKIGKLKKGTGKIA	-628.07
10	Androctonin	RSVCRQIKICRRRGGCYYKCTNRPY	-620.20
11	Magainin 1	GIGKFLHSAGKFGKAFVGEIMKS	-617.97
12	MRP	AIGSILGALAKGLPTLISWIKNR	-614.03
13	A	VVKKARKAAKKVAKK	-611.60
14	STAT 1	CTAGACTTCAGACCACACAAC	-610.34
15	Limandapleu-(rocidin(LmPle	GWKKWFKKATHVGKHVGKAALDAYL	-606.32
16	AVP 1074	RRKKAAVALLPAVLLA	-605.48
17	AVP 1072	RRKKAAVALLPAVLLALL	-604.52
18	Brevinin-1BYa	FLPILASLAAKFGPKLFCLVTKKC	-602.12
19	GLRC-1	GCRRLLGRLLRRLGRLLCR	-598.88
20	CP11	ILKKWPWWPWRRK	-598.73
21	Caerin 4.1	GLWQKIKSAAGDLASGIVEGIKS	-598.08
22	BR-C	CKLKNFAKGVAQSLLNKASKLSGQC	-593.08
23	Brevinin-1BYb	FLPILASLAAKLGPKLFCLVTKKC	-588.70
24	GLK-19	GLKKLLGKLLKKLGKLLLK	-588.66

25	GLRC-3	GLRRLCGRLGRRLCRLLLR	-582.37
26	Maculatin 1-1	GLFGVLAKVAAHVVPAIAEHF	-572.91
27	D	AIRRLARRGGVKRISGLI	-570.11
28	Ranatuerin 6	FISAIASMLGKFL	-569.85
29	HNP-1C-18	IAGERRYGTIYQGRLWAF	-568.98
30	GLRC-4	GCRRLCGRLGRRLCRLLCR	-567.25
31	B	VPKFKAGKILKQKVEKG	-565.01
32	HNP-1C	AYRIPAIAGERRYGTIYQGRLWAF	-562.57
33	Mx 1	AAGCCTGATCTGGTGGACAAAGGA	-559.58
34	AVP 1092	RRKKPAVLLALLAP	-557.72
35	Fv16	KKVGTSKVVAKTVTKK	-557.44
36	S4a	TLLKKVLKAAAKAALNAVLVG	-557.21
37	Brevinin-1BYc	FLPILASLAATLGPKLLCLITKKC	-550.42
38	Citropin 1.1	GLFDVIKKVASVIGGL	-549.84
39	Dahlein5.6	GLLASLGKVFGGYLAEKLKPK	-547.28
40	Vperin 3.6	GVIDAAKKWNVLKNLF	-544.72
41	GLR-19	GLRRLLGRLLRRLGRLLLR	-542.83
42	TAT-C	GRKKRRQRRRC	-541.96
43	Tachyplesin 1	KWCFRVCYRGICYRRCR	-541.09
44	Protegrin PG-1	RGGRLCYCRRRFCVCVGR	-539.44
45	AVP 1093	RRKKALLALLAP	-537.81
46	Magainin 2	GIGKFLHSAKKFGKAFVGEIMNS	-536.42
47	CP10A	ILAWKWAWWAWRR	-534.31
48	Polyphemusin 2	RRWCFRVCYKGFCYRKCR	-533.41
49	Caerin 1.1	GLLSVLGSVAKHVLPHVVPVIAEHL	-517.01
50	GAPdH	CACATGGCCTCCAAGGAGTAA	-507.75
51	STAT 2	GAGGAGAAGCAATGGGTCTTAG	-507.06
52	Aurein 1	GLFDIIKKIAESF	-505.53
53	F	KATKATITKKPVA	-501
54	HNP-1C-18A	IAAERRYATIYQARLWAF	-499.46
55	P1	WLVFFVIFYFFR	-491.62
56	DET2	PWLKPGDLDL	-490.71
57	Alloferon 1	HGVSGHGQHGVHG	-488.60

58	Indolicidin	ILPWKWPWWPWRR	-474.22
59	RTD 1	GFCRCLCRRGVCRCICTR	-473.18
60	P2	WLVFFVIFYIFR	-472.28
61	DET4	AGVKDGKLDF	-451.36
62	DET1	GWVKPAKLDG	-419.53
63	DET3	IGVRPGKLDL	-406.83
64	Alloferon 2	GVSGHGQHGVHG	-402.48
Indicated to the lowest selected energy value of peptide			

Then these 20 peptides were treated with other online programs to predict their characteristics, including cell penetration, isoelectric point, Boman index, hydropathicity, and molecular weight as shown in Table 14. The cell penetration test shows good penetration for some selected peptides, so from 20 peptides about 11 peptides can penetrate to cell. Also, this Table shows hydropathicity values.

Table (14): Predicted cell penetration, isoelectric point, Boman index, hydropathicity and molecular weight values of the selected peptides binds well to protease target (PDBID: 1VZV).

No.	Molecule Name	Prediction	SVM Score	PI	Boman index (kcal/(mol	Hydropathicity (kcal/mol)	Molwt (Dalton)
1	Lfcin B	CPP	0.18	11.85	2.75	-0.58	3126.17
2	MSI-78	CPP	0.46	10.91	0.49	-0.16	2478.54
3	BR-D	Non-CPP	-0.14	9.91	1.02	-0.16	2637.53
4	Brevinin-2R	Non-CPP	-0.14	9.91	1.02	-0.16	2637.53
5	GLRC-2	CPP	0.47	12.13	3.4	-0.06	2281.17
6	K4S4(1-16)a	CPP	0.41	10.49	-0.47	0.54	1583.25
7	AVP 1070	CPP	0.09	12.02	-0.59	1.23	2198.14
8	Caerin 1.9	Non-CPP	-0.52	8.94	-1.14	1.15	2594.59
9	C	Non-CPP	-0.18	10.61	0.83	-0.53	1500.10
10	Androctonin	Non-CPP	-0.12	10.23	3.93	-1.06	3081.01
11	Magainin 1	CPP	0.25	10.01	0.08	0.22	2410.23
12	MRP	Non-CPP	-0.22	11.17	-0.34	0.73	2393.28
13	A	CPP	0.51	11.48	2.29	-0.80	1653.34
14	STAT 1	Non-CPP	-0.37	5.70	0.89	1.50	1829.42
15	Limandapleurocidin(LmPle)	Non-CPP	-0.18	10.13	0.73	-0.49	2840.75

16	AVP 1074	CPP	0.03	12.02	0.25	0.89	1690.38
17	AVP 1072	Non-CPP	-0.20	12.02	-0.31	1.21	1916.74
18	Brevinin-1BYa	CPP	0.02	9.72	-0.96	1.08	2609.67
19	GLRC-1	CPP	0.35	12.13	3.4	-0.06	2281.17
20	CP11	CPP	0.42	12.03	2.1	-1.48	1880.51

.Indicated to the peptide that could perpetrated to cell

Indicated to peptide excepted value for hydropathicity

Table 15 shows the prediction of immunogenicity by class I immunogenicity test. From these 8 peptides, only 5 peptides pass the immunogenicity, and all these five peptides predicted to be non-toxic by toxicity prediction test. So these five peptides predicted to be effective against VZV.

Table (15): Predicted immunogenicity and toxicity of selected peptides with protease target (PDBID: 1VZV).

No.	Molecule Name	Score Class I Immunogenicity	Toxicity Prediction	SVM score of toxicity
1	Lfcin B	0.02174	Non-Toxin	-0.92
2	MSI-78	-0.99548	Non-Toxin	-0.86
3	GLRC-2	0.17076	Non-Toxin	-1.25
4	K4S4(1-16)a	-0.67828	Non-Toxin	-1.48
5	Magainin 1	-0.26042	Non-Toxin	-1.03
6	A	-0.80642	Non-Toxin	-0.65
7	AVP 1074	-0.10378	Non-Toxin	-1.62
8	GLRC-1	0.23118	Non-Toxin	-1.35

Indicated to non-immunogenic peptide.

Indicated to non-toxic peptide.

Then the selected 5 peptides sorted according to the lowest energy value to the highest one with the other properties of the peptide as shown in Table 16. Furthermore, the selected 5 peptides sorted according to Boman index value and according to the molecular weight.

Table (16): Peptides with the lowest E-values of binding to protease target (PDBID: 1VZV), and their prediction of cell penetration, immunogenicity, toxicity, isoelectric point, Bomam index, hydropathicity and molecular weight. Sorted according to E-values

No.	Molecule Name	E-value(kcal/mol)	Cell penetration Prediction	SVM Score of cell penetration	Score Class I Immunogenicity	Toxicity Prediction	SVM score of Toxicity	pI	(Boman index(kcal/mol	Hydropathicity(kcal/mol)	Molwt(Dalton)
1	MSI-78	-643	CPP	0.46	-0.99548	Non-Toxin	-0.86	10.49	0.49	-0.16	2478.54
2	K4S4(1-16)a	-632.87	CPP	0.41	-0.67828	Non-Toxin	-1.48	12.02	-0.47	0.54	1583.25
3	Magainin 1	-617.97	CPP	0.25	-0.26042	Non-Toxin	-1.03	11.48	0.08	0.22	2410.23
4	A	-611.60	CPP	0.51	-0.80642	Non-Toxin	-0.65	12.02	2.29	-0.80	1653.34
5	AVP 1074	-605.48	CPP	0.03	-0.10378	Non-Toxin	-1.62	9.72	0.25	0.89	1690.38
Indicated to energy value from lowest to highest values.											

Finally, Table 17 shows the three-dimensional structures (by Chimera software) of these 5 selected peptides with their binding site to their proposed target; Protease; and docking done using Hex 8.0.0 software.

Table (17): The three-dimensional structure of selected peptides with their binding site on their proposed protease target (PDBID: 1VZV), docking is done using Hex 8.0.0 software

No.	Molecule Name	Protease target (PDBID: 1VZV) –peptides complex	Focus docking
1	MSI-78 		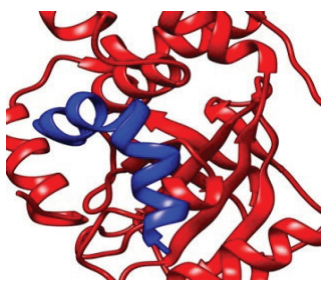

2	K4S4(1-16)a 	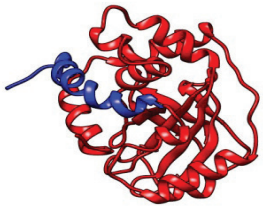	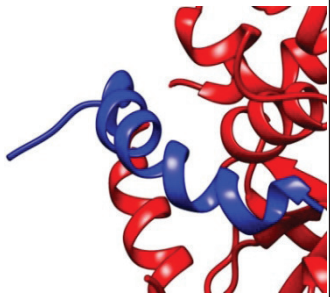
3	Magainin 1 	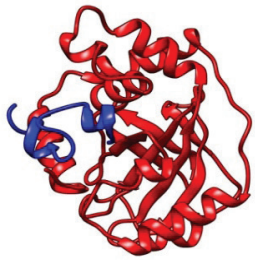	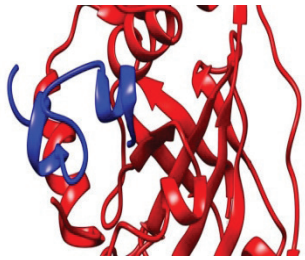
4	A 	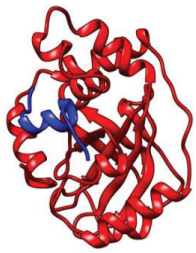	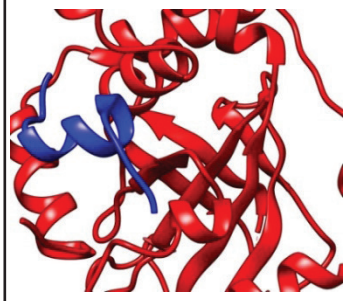
5	AVP 1074 	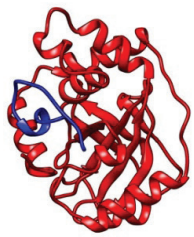	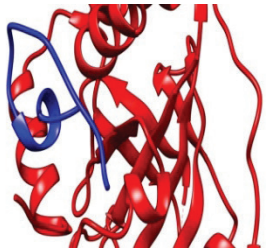

Table (18): The ability of the selected peptides to bind with more than one VZV targets

No.	Molecule Name	Peptide Sequence	Target	E-value (Kcal/ (mo
1	Polyphemusin 2	RRWCFRVCYKGFCYRKCR	Envelope glycoprotein H (PDBID:4XHJ)	-597.55
			Thymidine kinase (PDBID: 1OSN)	-876.07

2	K4S4(1-16)a	ALWKTLLKKVLKAA	Envelope glycoprotein H (PDBID:4XHJ)	-596.65
			Thymidine kinase (1OSN)	-827.8
			Protease (PDBID:1VZ)	-632.87
3	F	KATKATITKKPVA	Thymidine kinase (PDBID: 1OSN)	-837.74
4	AVP 1092	RRKKPAVLLALLAP	Thymidine kinase (PDBID: 1OSN)	-860.48
5	MSI-78	GIGKFLKKAKKFGKAFVKILKK	Envelope glycoprotein H (PDBID:4XHJ)	-791.49
			Thymidine kinase (PDBID: 1OSN)	-1027.32
			Protease (PDBID:1VZ)	-643
6	A	VVKKARKAAKKVAKK	Envelope glycoprotein H (PDBID:4XHJ)	-725.94
			Thymidine kinase (PDBID: 1OSN)	-967.51
			Protease (PDBID:1VZ)	-611.60
7	Fv16	KKVGTSKVVAKTVTKK	Envelope glycoprotein H (PDBID:4XHJ)	-582.14
			Thymidine kinase (PDBID: 1OSN)	-882.43
8	AVP 1074	RRKKAAVALLPAVLLA	Thymidine kinase (PDBID: 1OSN)	-848.62
			Protease (PDBID:1VZ)	-605.48
9	Magainin 1	GIGKFLHSAGKFGKAFVGEIMKS	Thymidine kinase (PDBID: 1OSN)	-840.59
			Protease (PDBID:1VZV)	-617.97
10	Dahlein 5.6	GLLASLGKVFGGYLAEKLKPK	Thymidine kinase (PDBID: 1OSN)	-803.63
11	GLK-19	GLKKLLGKLLKKLGKLLLK	Envelope glycoprotein H (PDBID:4XHJ)	-589.28
			Thymidine kinase (PDBID: 1OSN)	-883.56

4. Discussion

This research focused on using new computerized methods which involved studying affinity of the peptides to bind to specific receptor sites of varicella zoster virus by a specific computerized program (hex 8.0.).

A number of the selected peptides binds with the three varicella zoster virus (VZV) targets (envelope glycoprotein H, thymidine kinase, and protease) to know the interaction between targets and peptides using a process called molecular docking, so molecular docking is a widely used computer simulation procedure to predict the conformation of a receptor-ligand complex where the receptor is usually a protein or nucleic acid molecules and the ligand is either a small molecules or other proteins, and in this study the receptor is part of VZV (envelope glycoprotein H), and VZV enzymes (thymidine kinase and protease) as target while the ligand is a peptides, these peptides were selected because of their relatively low molecular weight, lesser toxicity, rapid elimination from the host, lesser side effects and cost effective.

After docking the ligand-receptor complex will form the expected output is docking energy. Among the different peptides, the best one can be selected based upon the lowest energy value which is an indicated of the highest stability (high negativity shows good binding to VZV target, so high negativity mean low energy so this will lead to high stability).

In the current study, several tests were done, to know the properties of the peptides then choose the best peptides that fit with VZV target and have the preferred properties. The first one is the cell penetration peptide (cpp) test; this test gives us an idea about the ability of the peptide for penetration into the cell membrane because of the VZV an intracellular virus so we need peptides that can enter into the cell to work on it, so this test is very important. If the cpp score is negative, this means the peptide is non-cell penetrating and if the cpp score is positive the peptide is cell penetrating, and it is ability to enter into the cell increase when the valve increase. Furthermore, the classI immunogenicity test was done, this test indicates the possibility of the reaction between the selected peptides and the immune system if the score of this test was positive this mean the immune reaction occur while the negative score mean there is no reaction. In addition to that, the toxicity test was done, this test suggests the possibility of the antimicrobial peptide either be toxic or not so, selection of the peptides must be carefully done to ensure that it isn't toxic. On the other hand, Boman index test was performed, this test shows the ability of the peptides to bind to other proteins rather than the protein targets, so if the Boman index value was high this mean the peptide has multifunction while if the E-value is low, this means there was a limited side effect. On the other hand, the hydropathicity test suggested the peptides will be dissolved in water or not. If the E-value is positive this mean it is insoluble in water while if it is negative this mean it is soluble

in water and the hydropathicity value of this peptide must be not very high or very low and be between them, in addition to that the molecular weight test was done, if the molecular weight of the peptides was low the properties will be better because of the adverse immune response is low so the efficacy will be better. After these tests were done, there is only eleven peptides meet the desired properties.

As shown in Table 6, from 64 peptides only 6 peptides are selected to be most appropriate to fit with the (envelope glycoprotein H) target and without the problem of cell penetration, immunogenicity, and toxicity. So these 6 peptides may be predicted as anti-VZV in the future. From the dimensional structure of the peptide with the target (as shown in Table 7) nearly the six peptides binding to their target in the same position.

The MSI-78 which has the highest E-value (-791.09 Kcal/mol), so it was indicated high binding affinity with the target, it was demonstrated broad spectrum in vitro antimicrobial activity against most of the common pathogens intact directly on the anionic phospholipid of the bacteria cell membrane which called lipopolysaccharide (LPC), so its mechanism based on the disruption of the bacterial membrane permeability barrier which in turn lead to loss of membrane integrity & ultimately to cell death [36].

Peptide A was the second highest E-value (-725.94 Kcal/mol) and Boman index value (2.29), in addition to that has the highest cpp test value (0.51), and both of these properties may enhance the theoretically estimated multi-functionality, due to the fact that the major fraction of protein is located inside the cell and bacterial membranes contain phospholipids with or without carbohydrate chains as the bulk material. As the binding of peptides to bacterial membranes involves the lipids rather than proteins, the index should be unrelated to the bactericidal effects of the peptides [35].

While polyphemusin, has good E-value (-597.55 Kcal/mol) and highest Boman index value (3.75) as compared with the others, so we expected this high value may be good and bad at the same time, it is good because the peptide may work on more than one protein sides and bad since it work on more sides so this may result in more adverse effects than other peptides. It was a cationic peptide CAP-derived from the horseshoe crab -Limulus polyphemus. These CAPs have been shown to be active in vitro against bacteria, fungi and even viruses, including vesicular stomatitis virus, influenza A virus, and human immunodeficiency virus (HIV-1). polyphemusins have also a pronounced activity against yeast and a lower activity against phylamentous fungi, also it can be predicted to be as anti-VZV [37].

K4-S4 (1–16) is potent to inhibit N. gonorrhoeae, it could be very useful in a variety of antimicrobial applications, especially against opportunistic fungal infections such as Candida, which is the most commonly encountered fungal pathogen in the human vagina. Since it has low molecular weight (1583.25 Dalton), so this mean it has a less predicted immuno-

genic reaction [38].

The peptide GLK-19 was found to be active against Gram-negative E. coli but not Gram-positive Staphylococcus aureus. But the results showed that the GLK-19 has a good binding and stability with the targets, the E-value was (-589.28 Kcal/mol) [39].

The FV16 peptide is a molecule with antiviral activity [5]. Due to limited researches concerning this molecule, and the scope of its action against the numerous virus targets still in need to be evaluated, this is done using another bioinformatics approach, the molecular docking. This peptide has the lowest E-value (-582.14 Kcal/mol) and cpp test value (0.02), so from this, it can be expected that this peptide having the lowest binding ability with the target than other peptides.

In another hand, from 64 peptides only 11 peptides are selected to be most appropriate to fit with the (Thymidine kinase) target and these have good cell penetration, immunogenicity, and toxicity properties, so these 11 peptides are predicted to be anti-VZV. From the three-dimensional structure of the peptide with the target the eleven peptides binding with their target in two different positions (five of them bind nearly to the same position and the remainder binds to the other position).

Magainins was found to be the best E-value (-840.59 Kcal/mol) with low Boman index value (0.08) as compared with the other peptides, so this low value may indicate that this peptide has limited adverse effects. This peptide is also known as PGS (peptide glycine-serine) [33], are 23 amino acid long peptides isolated from the skin of the African clawed frog Xenopuslaevis [34]. Magainins belong to a large family of amphibian amphipathic α-helicalantimicrobial peptides. Those peptides previously indicated to be characterized by a wide spectrum of antimicrobial activities. These were against Gram positive and Gram negative bacteria in addition to the fungi. In another hand, some researches indicated that the magainins have antiviral properties. For example, magainins-I exhibited inhibited Herpes Simplex Virus-1 and 2 [40].

Peptide F also has cell penetration possibility with its Boman index (equals 1.19). These results suggest that this peptide is oligo-functional. In addition, peptides A and F subjected to DNA binding inside microbial cells, this may expand their multi-functionality.

In another hand, Dahlein 5.6 peptide has the lowest E-value (-803.68 Kcal/mol), cpp test value (0.05) and Boman index value (-0.3), so this will indicate that this peptide has a low binding affinity to the target, also it is penetrating into the cell was little and has limited adverse effects. It is one member of Amphibian peptides, the dahlein 5.6 are amongst the most active neuronal nitric oxide synthase NOS inhibitors so far isolated from amphibians, and the NOS inhibit the formation of nitric oxide (NO). The NO is an anti-microbial agent.

Fur the rmore MSI-78, A, GLK-19, Fv16, Polyphemusin 2, AVP 1092 AVP 1074 and K4S4(1-16) all these peptides have high binding affinity, and the E-value for them were

-1027.32, -967.51, -883.56, -882.43, -876.07, -827.8, -848.62 and -860.48 respectively. The MSI-78 has a higher binding affinity due to its energy was the lowest one of these selected peptides but has the larger molecular weight among these peptides but it still weak immunogenic character which may reduce adverse immune response that eliminated peptides efficiency.

Finally, the last target was 1VZV- Protease it's docking values with the selection peptide. Only fifth peptides from 64 peptides suggested to be anti-VZV peptides they include MSI-78, K4S4 (1-16) a, Magainin 1, A and AVP 1074. The five peptides show a good binding their E-values are -643, -632.87- 617.97, -611.60 and -605.48 Kcal/mol respectively.

The best binding affinity wit0h these three targets was MSI-78, it shows the lowest energy among these peptides.

Some of these eleven peptides can bind with more than one targets, with K4S4(1-16)a, MSI-78, and A peptides, these three peptides can bind with the three targets, so this will indicate that their ability to act as anti- vzv drugs in the future was high, while Polyphemusin 2, Fv16, AVP 1074, Magainin 1, and GLK-19 peptides, all of these peptides can bind with two of the targets and this will be considered a good property for these peptides, on the other hand, the F, AVP 1092, and Dahlein 5.6 peptides act only on one target.

In conclusion, Since the antimicrobial peptides included Polyphemusin 2, K4S4(1-16) a, F, AVP1092, MSI-78, A, Fv16, GLK-19, Magainin 1, and Dahlen 5.6 bond with VZV targets with acceptable physical and chemical properites, so they may have the ability to inhibit VZV and may have the potential to work as promising inhibitors for VZV in the future.

References

[1] Sawyer MH, Chamberlin CJ, Wu YN, Aintablian N, Wallace MR. Detection of varicella-zoster virus DNA in air samples from hospital rooms. J. Infect. Dis.; 169:91–94,(1994).

[2] Gilden DH, Kleinschmidt-DeMasters BK, LaGuardia JJ, Mahalingam R, Cohrs RJ. Neurologic complications of the reactivation of varicella-zoster virus. N. Engl. J. Med.; 342:635–645,(2000).

[3] Gnann JW. Whitley RJ. Clinical practice. Herpes zoster. N. Engl . J. Med.; 347:340–346,(2002).

[4] Consensus conference on anti-infectious therapy of the French society of infectious disease, Management of infection due to Varicella-Zoster Virus. Mèd. Mal. infect.; 28: 1-8,(1998).

[5] Abo Almaali HM, Antimicrobial peptides potential of some microbial histones: In-silico modeling, Internation. J. Recent Scie. Res.,5(3):649-65,(2014).

[6] Sherman, R.A., Hall, M.J. & Thomas, S. Medicinal maggots: an ancient remedy for some contemporary afflictions. Annu. Rev. Entomol., 45, 55-81,(2000).

[7] Ehret-Sabatier, L., Loew, D., Goyffon, M., Fehlbaum, P., Hoffmann, J. A., Van Dorsselaer, A., and Bulet, P. Characterization of novel cysteine-rich antimicrobial peptides from scorpion blood. J. Biol. Chem.,271,29537–29544,(1996).

[8] Wegener K.L., Wabnitz P.A., Carver J.A., Bowie J.H., Wallace J.C. and Tyler M.J., Host defense peptides from the skin glands of the Australian blue mountains tree-frog Litoria citropa. Solution structure of the antibacterial peptide citropin, Eur. J. Biochem., 265, 627–637,(1999).

[9] Yaghoubi H, Asef A, Banki A. Solid phase chemical Synthesis and Structure Activity Study of Brevinin

-2R and Analogues as Antimicrobial Peptides. J. Med. Bacteriol., 2(1): 41-53,(2013).

[10] Conlon, J.M., Sonnevend, A., Patel, M., Davidson, C., Nielsen, P.F., Pa´l, T. & Rollins-Smith, L.A. Isolation of peptides of the brevinin-1 family with potent candidacidal activity from the skin secretions of the frog Rana boylii. J. Peptide Res.,, 62, 207–213,(2003).

[11] Wu M, Maier E, Benz R, Hancock REW. Mechanism of interaction of different classes of cationic antimicrobial peptides with planar bilayers and with the cytoplasmic membrane of Escherichia coli. Biochemistry, 38: 7242, (1999).

[12] Alhoot M A, Rathinam A K, Wang S M, Manikam R, and Sekaran S D, Inhibition of Dengue Virus Entry into Target Cells Using Synthetic Antiviral Peptides,Intern. J. Med.Sci.,;10(6):719-729,(2013).

[13] Scott E. VanCompernolle, R. Taylor J., Oswald-Richter, K., Jiang, J., Youree B. E., Bowie J. H., Tyler M. J., Conlon J. M., Wade D., Aiken C., Dermody T. S., KewalRamani V.N.,

[14] Rollins-Smith L. A., and Unutmaz D., Antimicrobial Peptides from Amphibian Skin Potently Inhibit Human Immunodeficiency Virus Infection and Transfer of Virus from Dendritic Cells to T Cells, J. Virol., p. 11598–11606,(2005).

[15] Ganz, T. Defensins: antimicrobial peptides of innate immunity. Nat. Rev. Immunol.,3:710–720,(2003).

[16] Krugliak M., Feder R., Zolotarev V. Y., Antimalarial activities of dermaseptin S4 derivatives, Antimicrob. Agents and Chemother., 44(9): 2442–2451,(2000).

[17] Shestakov A., Jenssen H., Nordstr¨om I., and Eriksson K., Lactoferricin but not lactoferrin inhibit herpes simplex virus type 2 infection in mice. Antivir. Res.,, 93(3): 340–345,(2012).

[18] Brocal I, Falco A, Mas V, Rocha A, Perez L, Coll JM, et al. STable expression of bioactive recombinant pleurocidin in a fish cell line. Appl. Microbiol. Biotechnol., 72:1217e28,(2006).

[19] Conlon, J. M., A. Sonnevend, M. Patel, V. Camasamudram, N. Nowotny, E. Zilahi, S. Iwamuro, P. F. Nielsen, and T. Pal.. A melittin-related peptide from the skin of the Japanese frog, Rana tagoi, with antimicrobial and cytolytic properties. Biochem. Biophys. Res. Commun., 306:496–500,(2003).

[20] Ge, Y., MacDonald, D., Henry, M.M. In vitro susceptibility to pexiganan of bacteria isolated from infected diabetic foot ulcers. Diagnostic Microbiol. and Infect. Dis., 35: 45–53,(1999).

[21] Gottler L.M., and Ramamoorthy A., Structure, membrane orientation, mechanism, and function of pexiganan A highly, potent antimicrobial peptide designed from magainin, Biochimica et Biophysica Acta,: 1680–1686, (2009).

[22] Bastl K, Skalickova S, Heger Z, Zitka O, Adam V, et al. Modeling of the Antiviral Peptide for Specific Inhibition of Influenza Virus Entry. J. Drug. Des. Res., 2(1): 1010,(2015).

[23] Bultmann, H., and C. R. Brandt. Peptides containing membrane transiting motifs inhibit virus entry. J. Biol. Chem., 277:36018–36023,(2002).

[24] Ku C-C, Zerboni L, Ito H, Graham BS, Wallace M, Arvin AM. Varicella-zoster virus transfer to skin by T cells and modulation of viral replication by epidermal cell interferon. J. Exp. Med., 200:917–925,(2004).

[25] Wang G., Database-guided discovery of potent peptides to combat HIV-1 or Superbugs, Pharmaceuticals, 6: 728- 758, (2013).

[26] Xing, Y., Oliver, S.L., Nguyen, T., Ciferri, C., Nandi, A., Hickman, J., Giovani, C., et al., A site of varicella-zoster virus vulnerability identified by structural studies of neutralizing antibodies bound to the glycoprotein complex gHgL. Proc. Natl. Acad. Sci. USA,112: 6056-6061,(2015).

[27] Bird, L.E., Ren, J., Wright, A., Leslie, K.D., Degreve, B., Balzarini, J., Stammers, D.K. Crystal structure of varicella zoster virus thymidine kinase. J. Biol. Chem., 278: 24680 - 24687, (2003).

[28] Qiu, X., Janson, C.A., Culp, J.S., Richardson, S.B., Debouck, C., Smith, W.W., Abdel-Meguid, S.S. Crystal structure of varicella-zoster virus protease.

Proc. Natl. Acad. Sci. USA, 94: 2874-2879,(1997).

[29] Ritchie D. and Venkatraman V., Ultra-Fast FFT protein docking on graphics processors, Bioinformatics, 26(19): 2398-2405,(2010).

[30] Huang CC, Couch GS, Pettersen EF, and Ferrin TE., Chimera: an extensible molecular modeling application constructed using standard components. Pacific Symposium on Biocomputing, 1:724,(1996).

[31] Kaur, H., Garg, A. and Raghava, G.P.S. PEPstr: A de novo method for tertiary structure prediction of small bioactive peptides. Protein Pept. Lett., 14: 626-30,(2007).

[32] Calis JJA, Maybeno M, Greenbaum JA, Weiskopf D, De Silva AD, Sette A, et al., Properties of MHC class I presented peptides that enhance immunogenicity. PloS Comp. Biol., 9(10): e1003266,(2013).

[33] Gupta S, Kapoor P, Chaudhary K, Gautam A, Kumar R, et al. In silico approach for predicting toxicity of peptides and proteins. PLoS ONE, 8(9): e73957,(2013).

[34] Kyte J. and Doolittle R.F., A simple method for displaying the hydropathic character of a protein, J. Mol. Biol., 157: 105-32,(1982).

[35] Gautam A, Chaudhary K, Kumar R, Sharma A, Kapoor P and Tyagi A, et al. In silico approaches for designing highly effective cell penetrating peptides, J. Translational Med., 11:74,(2013).

[36] Boman, H. Antibacterial peptides: basic facts and emerging concepts. J. Int. Med., 254:197–215,(2003).

[37] Maloy, W.L., and Kari U.P. Structure-activity studies on magainins and other host-defense peptides. Bio. poly., 37:105-122,(1995).

[38] Miyata T., Tokunaga F., Yoneya T., Yoshikawa K., Iwanaga S., Niwa M., Takao T., and Shimonishi Y.J. Biochem., 106: 663–668,(1989).

[39] Rao, A. G. Conformation and antimicrobial activity of linear derivatives of tachyplesin lacking disulfide bonds. Arch. Biochem. Biophys., 361: 127-134,(1999).

[40] Naglik J.R., Challacombe S.J., and Hube B., Candida albicans secreted aspartyl proteinases in virulence and pathogenesis, Microbiol. And Molecular Biol. Rev., 67(3): 400–428,(2003).

[41] Perry C.M., Wagstaff A.J. Famciclovir: a review of its pharmacological properties and therapeutic efficacy in herpes virus infections. J. Drugs.; 50: 396–415,(1995).